Establishing Percent Embedment Limits to Improve Chip Seal Performance

FINAL REPORT

SPR-1679

Project Research No. OR17 -102

The Michigan Department of Transportation
Research Administration
8885 Ricks Road
P.O. Box 33049
Lansing, Michigan 48909

Authors:

Ilker Boz, Ph.D.
(Research Associate)

Yogesh Kumbargeri, E.I.T.
(Research Assistant)

M. Emin Kutay, Ph.D., P.E.
(Associate Professor)
Principal Investigator (PI)

Syed Waqar Haider, Ph.D., P.E.
(Associate Professor)

Michigan State University
Department of Civil & Environmental Engineering
428 S. Shaw Lane, Room no. 3546,
Engineering Building
East Lansing, MI 48824

August 15, 2018

TECHNICAL REPORT DOCUMENTATION PAGE

1. Report No. SPR-1679	**2. Government Accession No.** N/A	**3. Recipient's Catalog No.** N/A
4. Title and Subtitle Establishing Percent Embedment Limits to Improve Chip Seal Performance		**5. Report Date** August 15, 2018
		6. Performing Organization Code OR17 – 102
7. Author(s) Ilker Boz, Yogesh Kumbargeri, M. Emin Kutay and Syed Waqar Haider		**8. Performing Organization Report No.** N/A
9. Performing Organization Name and Address Michigan State University, 428 S. Shaw Lane, Room no. 3546, Engineering Building East Lansing, MI 48824		**10. Work Unit No.** N/A
		11. Contract or Grant No. Contract 2013-0066 Z11
12. Sponsoring Agency Name and Address Michigan Department of Transportation (MDOT) Research Administration 8885 Ricks Road, P.O. Box 33049 Lansing, Michigan 48909		**13. Type of Report and Period Covered** FINAL REPORT, 05/01/17 to 08/15/18
		14. Sponsoring Agency Code N/A

15. Supplementary Notes

Conducted in cooperation with the U.S. Department of Transportation, Federal Highway Administration. MDOT research reports are available at www.michigan.gov/mdotresearch.

16. Abstract

Long-term performance of a chip seal treatment is affected by several factors including the type and morphology of the aggregates, emulsion/binder type and most importantly, the mictrostructural characteristics such as the percent embedment and aggregate orientation. As part of a previous MDOT project (OR15-508), a methodology (and a software named CIPS) was developed to directly calculate the aggregate percent embedment based on digital image analysis. The most important aspect of this methodology is that it involves direct calculation of the embedment of individual aggregates from the images of vertical saw-cut slices. The CIPS methodology does not suffer from the major drawbacks of the traditional methods of estimating percent embedment (i.e., sand patch and laser-based methods), which assume the pavement surface to be perfectly smooth, ignore penetration of aggregates into the substrate and ignore the aggregate size distribution and orientation. The CIPS methodology provides the percent embedment objectively; however, the appropriateness of the computed percent embedment for a given field application could not be assessed due to a lack of data relating the percent embedment to chip seal performance. The primary objective of this study was to relate the image-based percent embedment to performance measures such as resistance to bleeding and chip loss. To meet this objective, an extensive laboratory testing program was completed. This included tests for chip loss and bleeding using a retrofitted Hamburg Wheel Tracking (HWT) device. Two emulsion types (CRS-2M and CSEA), one binder (PG70-28) for hot-applied chip seal application, and three aggregate sources (one slag and two different kinds of natural aggregate) were included in the testing program. Digital image techniques of the CIPS methodology were utilized to quantify and analyze the laboratory test results to develop the percent embedment thresholds. Finally, pay adjustment factors and procedures for chip seals were developed based on the percent embedment thresholds.

17. Key Words Chip seal, pavement preservation, percent embedment, image processing, sand patch test	**18. Distribution Statement** No restrictions. This document is also available to the public through the Michigan Department of Transportation.

19. Security Classif. (of this report) Unclassified	**20. Security Classif. (of this page)** Unclassified	**21. No. of Pages** 109	**22. Price** N/A

Form DOT F 1700.7 (8-72) Reproduction of completed page authorized

ACKNOWLEDGEMENTS

The authors would like to acknowledge the U.S. Department of Transportation (USDOT) for funding the University Transportation Center for Highway Pavement Preservation (UTCHPP). This project was MDOT's match to the UTCHPP funding. The authors also thank Dr. Karim Chatti (the PI of the UTCHPP), and Larry Galehouse from the National Center for Pavement Preservation (NCPP).

RESEARCH REPORT DISCLAIMER

"This publication is disseminated in the interest of information exchange. The Michigan Department of Transportation (hereinafter referred to as MDOT) expressly disclaims any liability, of any kind, or for any reason, that might otherwise arise out of any use of this publication or the information or data provided in the publication. MDOT further disclaims any responsibility for typographical errors or accuracy of the information provided or contained within this information. MDOT makes no warranties or representations whatsoever regarding the quality, content, completeness, suitability, adequacy, sequence, accuracy or timeliness of the information and data provided, or that the contents represent standards, specifications, or regulations."

TABLE OF CONTENTS

EXECUTIVE SUMMARY

Chip seal treatments are commonly used to extend the life of asphalt pavements. They typically seal minor fatigue and low temperature cracks, retard raveling by reducing the moisture infiltration and improve friction. Long-term performance of a chip seal treatment is affected by several factors including the type and morphology of the aggregates, emulsion/binder type and most importantly, the microstructural characteristics such as the percent embedment and aggregate orientation. As part of a previous MDOT project (OR15-508), a methodology (and a software named CIPS) was developed to directly calculate the aggregate percent embedment based on digital image analysis. The most important aspect of this methodology is that it involves direct calculation of the embedment of individual aggregates from the images of vertical saw-cut slices. The CIPS methodology does not suffer from the major drawbacks of the traditional methods of estimating percent embedment (i.e., sand patch and laser-based methods), which assume the pavement surface to be perfectly smooth, ignore penetration of aggregates into the substrate and ignore the aggregate size distribution and orientation. The histogram of the percent embedment of individual aggregates allows computation of Percent Within Limits (PWL), which can be used to compute the pay adjustment factors. The CIPS software can compute the percent embedment accurately; however, the appropriateness of the computed percent embedment could not be assessed due to the lack of data relating the percent embedment to chip seal performance. Therefore, there was a need to find appropriate range of percent embedment (computed for each aggregate) to performance measures.

This report documents the efforts towards establishing performance-based threshold values of the percent embedment to minimize common chip seal distresses (i.e., bleeding and aggregate loss). The extensive laboratory testing program included tests for chip loss and bleeding using a retrofitted Hamburg Wheel Tracking (HWT) device. Two emulsion types (CRS-2M and CSEA), one binder (PG70-28) for hot-applied chip seal application, and three aggregate sources (one slag and two different kinds of natural aggregate) were included in the testing program. Digital image techniques of the CIPS methodology were utilized to quantify and analyze the laboratory test results with respect to the percent embedment. During this project, a new image-based parameter (i.e., aggregate orientation) was introduced and added to the CIPS software. Additionally, mean texture depth of laboratory-fabricated chip seal samples was also used in analysis of the test results. The mean texture depths of the samples were calculated from the mean profile depth profile that is obtained from a 3D image of chip seal surface. The 3D surface profiles of the chip seal samples were reconstructed by using commercially available photogrammetry software and then processed by a MATLAB-based algorithm developed during this project for calculation of the mean profile depth. Furthermore, an image analysis algorithm was also developed to convert the chip seal cross-sectional images to finite element mesh that can be used as an input to ABAQUS software. The selected levels of percent embedment and other microstructural properties (e.g., aggregate orientation) were mechanistically evaluated, and a comparative analysis was made. Finally, pay adjustment factors and procedures for chip seals were developed.

1. INTRODUCTION

The use of chip seals dates to the 1920s as a method of re-surfacing pavements. Even though chip seals have been mainly used in the construction of new low-volume roads in early projects, they have emerged into a maintenance and preservation treatment in the past few decades for low-volume roads that show slight to moderate levels of deterioration. With the advancement in binder/emulsion technology and improvements in design and construction practices, chip seals have also been applied to treat high-volume roads in recent years (Im and Kim, 2016). Although chip seals can be applied in several different forms (i.e. as single seals, cape seals, and stress absorbing membrane interlayers), single-layer chip seal treatments are the most commonly applied form of chip seals in the US (D. Gransberg and James, 2005; Pierce and Kebede, 2015). Construction sequence of single chip seals consists of spraying hot asphalt binder or emulsion over the surface of an existing pavement, followed by immediate spreading of aggregates (chips) on the surface. The chips are then seated into the binder/emulsion through roller compaction, achieved by pneumatic rollers. After curing period, the treated surface is swept off for removal of any loose aggregates. While the asphaltic component of chip seals fills and seals existing cracks and acts as a waterproof layer to prevent moisture infiltration and aging of the underlying pavement, aggregates act as a protective membrane for the asphaltic component of the seal and provide the required skid resistance for the pavement (Janisch and Gaillard, 1998). In addition to its proven benefits in improving the serviceability level and extending life of deteriorating pavements, many construction agencies frequently prefer chip seals as a preventive maintenance method due to their cost-effective application as well as simplicity and ease of construction procedures (D. Gransberg and James, 2005).

The performance of chip seals depends on many factors including design of the treatment, condition of the existing pavement, quality of the materials being used and construction practices, climate, and traffic (D. Gransberg and James, 2005). The performance of such treatments as it relates to the design is affected by the joint interaction of its constituent materials (aggregate and emulsion/binder). Such interaction is governed by the application rates of aggregate and binder, as well as their properties, such as aggregate size and shape, gradation, and stiffness. For a given aggregate and binder, the extent of embedment of aggregate chips into the binder dominates the behavior of the aggregate-binder interaction, including aggregate orientation and dictates the performance of chip seals (Kumbargeri, Boz and Kutay, 2018). Thus, making the embedment of aggregates one of the most significant parameters affecting the performance of chip seals. Excessive or insufficient aggregate embedment may result in severe distresses such as bleeding or aggregate loss in chip seal applications. Hence, having proper limits of the percent embedment of aggregates established based on performance-based test measures are of paramount importance for successful application of such treatments.

In a previous project (OR15-508) (Kutay et al. 2017) funded by Michigan Department of Transportation (MDOT), a procedure (and a software named CIPS) was developed to directly calculate the percent embedment of aggregates into the asphalt binder for a chip seal application based on digital image analysis. This procedure can be used as;

(i) An acceptance test (or part of an acceptance specification) for MDOT,
(ii) A quality control measure for contractors and for MDOT quality assurance,
(iii) An objective tool for forensic investigations,

(iv) A method for future conflict resolutions.

However, all these potential applications rely heavily on maximum and minimum limits of the percent embedment, which should be determined through performance testing of chip seals.

The image-based software (CIPS) developed as part of OR15-508 was able to compute the percent embedment using three different methods, namely; (i) peak valley method, (ii) surface coverage area method and (iii) embedment of each aggregate method. Among these methods, the third method, embedment of each aggregate method was found to be the most robust method delivering repeatability. The CIPS software can compute the percent embedment accurately and objectively; however, the appropriateness of the computed percent embedment could not be assessed due to a lack of data relating the percent embedment to chip seal performance. There is a need to relate the percent embedment to performance measures such as resistance to bleeding (which can impact surface friction and texture) and aggregate loss.

The research results presented in this report details the effort towards establishing performance-based threshold values of the percent embedment to minimize common chip seal distresses (i.e., bleeding and aggregate loss) through an extensive experimental program. The laboratory performance-based test results for chip loss and bleeding were obtained using a retrofitted Hamburg Wheel Tracking (HWT) device. Digital image techniques were utilized to quantify and analyze the laboratory test results with respect to the percent embedment. During this project, a new image-based parameter (i.e., aggregate orientation) was introduced. Additionally, mean texture depth of laboratory-fabricated chip seal samples was also used in analysis of the test results. The mean texture depth of the samples was calculated from the mean profile depth profile that is obtained from a 3D image of chip seal surface. The 3D surface profiles of the chip seal samples were reconstructed by using commercially available photogrammetry software and then processed by a MATLAB-based algorithm developed during this project for calculation of the mean profile depth. Furthermore, an image analysis algorithm was also developed to convert the chip seal cross-sectional images to finite element mesh that can be used as an input to ABAQUS software. The selected levels of percent embedment and other microstructural properties (e.g., aggregate orientation) were mechanistically evaluated, and comparative analysis with respect to the laboratory-obtained test results was completed. Finally, pay adjustment factors and procedures for chip seals were developed based on the test results.

This report is divided into several chapters. Chapter 2 documents a relevant review of the literature on chip seals, mainly covering the studies completed in the past two decades. The objectives of this research as well as research plan and the pertaining tasks are listed in Chapter 3. Chapter 4 presents the experimental program, materials, and methods used in this research. Chapter 5 includes the descriptions of image-based evaluation methods and parameters. Chapters 6 and 7 are devoted to presentation, analysis, and discussion of the aggregate loss and bleeding susceptibility test results, respectively. Chapter 8 details the development of pay adjustment factors and procedures for chip seals. Finally, the summary and findings of the performed research as well as recommendations for potential future work are presented in Chapter 9.

2. LITERATURE REVIEW

In the United States, chip seal design has been reported to be somewhat of an art rather than a science (D. D. Gransberg and James, 2005). Initial efforts to design chip seals used a purely empirical approach. With further research, this approach was slightly modified with inclusion of aggregate shape and other morphological characteristics. McLeod and Kearby design procedures are some of the popular examples of this approach. Geographical differences, variable nature of materials, and surface conditions were impediments to the establishment of a nationwide design method. Experience-based design is still very popular among road agencies in the US. It is performed by starting with a base rate for the binder and aggregate determined after years of experience in the field. Road agencies that predominantly use empirical methods state that, in many instances chip seal projects merely specify a base rate for binder and aggregate. Hence, empirical approaches are used by these agencies essentially to estimate the quantities of each to be used during the bidding phase. This empirical approach in design of chip seals further gets transferred to quality assurance (QA) and quality control (QC) methods. In practice, the sand patch test has been widely used as QA protocol by various state as well as county road agencies. The sand patch method is based on approximation and assumptions related to aggregate embedment in the emulsion/binder layer. The shortcomings of this method have been described in depth as part of previous in a previous project (OR15-508) (Kutay et al. 2017; Ozdemir et al. 2018.) funded by Michigan Department of Transportation (MDOT).

In order to develop performance related specifications, it is important to understand the performance distresses involved in chip seal pavements. A survey of US public road agencies was conducted by Gransberg (Gransberg, 2005). This survey covered the agencies that use chip seals as an important pavement preservation solution. It identified bleeding and aggregate loss as the two most common distresses for chip seals. Further, bleeding was pointed out to be the most common distress by 81% of respondents which was followed by aggregate loss (67%) (Gransberg, 2005). This survey further highlighted the importance of aggregate loss and bleeding, as major performance distresses in chip seals. The following paragraphs deal with these distresses as well as methods to characterize these distresses.

2.1 Aggregate loss in chip seals

Aggregate loss occurs because of a weak or insufficient bond between the binder and aggregate. Low binder application rates or high aggregate application rates can lead to low percent embedments, which in turn leads to aggregate loss. The other factors affecting chip loss can be listed as follows:

1. High traffic stress: This can happen due to high volumes of activity, excessive weights of vehicles, braking and acceleration.
2. Environmental conditions: Precipitation immediately after chip seal construction can have an adverse effect on development of the bonding of aggregates and binder, leading to high susceptibility to aggregate loss.
3. High dust content: If the aggregates used for chip seal applications have a high dust content, it adversely affects the bonding of the aggregate and binder. This results in higher susceptibility to aggregate loss.

Several methods have been developed to characterize aggregate loss in chip seals. A summary of each procedure is presented in the following subsections.

2.1.1 Vialit Adhesion Test

The Vialit Adhesion Test was first introduced in France to measure the effect of binder and aggregate type on performance (Louw, Rossman and Cupido, 2004). Figure 2-1 shows the *Vialit* test setup. It consists of three component metal base with the vertical rod, a steel ball, and metal test plates. Jordan and Howard (2010) studied applicability of the Vialit test on surface seal treatments with respect to performance (Jordan and Howard, 2010). It was concluded that results from the Vialit test are always questionable and it is not sufficient to make conclusions regarding performance of seal treatments. Another study by Epps-Martin et al (2001) also suggested that results from the Vialit test are inconsistent and they cannot differentiate between good and poor performance of the seal treatments (Epps-Martin, Glover and Barcena, 2001).

Figure 2-1 *Vialit* test setup (source: Louw et al. 2004)

2.1.2 Frosted Marble Test

The Frosted Marble Test (FMT) was developed to measure binder adhesion by applying torque to marbles fixed to a base tray with the binder. The test setup consists of a torque wrench, a hooked foot for applying shear and a tray on which binder is spread and marbles are placed, respectively. Howard et al. (2009) made a modification to the FMT setup by including temperature control using an environmental chamber. They also modified the curing procedure. Howard et al. (2009) stated that although the results from the FMT seem to be valuable for evaluating the performance of binder adhesion and curing, it is not enough by itself and other test methods should be used to make comprehensive evaluation. Figure 2-2 shows the Frosted Marble Test setup.

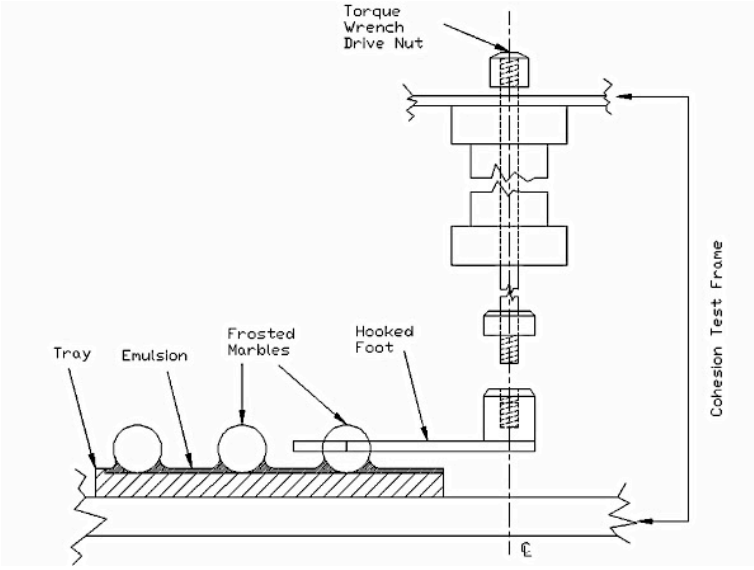

Figure 2-2 FMT test setup (source: Howard et al. 2009)

2.1.3 Australian Aggregate Pull-out Test

This test method was developed for finding the necessary pull-out force to separate aggregates from the asphalt bitumen material in surface seal treatments. It has been illustrated in Figure 2-3 (Akilli *et al.*, 2012).After the surface seal treatment is prepared, the embedded aggregates are fixed by a crocodile clip and a 20 g/sec pull-out rate is applied to the stone until it is detached. During this procedure, load measurements are taken continuously. One of the uses of this test method can be found in determining the duration of traffic control after construction. In addition, coated average area of the binder on the aggregate can be observed visually to correlate with the peak tensile stress needed to pull out the aggregate (Sendheera *et al.*, 2006).

Figure 2-3 Aggregate pullout test setup (source: Akýllý et al. 2012)

2.1.4 Pennsylvania Aggregate Retention Test

The Pennsylvania Aggregate Retention Test (PART) was first developed by National Center for Asphalt Technology Auburn University (Kandhal and Motter, 1991). The test simulates the effect of traffic on surface seal treatments by using a laboratory sieve shaker. A surface seal treatment sample is prepared within the pan and after the compression and curing process, initial aggregate loss is obtained by turning the pan upside down. Then, the pan is placed in the sieve shaker (as shown in Figure 2-4) upside down at an inclination of 45^{o}. After 5 minutes of shaking, aggregate loss is measured and calculated as a percentage.

Figure 2-4 Mary Ann sieve shaker used for Pennsylania Aggregate Retention Test (source: Kandhal and Motter 1991)

2.1.5 Pneumatic Adhesion Tension Test

The Pneumatic Adhesion Tension Testing Instrument (PATTI) (ASTM D4541, 2009)is used for evaluating bond strength of an asphalt binder by applying direct tension. Figure 2-5 shows the PATTI test setup (Santagata *et al.*, 2009).

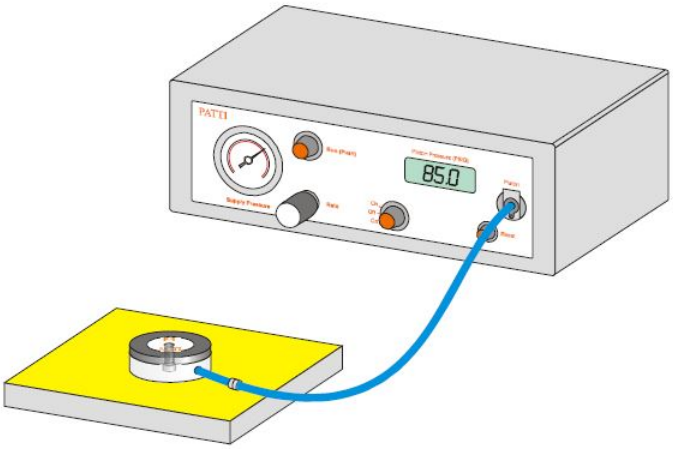

Figure 2-5 PATTI test setup (source: (Watson, no date))

2.1.6 ASTM D7000 Sweep Test

The sweep test (ASTM-D7000, 2011) is one of the laboratory test methods suggested by the NCHRP Report 680 for evaluation of the performance of asphalt chip seals in terms of aggregate loss. The test procedure includes fabrication of asphalt chip seal samples, and testing by applying shear force to the surface of aggregates by using a nylon strip brush affixed to the mixer. Before and after testing, the sample is weighed and the percentage of mass loss is calculated (ASTM-D7000, 2011). The goal of the sweep test is to measure the adhesive properties of an emulsion just after the construction, not to simulate the effect of traffic. In other words, this test method is designed to assess the curing characteristics of chip seals. However, researchers have used this method to evaluate the aggregate loss performance of the chip seals. Figure 2-6 illustrates sweep test apparatus.

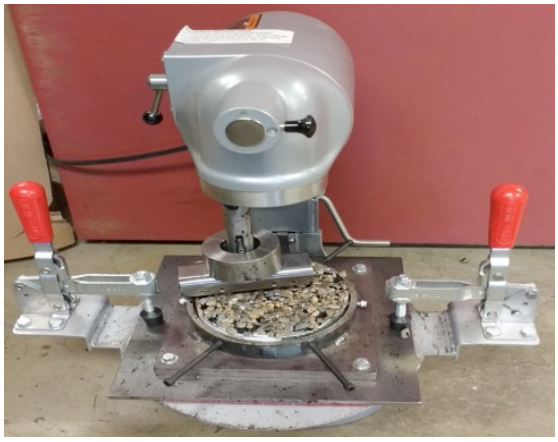

Figure 2-6 Sweep test setup

Among the different test methods mentioned above, sweep test was recommended to be the best for aggregate loss characterization of chip seals. Previous studies compared different asphalt emulsions and binders, and suggested the use of modified binders and emulsions for better performance (Gransberg and Zaman, 2005; Lee and Kim, 2012; Aktaş *et al.*, 2013; Rizzutto *et al.*, 2015; Abedini *et al.*, 2017). Furthermore, studies analyzing the effect of binder and aggregate application rates on the aggregate loss of chip seals have also been conducted (Lee and Kim, 2008; Lee *et al.*, 2013). These studies focused on chip seal aggregate loss performance from an empirical perspective. The ASTM D7000 sweep test (ASTM-D7000, 2011) was originally intended to investigate the curing characteristics of emulsion-based chip seals to determine the amount time required for the chip seal to sufficiently cure before traffic could be allowed on the surface. Additionally, the sweep test has successfully been utilized (with slight modifications) by various researchers to study the effect of several other factors on performance characteristics of chip seals, including hot applied chip seals (Aktaş *et al.*, 2013; Rizzutto *et al.*, 2015). The sweep test was found to be effective in discerning the performance of chip seals due to differences in aggregate minerology and gradation, curing temperature, humidity and time, type of emulsions, aggregate pre-coating and moisture content (Miller, Arega and Bahia, 2010; Johannes, Mahmoud and Bahia, 2011; Wasiuddin *et al.*, 2013; Howard *et al.*, 2017). Ranking of field performances of emulsion-based and hot applied chip seals were also evaluated based on the aggregate loss calculated from the sweep test. It was found that the sweep test performed in the laboratory can properly rank specimens to match the field performance (Wasiuddin *et al.*, 2013). Moreover, the sweep test was recommended as the optimal aggregate retention test method among other performance tests (the Vialit and FMT) for emulsion-based chip seals (Howard *et al.*, 2017). All these studies have generally focused on aggregate loss of chip seals from an empirical perspective.

In summary, there are numerous studies on the effect of application rates on aggregate loss in chip seals. It has been reported that aggregate loss increases with increase in aggregate rate and decrease in binder application rate. The ASTM D7000 sweep test has been typically used to characterize aggregate loss in these studies. The main drawback of the sweep test is that the load levels are much lower than those of field conditions. The amount of aggregate loss in chip seals significantly depends on the bond strength between aggregates and the binder. Since chip seal consists only of a surface layer with binder and aggregate and not a strong structural layer, the effects of heavy traffic are magnified. There is a need to develop a test protocol that requires chip seal specimens to be subjected to relatively heavy loading conditions. Additionally, the previous studies have characterized aggregate loss from an empirical perspective, without direct consideration of its microstructure (i.e., aggregate embedment and orientation). Hence, there is a need to analyze and correlate abrasion loss results with chip seal microstructure.

2.2 Bleeding of chip seals

Bleeding, i.e., the rise of asphalt binder to the surface, is one of the major chip seal distresses. The binder fills the voids in the aggregate and spreads on the surface which leads to lower skid resistance. It is usually observed in the wheel path and areas of frequent loading such as intersections where slow traffic and turning movements cause a higher stress condition at the chip seal surface. Also, at elevated temperatures, binder might be picked up by the tires and lead to catastrophic failures in chip seals.

2.2.1 Causes of bleeding

Several factors affect the susceptibility of chip seals to bleeding. These include but not limited to:

1. *Binder application rate*: Optimum binder application rate is extremely important to ensure efficient performance of chip seals. Very high content of binder leads to bleeding. Additionally, there is a trade-off between binder and aggregate application rates, which also depends on the type and gradation of aggregates.
2. *Traffic volume*: Traffic volume plays an important role in selection of the binder application rates for bleeding. It has been reported by some studies that roads with high traffic volumes need lower binder application rates. This is because the heavy traffic can cause aggregates to penetrate into underlying surface after the road is opened to traffic (Texas Department of Transporation, 2010)
3. *Aggregate properties*: Aggregate properties such as gradation, shape, size and toughness have been reported to be factors affecting bleeding performance (Chaturabong, Hanz and Bahia, 2015). Non-uniform gradation (i.e., well graded aggregates) has been identified as an important concern (Senadheera, Gransberg and Kologlu, 2000). However, many state agencies pay sufficient attention to the type of gradation (e.g., uniform versus well graded aggregates) of chip seal aggregates. Non-uniform gradation prevents the aggregates from attaining uniform percent embedment (Shuler *et al.*, 2011). Larger aggregates become less embedded whereas smaller aggregates get highly or almost fully embedded inside the binder. Such non-uniformity in embedment creates localized distresses which later spreads to the whole surface due to tire-pickup phenomenon.
4. *Type of binder*: Type and grade of asphalt binder significantly influences the susceptibility of chip seals to bleeding (Shuler *et al.*, 2011). Modified binders typically improve the performance of chip seals with respect to bleeding. Recently, performance related specifications have been developed to choose appropriate emulsion for particular climatic conditions (Shuler *et al.*, 2011). Similar studies need to be performed for hot applied chip seals as well.
5. *Climate*: Climate plays a key role in potential for chip seal bleeding. In order to properly address the effect of climate on chip seals, an emulsion performance grading procedure has been developed as part of a recent NCHRP study (NCHRP project 9-50) (Kim *et al.*, 2017) .
6. *Existing pavement surface*: Existing pavement surface should not be treated with chip seals during hot weather. This leads to aggregates penetrating pre-existing pavement surfaces.

The following subsection presents chip seal bleeding studies performed by several researchers in the past.

2.2.2 Laboratory studies on chip seal bleeding

Few research studies have focused on characterizing bleeding in the laboratory. These studies used several kinds of small scale loaded wheel tracking devices described below:

1. *Accelerated Chip Seal Simulation Device (HSKSC)*: Accelerated Chip Seal Simulation Device (abbreviated in Turkish language as HSKSC) is a vehicle load simulator that was developed in Turkey (Aktaş *et al.*, 2013) to assess the chip seal performance in the laboratory (Figure 2-7). The loading system is built inside a temperature-controlled cabin, so that moving load can be applied under different temperatures. It provides back and forth movement of the wheel through a pneumatic piston. The diameter of the tire is 48.5 cm, and it is inflated to 70 psi. The wheel travels at a speed of about 1500-wheel application per hour. More than one wheel can be fixed to the transverse shaft to allow for testing of multiple samples at the same time. These units are operated by an external microprocessor-controlled, programmable electronic panel. Although this device considers the effect of moving loads and temperatures, it does not account for real field loads and loading pattern. It has been mostly used to understand performance of surface treatments on a comparative basis.

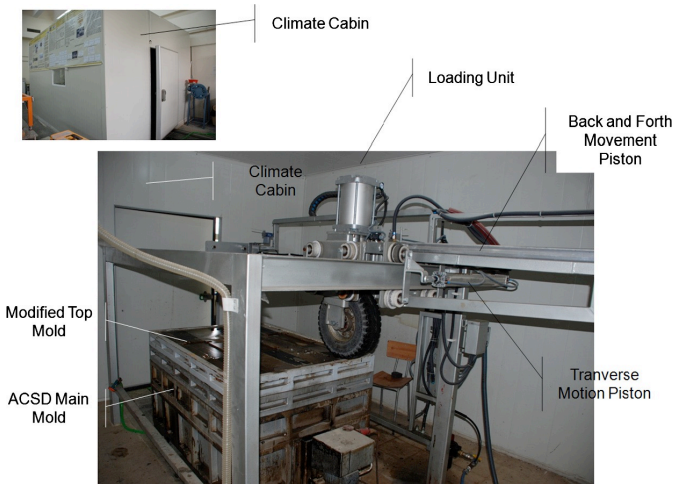

Figure 2-7 HSKSC setup (source: Aktas et al. 2013)

2. *Modified Loaded wheel test (LWT)*: The loaded wheel test (LWT) has been specified in ASTM D6372 (ASTM-D6372, 2005) and is intended for use to assess bleeding potential in slurry seal and microsurfacing applications (Figure 2-8). The test applies a rubber-tired wheel (7.62 cm in diameter) with a load of approximately 57 kg to a microsurface for 1,000 cycles at a frequency of 44 cycles per minute. The weight of the dry sample is recorded, and hot sand, heated to 85°C, is added to the sample. The sample is further subjected to 100 cycles with the sand on top of it. The sand is dusted off the sample at the end of 100 cycles, and the weight of the sample is recorded again. Bleeding is determined indirectly through limitation of the amount of sand that adheres to the samples. In a study by Chaturabong et al. (2015), LWT was modified in order to be applied to chip seal bleeding characterization. The test was modified to better represent field conditions through the provision of a mechanism to control. During initial testing, significant ravelling (i.e., aggregate loss) was observed. This behaviour was attributed to the stiffness of the steel plate used to support the sample in the original LWT device. One cause of bleeding was embedment of aggregate chips into the existing pavement.

For the representation of this condition and to provide a flexible support, a neoprene foam pad was placed between the steel plate and sample.

Figure 2-8 Loaded wheel test (LWT) setup (source: Chaturabong et al. 2015)

3. *Third scale model mobile loading simulator (MMLS3)*: The third scale model mobile loading simulator (MMLS3) is one of accelerated pavement testing devices for determining performance of different kinds of pavements by simulating traffic effect in a determined scale. Lee (2003) first introduced the MMLS3 to measure hot mix asphalt (HMA) performance with respect to fatigue cracking and rutting. This test machine consists of 4 bogies, 1 axle per bogie and 1 wheel/tire per axle (Bhattacharjee *et al.*, 2004). Each wheel has a diameter of 80 mm and can apply a maximum of800 kPa pressure, and between 1.9 kN and 2.7 kN load. It has been illustrated in Figure 2-9 .Since the MMLS3 is inside an environmental chamber, the desired temperature can be sustained. In addition to applicability of MMLS3 to HMA pavements, this test is also applicable to surface seal treatments. MMLS3 has been extensively used to characterize bleeding performance of chip seals in recent years. The latest NCHRP project 9-50 (Kim *et al.*, 2017) used MMLS3 as the sole bleeding analysis tool for chip seal pavements.

Figure 2-9 MMLS3 setup (source: Adams et al. 2014)

There have been several research studies to characterize bleeding in chip seals. Chaturabong et al. (Chaturabong, Hanz and Bahia, 2015) developed a modified loaded wheel tracking test as a laboratory test procedure to evaluate bleeding. Bleeding was evaluated as the relative percentage of asphalt appeared on the surface. Results indicated that the modified LWT method could quantify bleeding potential and bleeding development of laboratory prepared chip seal samples. Lee et al. (2006) used Third-Scale Model Mobile Loading Simulator (MMLS3) to characterize bleeding in laboratory. It has been reported to show promising results for bleeding analysis with respect to laboratory and field chip seal specimens (Adams and Kim, 2010). Aktaş et al., (2013) developed a similar wheel tracking device called an 'Accelerated Chip Seal Simulation Device' to study bleeding potential of chip seal design scenarios. These studies developed customized equipment to test and analyze bleeding performance. Although these studies showed promising results, it may not be economically feasible for the road agencies to buy a specialized equipment for chip seal bleeding evaluation. Because chip seals are applied to low volume roads, road agencies and companies may not be keen on investing additional money on such equipment. Thus, it is important to use readily available equipment to save additional cost of procuring a new equipment. Hamburg wheel tracking device (HWT) is one of the most popular pieces of equipment used to characterize rutting in asphalt pavements. All the major road agencies and laboratories typically have access to HWT. Consequently, it is a feasible option to characterize chip seal bleeding through HWT. Furthermore, it is important to analyze the bleeding results (from HWT) through the perspective of percent embedment. This would yield the upper threshold limits for percent embedment, to control bleeding of chip seal projects in the state of Michigan.

3. OBJECTIVES AND RESEARCH PLAN

The main objective of this research project was to establish performance-based minimum and maximum limits of the percent embedment of aggregates through evaluation of common chip seal distresses (bleeding and aggregate loss). A research plan was devised through a series of tasks to achieve the objectives of this research study. The following sections briefly describe the tasks undertaken to complete the research study presented in this report. Details of the tasks are provided later in the report, with the exception of Task 1, as it is provided in Chapter 2.

3.1 Task 1: Literature Review

A critical review of the literature was completed to identify and synthesize current research, emerging testing methods and equipment available for evaluating the performance of chip seals in the laboratory and their relation to the performance. Emphasis was placed on test methods utilizing laboratory wheel tracking devices as well as the procedures to evaluate performance of chip seals in respect to aggregate loss and bleeding. The review and summary of the literature is provided in Chapter 2.

3.2 Task 2: Laboratory Testing and Analysis

Material procurement and characterization, sample preparation, setting-up the laboratory test procedures and equipment, and performing laboratory performance tests were the activities accomplished under this task. Additionally, evaluating the impact of chip seal substrate surface conditions (field vs. lab) on the laboratory test results for chip seals through aggregate loss was performed as part of this task.

3.3 Task 3: Image-based Analysis

The work under this task included determination of the percent embedment and a newly-introduced parameter (i.e., aggregate orientation) through the revised CIPS software. Also, evaluation of changes in chip seal surface characteristics (i.e., percent bleeding area and mean texture depth) due to the loading of the HWT device through the analyses of digital images was conducted under this task. Moreover, the effect of percent embedment and microstructural properties of chip seals on the resultant performance were studied through the finite element method. The results obtained in Task 2 were analyzed in conjunction with the results from this task to establish performance-based threshold values of the percent embedment that can be used as the basis for chip seal design specifications.

3.4 Task 4: Establishing Pay Adjustment Factors and Procedures

Establishing a sampling plan and the procedure of the field cores for pay adjustment factors were developed based on the test results of Tasks 2 and 3. The framework as part of this task can serve as a benchmark towards developing quality assurance and acceptance protocols for the future chip seal projects.

3.5 Task 5: Development of Final Report

The final task of this research project was the preparation of the final report.

4. MATERIALS AND METHODS

This chapter covers detailed descriptions of the work performed under Task 2: Laboratory Testing and Analysis. This task consisted of series of activities that had been performed either in parallel or sequential order.

4.1 Material Procurement and Characterization

Through consultation with MDOT, two emulsion types (CRS-2M and CSEA) and two aggregate sources (slag (MDOT Pit#92-35) and natural aggregate (MDOT Pit#31-87)) were identified and brought to the laboratory for testing. During the study, another source of aggregate (natural aggregate—referred to as Gerkin aggregate) and binder (with a performance grading of PG70-28) were added to the experimental program. The reason(s) for this decision has been provided under the experimental design and sample preparation section.

4.1.1 Aggregate Properties

In this study, the following physical properties of aggregates were measured: particle size distribution (gradation), specific gravity, unit weight, and flakiness ratio. These properties are used as input parameters in the existing empirical design procedures for chip seals to calculate aggregate application rates. They are also used for quality control and assurance purposes as well as comparative performance ranking of chip seals.

Aggregates were brought to the laboratory in canvas bags, each weighing approximately 50 lbs. For a given source of aggregate, two bags of aggregate were poured on the floor and mixed thoroughly with shovels. Then, the mixed aggregate stockpile was quartered into four mini stockpiles, as shown in Figure 4-1 Illustration of a) four mini stock piles of aggregates, b) representative samples from stockpiles, c) separation based on the sieve size, d) metal plate for flakiness index computation (MTM 130). Figure 4-1(a). The appropriate aggregate samples were randomly scooped from each of the four mini stockpiles to obtain representative samples for testing (Figure 4-1 (b)). Once the representative samples were obtained, the aggregate properties of interest were determined by following appropriate test standards. The particle size distribution of aggregates (gradations) for each source was determined by the sieve analysis using AASHTO T 11 and T 27 standards. While the bulk specific gravities of the aggregates were determined following AASHTO T 84 and T 85 standards, the standard test procedure outlined in ASTM C 29 was performed to determine the bulk density (unit weight) of the aggregates. Finally, the flakiness index (ratio) test were performed to determine the percentage of flat particles in each aggregate source using the procedure implemented by Minnesota Department of Transportation for seal coat aggregates. The test was performed using the aggregates retained on sieves larger than the #4 sieve. Based on the results of the particle size distribution of aggregates used in this study, the sieves utilized for the flakiness index were 3/8", ¼", and #4. The test procedure involved separating aggregates retained on each respective sieve into containers (Figure 4-1(c)), followed by washing and oven-drying the samples to a constant mass at 110 ± 5°C. Then, the aggregates retained on each sieve comprising 4 percent of the total of representative sample were tested through a metal plate with slotted openings (Figure 4-1(d)). In other words, each of the particles in each sieve fraction was tried through the slot opening for each respective sieve size. The total mass of particles passing through the respective slot openings were determined. The mass was then divided by the

total mass of passing and retained aggregates. The resultant number multiplied by 100 and rounded up to the nearest whole number was reported as a percent flakiness index. The dimensions (width by length) of the slot openings were determined to be 0.263 by 1.57, 0.184 by 1.18, and 0.131 by 0.79 inches for the sieves 3/8", ¼", and #4, respectively. Two replicates for each aggregate source were prepared and tested in conjunction with each of the tests described above.

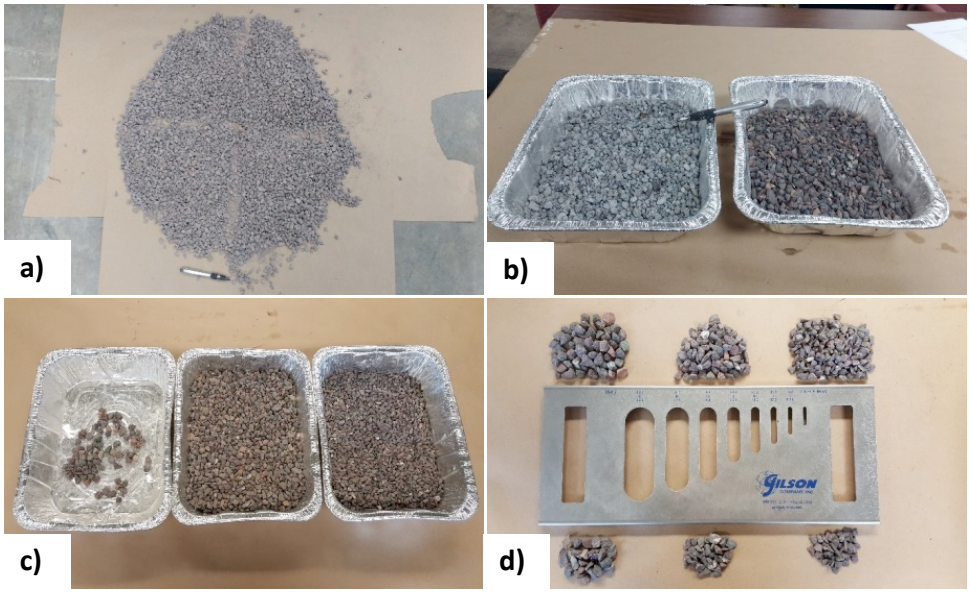

Figure 4-1 Illustration of a) four mini stock piles of aggregates, b) representative samples from stockpiles, c) separation based on the sieve size, d) metal plate for flakiness index computation (MTM 130).

The particle size distribution of the three aggregate sources used in this study are shown in Figure 4-2 along with MDOT boundary sieve size requirements for single chip seal gradations. Additionally, the corresponding percent passing values of each sieve size to the MDOT respective boundary sieve sizes are tabulated in Table 4-1 for each aggregate source. As it can be seen from the table, the three aggregate sources confirmed the MDOT gradation requirements for single chip seal aggregates for each sieve size, except sieve No.4 for Gerkin aggregates. It must be noted that natural and Gerkin aggregates met the requirements for Type B gradation in AASHTO MP 27 Standard Specification for Materials for Emulsified Asphalt Chip Seals. However, aggregate gradation for slag did not confirm the requirements set forth for Type B gradation in the AASHTO specification. Slag aggregate gradation exceeded the maximum limits for the sieves No.8, 30 and 200, which were 10, 2, and 1 percent passing, respectively.

Aggregate gradation is among the major factors driving chip seal performance (Lee and Kim, 2009; Johannes, Mahmoud and Bahia, 2011; Wasiuddin *et al.*, 2013). Uniformly graded aggregates are typically less prone to chip seal distresses compared to well graded aggregates, when all other characteristics are the same. The extent of aggregate gradation uniformity can be quantified using the uniformity coefficient (C_u), a parameter widely used in geotechnical engineering to classify soils and aggregates. The C_u is defined as the ratio of the particle diameter corresponding to 60 percent finer (D_{60}) to the particle diameter corresponding to 10 percent finer (D_{10}) on the aggregate gradation curve (Das and Sobham, 2013).

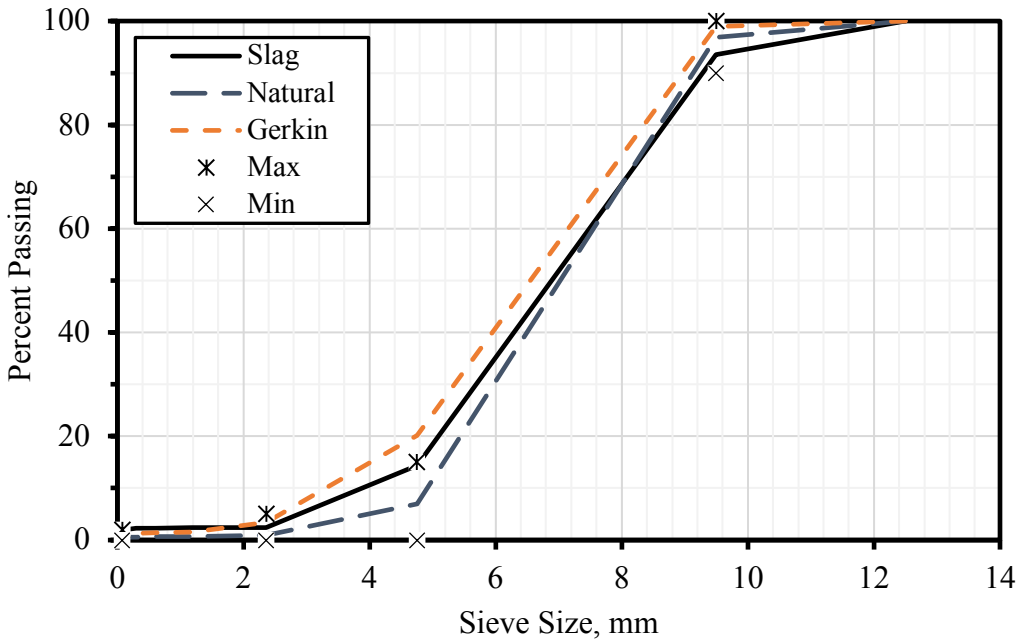

Figure 4-2 Particle size distrubution of the aggregates (see Table 4-1 for the magnitudes of the percent passing and sieve sizes).

Table 4-1 Gradations of Aggregates with respect to MDOT Sieve Limits

Sieve Size		MDOT Min	MDOT Max	Slag	Natural	Gerkin
US	SI (mm)	% Passing				
1/2"	12.5	100	100	100.00	100.00	100.00
3/8"	9.5	90	100	93.50	96.80	98.90
#4	4.75	0	15	14.38	6.94	20.20
#8	2.36	0	5	2.45	0.94	3.40
#16	1.18	-	-	2.36	0.67	1.60
#30	0.6	-	-	2.31	0.63	1.40
#50	0.3	-	-	2.23	0.61	1.30
#100	0.15	-	-	2.03	0.59	1.00
#200	0.075	0	2	1.72	0.51	0.70

In a study by Lee and Kim (Lee and Kim, 2009), the ranking of chip seal performance was evaluated using the C_u as a performance parameter index. The work was conducted using three different aggregate gradations of the same source with the same median particle size. The performance criteria chosen was raveling distress, quantified via the MMLS3 testing. The test results indicated that the C_u -based uniformity ranking did not show the expected trend of chip seal performance. In the same study, the authors introduced a new gradation-based coefficient to rank the degree of uniformity of aggregate gradation, called the performance-based uniformity coefficient (PUC), to optimize chip seal aggregate gradation for a given source. The test results showed that the effect of particle size uniformity on the chip seal performance (i.e. raveling) was properly ranked by the PUC parameter, which is defined as follows (Lee and Kim, 2009):

$$PUC = \frac{P_{0.7D_{50}}}{P_{1.4D_{50}}} \quad (1)$$

where PUC = performance-based uniformity coefficient (PUC), $P_{0.7D_{50}}$ = percent passing corresponding to $0.7 * D_{50}$, and $P_{1.4D_{50}}$ = percent passing corresponding to $1.4 * D_{50}$, where D_{50} is the median particle size. In the PUC equation, it is assumed that the percent embedment of the aggregates is 70%. Figure 4-3 illustrates the steps of determining $P_{0.7D_{50}}$ and $P_{1.4D_{50}}$ from a gradation curve. First, the median particle size (D_{50}) corresponding to 50 percent passing is determined. Then, assuming 70 percent aggregate embedment, the percent passing that corresponds to 70 percent of the median particle size ($P_{0.7D_{50}}$) is determined. Likewise, the percent passing that corresponds to 140 percent of the median particle size ($P_{1.4D_{50}}$) is also determined. The $P_{0.7D_{50}}$ represents the percent of aggregates contributing to the bleeding of chip seals, whereas 100-$P_{1.4D_{50}}$ corresponds to the percent of aggregates contributing to the chip seal aggregate loss (Lee and Kim, 2009).

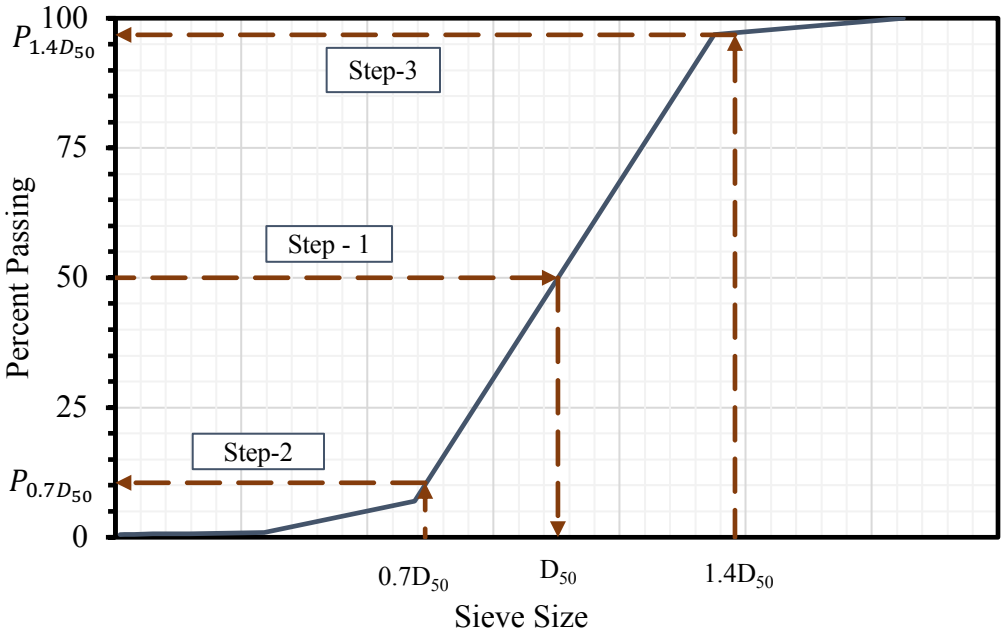

Figure 4-3 Determining chip seal performance indicators from gradation chart.

The calculated C_u and PUC parameters are shown in Table 4-2. The gradation uniformity of the aggregate sources used in this study is ranked in the same order by the two parameters. As the table displays, natural aggregate is ranked as the most uniformly graded aggregate source, followed by slag and Gerkin aggregates.

As indicated previously, chip seal aggregate gradation is among the factors affecting chip seal performance, and it is imperative to select an optimal chip seal aggregate gradation for the desired performance. However, caution should be exercised when interpreting the chip seal performance solely based on the PUC due to the assumptions made in developing the parameter. The PUC was developed based on incorporation of the chip seal design concept by McLeod (Mcleod, 1969) and the concept of C_u (Lee and Kim, 2009).

Table 4-2 Gradation-based Properties for Aggregates

	Slag	Natural	Gerkin
D_{60} (in)	0.29	0.30	0.28
D_{10} (in)	0.15	0.19	0.13
C_u	1.93	1.54	2.17
$P_{0.7D_{50}}$ (%)	15.58	10.12	17.45
$P_{1.4D_{50}}$ (%)	93.81	97.16	93.40
PUC	0.17	0.10	0.19

The McLeod design concept assumes that single chip seals forms one-stone thick aggregate layer and the aggregates lies on their flat side. Moreover, the voids among chip seal aggregates are assumed to be filled by approximately 70 percent of the emulsion residue for a better performance of chip seals. The McLeod procedure also assumes that the aggregates that are embedded less than 50 percent into the emulsion residue are to be expected to dislodge by traffic. In validating the PUC index, Lee and Kim (Lee and Kim, 2009) treated the 70 percent of the voids filled with emulsion residue as a percent embedment of aggregates. The authors postulated that aggregates that are smaller than 70 percent of the median particle size are prone to bleeding of chip seals, and aggregates that are larger than twice $0.7D_{50}$ are likely to result in aggregate loss. *However, in reality, the percent of void filling among aggregate particles does not necessarily translate through one-by-one conversion to the aggregate embedment depth due to the complex interaction in aggregate-binder microstructure (i.e. percent embedment and aggregate orientation). Such interaction is governed by various factors such as aggregate size, shape, and aggregate and binder application rates. One aspect of this phenomenon is presented in Figure 4-4.* The schematic displayed in Figure 4-4(a) is the schematic presented in the work of Lee and Kim (Lee and Kim, 2009)for describing McLeod's chip seal failure criteria. As it can be seen, the chip seal aggregate-binder structure is much idealized and does not account for aggregate spatial distribution and orientation. In this case, the filling of 70 percent of the voids results in 70 percent aggregate embedment. However, depending on the shape of aggregates and their resultant distribution and orientation, the filling of 70 percent of the voids may result in less or more aggregate embedment than 70 percent, as shown in Figure 4-4(b). Additionally, the gradation-based parameters cannot take into account the effects of the rheological characteristics of emulsion residue or the effects of the chemical interaction between aggregate mineralogy and emulsion, which was discovered to be a more significant factor than aggregate gradation in affecting final chip seal performance (Johannes, Mahmoud and Bahia, 2011; Wasiuddin *et al.*, 2013) . Furthermore, the developers of the PUC parameter compared the measured aggregate loss from the MMLS3 testing to that of the calculated aggregate loss from the PUC (Lee and Kim, 2009). It was observed that the measured aggregate loss was smaller than the calculated aggregate loss. As described by the authors, one of the reasons for such an observation was attributed, by the authors, to the potential formation of multistone-thick aggregate layer in a chip seal, which is also not accounted for in the PUC parameter. Lastly, it is not well established that the filling of 70 percent of the voids or 70 percent aggregate embedment depth provides the optimal chip seal performance. As shown later in this report, for example, an aggregate embedment of 70 percent could be a failure point for some chip seals.

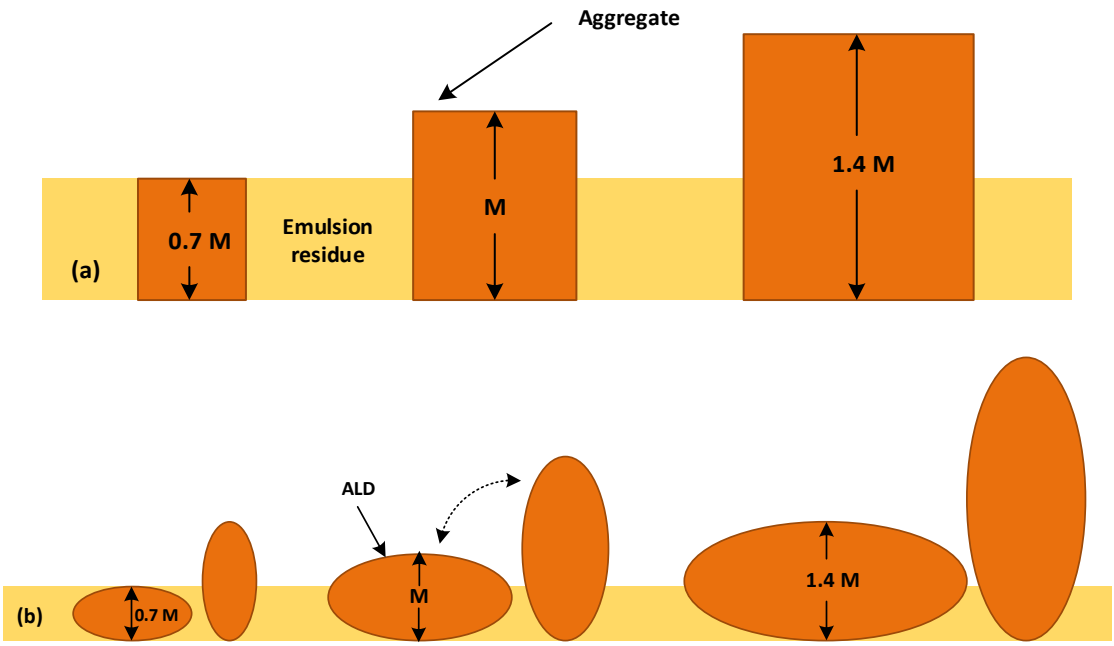

Figure 4-4 Concept of chip failure criteria and the assumptions. Note that M = D_{50}, i.e., the median particle size

Other aggregate properties measured as part of this project are presented in Table 4-3. These properties are used as inputs in chip seal design procedures (e.g. AASHTO PP 82 Standard Practice for Emulsified Asphalt Chip Seal Design). Many, if not all, Departments of Transportation in the US require a limit on the use of flaky aggregates in chip seals because of their detrimental impact on chip seal durability. For example, MDOT specifies a maximum of 15 percent flakiness ratio, measured based on ASTM D 4791.

Table 4-3 Aggregate Properties

Aggregate Property	Test Method	Aggregate Type		
		Slag	Natural	Gerkin
Bulk Specific Gravity	AASHTO T84&85	2.417	2.734	2.678
Voids in Loose Aggregate	ASTM C29	0.46	0.45	0.42
Loose Unit Weight (lbs/ft^3)	ASTM C29	82.9	96.1	97.1
Median Particle Size (in)	McLeod (1969)	0.27	0.28	0.26
Flakiness Ratio (%)	Mn/DOT FLH T 508	3	20	26
Average Least Dimension (in)	McLeod (1969)	0.22	0.2	0.18
Flat and Elongated Ratio	MTM 130	N/A	9	N/A

The limit on flakiness ratio in AASHTO MP 27 Standard Specification for Materials for Emulsified Asphalt Chip Seals is based on traffic levels of a roadway considered for a placement of chip seal. The maximum limits of the flakiness ratio are specified as 35, 30, and 25 percent for traffic levels of less than 500, between 501 and 5000, and greater than 5000 AADT (Annual

Average Daily Traffic), respectively. The procedure used in this project to measure the flakiness ratio was the procedure recommended by AASHTO MP 27. It can be seen from Table 4-3, slag and natural aggregates can be used for traffic levels greater than 5000 AADT, whereby Gerkin aggregates can be utilized in chip seals with a traffic level of up to 5000 AADT, provided that all other aggregate requirements are met for the respective traffic limits, such as abrasion characteristics.

4.1.2 Emulsion and Binder Properties

The emulsions (CRS-2M and CSEA) used in this study were supplied from Michigan Paving and Materials company located in Alma, MI. The binder (PG 70-28) was, obtained from Owens Corning, Inc. The emulsions were received in 5-gallon buckets and split into smaller cans for ease of handling and use in future testing, as shown in Figure 4-5. Residual asphalt content, spray ability and drain-out characteristics of the emulsions were determined as part of this study. Also, rheological properties (i.e., dynamic shear modulus, phase angle, and non-recoverable creep compliance) of the emulsified asphalt residue and the binder were also determined. Residual asphalt content is used as an input parameter in the existing empirical design procedures for chip seals to calculate emulsion application rates, and it is also used for quality control and assurance purposes. For example, many agencies, including MDOT, require at least 65 percent emulsified asphalt residue for an emulsion to be used in construction of chip seals. Sprayability is defined as the ability of an emulsion to be sprayed in a uniform thickness over the surface of an existing pavement, and drainout is the ability of an emulsion to resist draining off the pavement surface due to gravity (Rizzutto *et al.*, 2015; Kim *et al.*, 2017). An emulsion without a proper spray ability and drain-out characteristics will cause early chip seal failures such as streaking and aggregate loss (Johannes, Johannes and Bahia, 2013). Evaluating spray ability and drain-out characteristics of emulsions were recently recommended as specifications in NCHRP Report No.837 (Kim *et al.*, 2017). The rheological properties of emulsified asphalt residue and binders are one of the key factors for a sound chip seal design and long-term performance of such treatments. Improper selection of an emulsion will result in severe chip seal distress such as aggregate loss and bleeding. This fact was clearly highlighted by the results of NCHRP Report No.837 in which specifications based on rheological properties of emulsified asphaltic binders were recommended against critical chip seals distresses (bleeding and low-temperature aggregate loss).

Residual asphalt contents of the each emulsion used in this study were determined in accordance with ASTM D6943 (ASTM-D6943, 2015) Procedure A. The residual contents of CRS-2M and CSEA were found to be 69.1 and 69.5 percent by the weight of emulsion, respectively. The maximum coefficient of variation observed between the replicate measurements for each emulsion did not exceed 1.4 percent. The test results indicated that both emulsions had higher emulsion residue content than 65 percent, a minimum content for an emulsion to be used in chip seal projects per MDOT and AASHTO M 316 specifications.

The viscosity of each emulsion was measured following the procedure outlined in NCHRP Report No. 837 to determine sprayability and drainout characteristics of the emulsions. The viscosity test, also known as the three-step shear test, is conducted by varying a shear rate in three-steps in a rotational viscometer at a specified temperature. In the first step, emulsion is subjected to a shear rate of 4.65 s^{-1} (5 RPM) for 15 minutes, followed by testing at a shear rate of 142 s^{-1} (150 RPM) for 5 minutes. Then, the shear rate is changed back to 4.65 s^{-1} (5 RPM) and the test is

run for 5 minutes for this third step. The test is performed without any rest periods between the steps. As shown in Figure 4-6, the first step of the test represents the pumping and handling conditions of the emulsion until spraying. No limits were specified in the NCHRP report for this step. The second step is assumed to mimic the spraying of emulsions through a nozzle. A maximum limit of 400 centipoise was specified for this part of the testing in the NCHRP report. The final step in the test simulates the emulsion resistance characteristics to flow off under gravitational forces once it is placed in the field. For this step, a minimum limit of 50 centipoise was specified in the NCHRP report. The emulsions utilized in this study were tested at a temperature of 60°C. The test results are plotted in Figure 4-7. It is seen that the emulsions fall within the limits presented in the NCHRP report. This indicates that, from a material quality standpoint, both emulsions should not result in non-uniform spraying during the construction and flow off once placed in the field.

Figure 4-5 Image showing emulsions split and stored into small containers for further testing.

Past research shows various efforts toward linking the contribution of rheological properties of emulsified asphalt residue to chip seal distresses, especially bleeding and aggregate loss (Miller, Arega and Bahia, 2010; Islam and Hossain, 2011; Shuler, 2011; Kim *et al.*, 2017) The study presented in NCHRP Report No.837 explored such potential in an effort to establish performance-based specifications for emulsions used in chip seals and other surface treatments. The study proposed two testing schemes conducted on emulsified asphalt residue for evaluating the contribution of emulsions to the bleeding and aggregate loss of chip seals at high and low-temperatures, respectively. The multiple stress creep and recovery (MSCR) test, as outlined in AASHTO T 350, was recommended for assessing the bleeding potential of chip seals. Performance limits considering traffic levels were established based on the non-recoverable creep compliance (Jnr) value obtained at a stress level of 3.2 kPa at a temperature of interest. Likewise, the dynamic shear rheometer (DSR) frequency sweep test was proposed to evaluate the low-temperature aggregate loss resistance of chip seals. Performance limits incorporating traffic levels were also selected based on the dynamic shear modulus at a critical phase angle, which is specified as a function of the climate condition under which the emulsion is placed. The aforementioned two tests were utilized to evaluate the properties of the residue of the emulsions and the binder used in this study. The residue of emulsions was recovered for testing using AASHTO R 78 Method B.

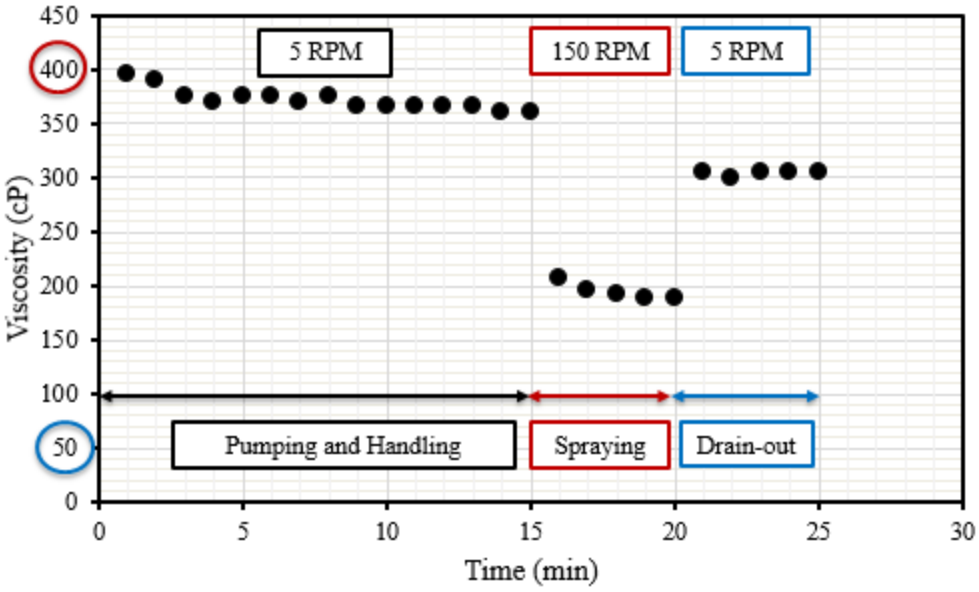

Figure 4-6 Steps of emulsion viscosity testing using rotational viscometer.

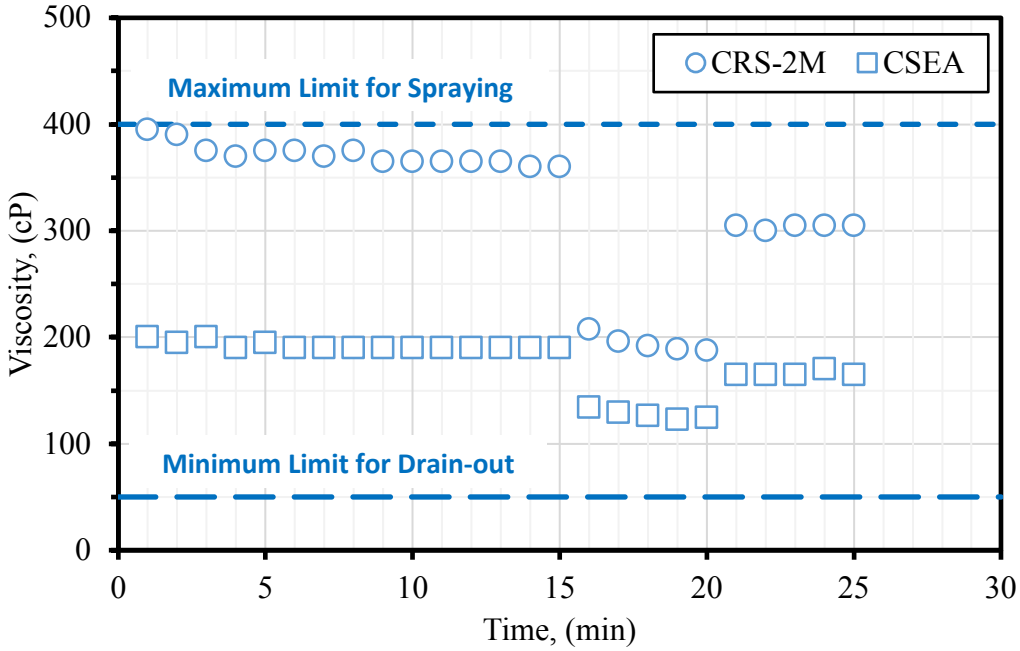

Figure 4-7 Three-step viscosity testing of the emulsions.

The MSCR test is conducted at two stress levels (i.e. 0.1 and 3.2 kPa) to determine the non-recoverable creep compliance (Jnr) and elastic recovery of asphaltic binders. However, the Jnr value obtained at a stress level of 3.2 kPa is used for assessing the bleeding potential of chip seals. The higher magnitude of the Jnr value at a given temperature is indication of a higher bleeding potential of chip seals, provided that all other chip seal design characteristics are maintained the same. The MSCR testing of the residue of the emulsions and the binder used in this study was conducted at two temperatures: 54 and 61°C. The test temperature of 54°C was the temperature at which the chip seal bleeding tests were performed in this study. The test temperature of 61°C was

included in the testing campaign for informational purposes only as it corresponds to a high-temperature emulsion performance grade for Michigan (for the lower peninsula), as mapped in NCHRP Report no. 837. The MSCR test results at the two test temperatures are plotted in Figure 4-8 for the emulsions and the binder used in this study. The whisker bars in the figure indicate one standard deviation around the mean. The test results show that, for a given location (temperature), a chip seal application with CSEA emulsion is expected to outperform the performance of a chip seal application with CRS-2M emulsion, assuming the change in chemistry of the emulsions does not have an impact on the performance. However, the extent of which the Jnr differs for the two emulsions in this research may not result in considerable differences in chip seal performance. This is also evident from close inspection of the data presented in NCHRP Report No. 837, where such close values of the Jnr did not show any differences in terms of chip seal bleeding susceptibility. Even though the Jnr value of the binder is higher than those of the emulsions, suggesting a higher potential for bleeding, a direct performance comparison between hot-applied and emulsion-based chip seals should be avoided. This is because other factors may contribute to the final performance of chip seals. Such factors include, but are not limited to, potential differences in aggregate-binder and aggregate-emulsion microstructures and chemistry of binder and emulsified binder and their resultant effect on the adhesive behavior between the two components (i.e. aggregate and binder).

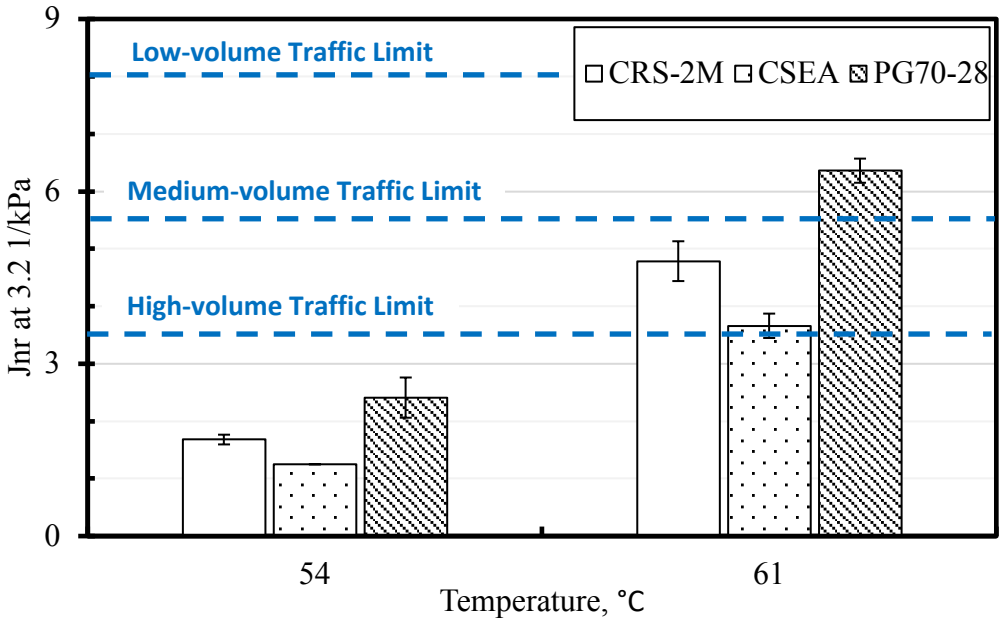

Figure 4-8 Non-recoverable creep compliance (J_{nr}) of the emulsions and the binder.

Three traffic classes according to average annual daily traffic (AADT) volume are specified in NCHRP Report No. 837 for chip seal applications. AADT of less than 500, between 501 and 2500, and greater than 5000 vehicles are defined as a limit for low, medium, and high-volume traffic, respectively. Figure 4-8 also shows the Jnr limits for low, medium, and high-volume traffics. Based on these classifications, both emulsions are suitable to be placed on a roadway subject to high-traffic volume when the maximum pavement surface temperature is no more than 54°C. Similarly, the emulsions can be placed on a roadway subjected to medium-traffic volume when the maximum pavement surface temperature is no more than 61°C, as can be seen

from the figure. Since these classifications were established for emulsion-based chip seals, the traffic-based limits may not be applicable to hot-applied chip seals.

The results from NCHRP Report No.837 indicated that the low-temperature chip seal aggregate loss correlated with the dynamic shear modulus (G*) at a critical phase angle (δc). The higher magnitude of the G* value at a given δc is indication of a higher aggregate loss potential of chip seals, given that all other chip seal design characteristics are kept the same. In NCHRP Report No. 837, the δc values are specified as a function of the low-temperature performance grade of a climatic region of interest. For example, the minimum pavement surface temperature for Lansing, MI corresponds to -25°C, and the δc for this temperature, per NCHRP Report No. 837, is specified as 45°.

The illustration of determining the G* at δc is presented in Figure 4-9. First, after constructing G* and δ master curves through implementing time-temperature superposition, the reduced frequency that corresponds to δc is determined. Secondly, the G* at that reduced frequency is determined, and it is used for assessing the aggregate loss potential of chip seals. The G* and δ values of the emulsified asphalt residues and the binder used in this study were determined at temperatures of 5, 15, and 30°C covering frequency range from 1 to 100 rad/s. The DSR test was conducted according to AASHTO T 315. The maximum coefficient of variation found between replicate samples in the DSR testing of the materials was 7.3 and 1.48 percent for the values of G* and δ, respectively. The G* master curve was developed using Christensen-Anderson-Marasteanu (CAM) model (Marasteanu and Anderson, 1999) at a reference temperature of 15°C. Then, the optimized fitting parameters in the G* master curve were used to develop the δ master curve. The resultant master curves for each material are presented in Figure 4-10 through Figure 4-12.

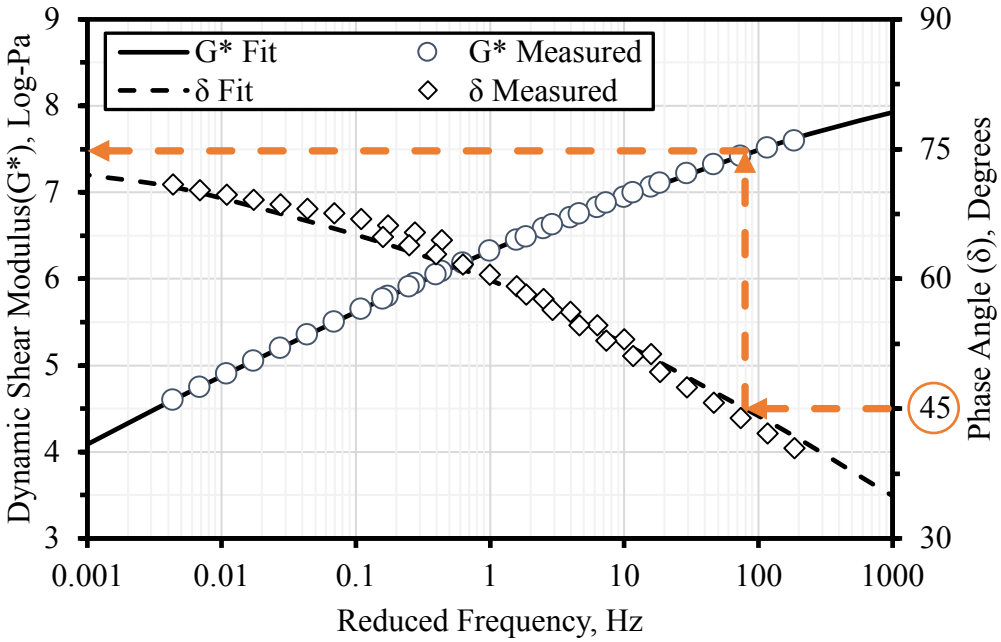

Figure 4-9 Determining dynamic shear modulus at the critical phase angle.

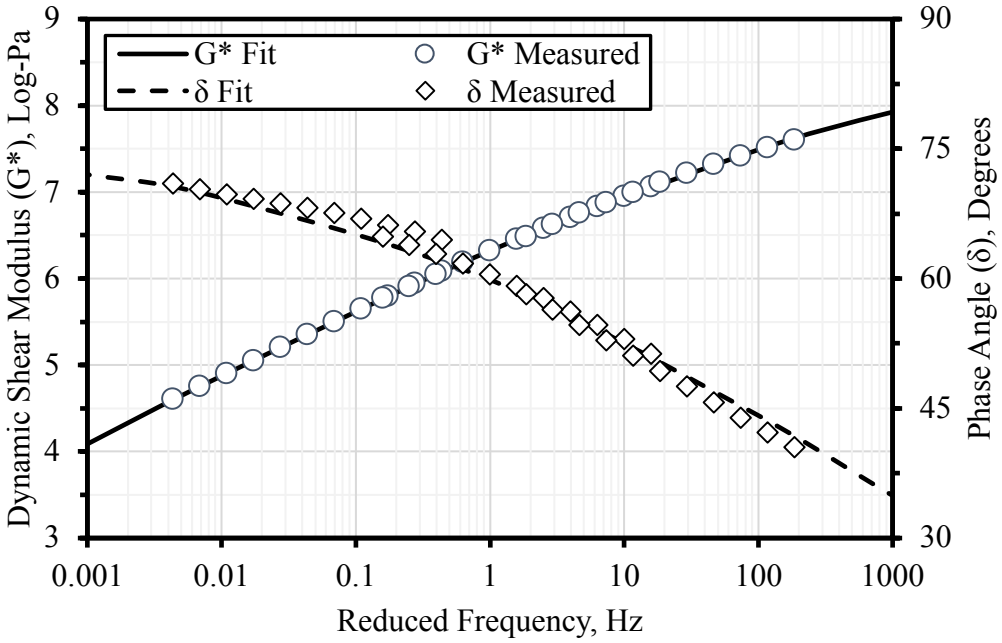

Figure 4-10 Dynamic shear modulus and phase angle master curves for CRS-2M residue.

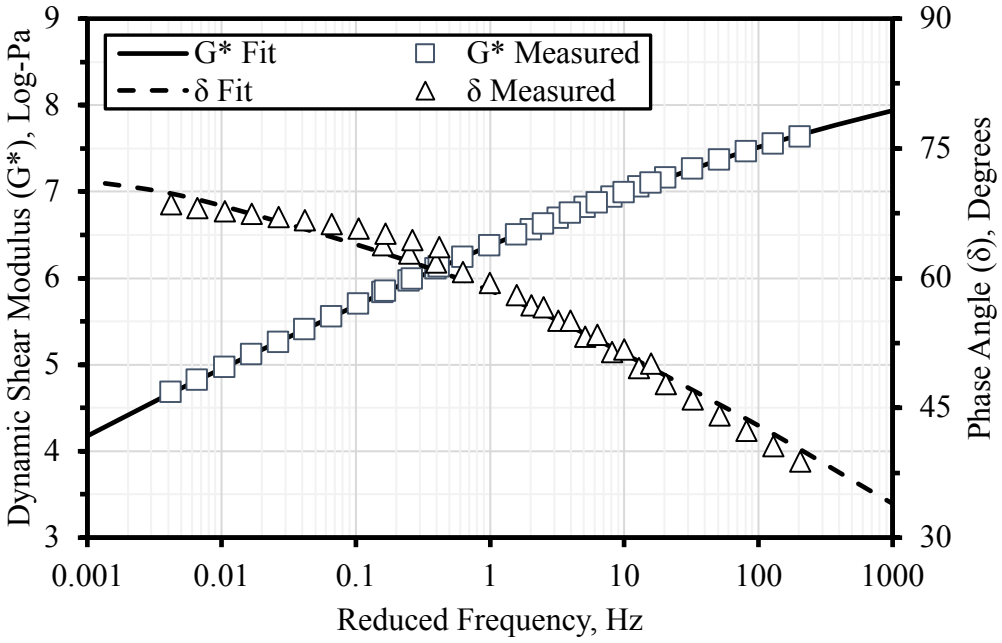

Figure 4-11 Dynamic shear modulus and phase angle master curves for CSEA residue.

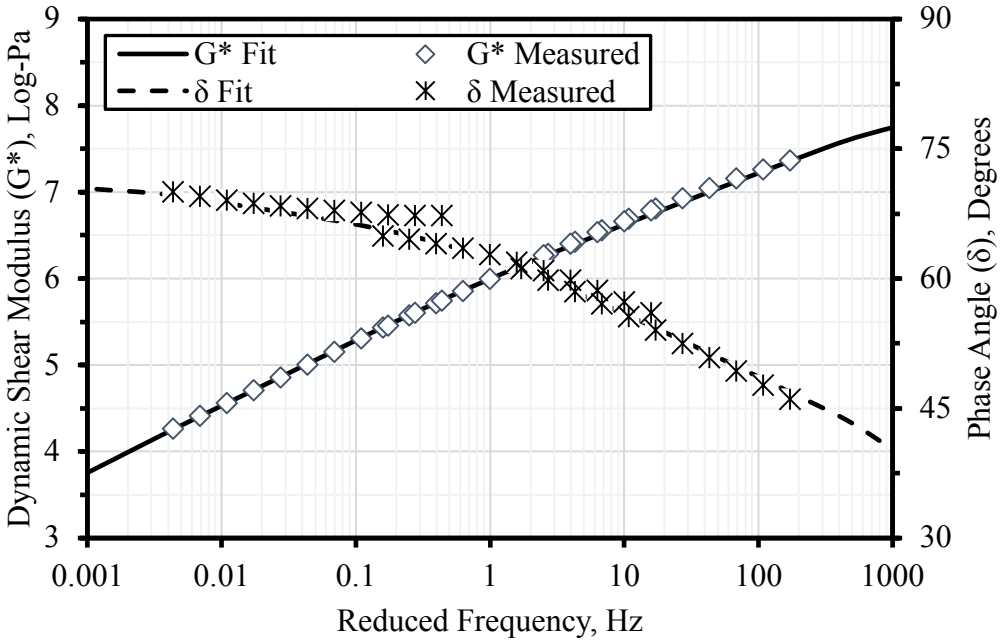

Figure 4-12 Dynamic shear modulus and phase angle master curves for PG 70-28 binder.

As indicated previously, the δc corresponding to the emulsion performance-grade climate of Lansing, MI is 45°. The corresponding G* values at the δc of 45° were 27.3, 24.6, and 31.8 MPa for CRS-2M, CSEA, and PG 70-28 binder, respectively. Based on the test results, for a given location (temperature), a chip seal application with CSEA emulsion is expected to perform better than a chip seal application with CRS-2M emulsion in terms of the aggregate loss susceptibility. Like the discussion on the Jnr values of the two emulsions, the susceptibility of chip seals to aggregate loss may not be different for the two emulsions used in this research due to the extent of the variations of the relevant data in NCHRP Report No. 837. Based on the comparative analysis of G*, the hot-applied chip seal application with PG70-28 binder is expected to perform the worst, but, again, the differences in the 'mixture' performance behavior of different kinds (i.e., emulsion or hot-applied) of chip seals may render such conclusion meaningless.

The limits of the G* at the δc for low, medium, and high-volume traffics specified in NCHRP Report No. 837 are 30, 20, and 12 MPa, respectively. Based on these classifications, both emulsions are suitable to be placed on a roadway subject to low-traffic volume in Lansing, MI. The binder is not suitable to be placed for chip seals in Lansing, MI based on the NCHRP Report No.837 criteria. Once again, such conclusion is possibly invalid as the limits were derived for the emulsion-based chip seals.

Although the rheological properties of the residue of the emulsions used in this study were analyzed with respect to the proposed specifications in NCHRP Report No. 837, it is very important to note that caution should be exercised with the use of the specifications. This is due to the face that in developing the specifications, the chip seal mixture specimens were prepared with different types of emulsions using a single source of aggregate, single aggregate and emulsion application rates, and single embedment depth, the extent of which was not stated in the report. Since a change in any of these factors can affect the performance of chip seals to a considerable

extent, an emulsion selected based on such limits may, in some instances, result in premature chip seal failures.

4.2 Experimental Design and Sample Preparation

The preliminary experimental design included various emulsion types and emulsion application rates (EARs) to study the effect of the percent embedment on aggregate loss and bleeding distresses for different types of aggregates. Consequently, it was proposed to include two most commonly used aggregates and emulsions throughout the state of Michigan for testing under this research. Additionally, investigating the effect of aggregate size (gradation) on the limits of the percent embedment was recommended. The suggested method of studying the effect of aggregate size was to have one of the two aggregate sources fractioned into fine and coarse gradation, the distinction for the gradation were to be made based on the sieve # ¼", thereby, creating an additional variable in the experimental design. However, based on the particle size distribution of the aggregates used as well as MDOT restriction limits on aggregate gradation, it was observed that such fractionation would not result in significant distinction between the targeted gradations (fine and coarse). Hence, the research team did not pursue that objective any further but did include another source of aggregate and binder into the experimental program.

Aggregate application rate (AAR) used in this study was limited to a single AAR (i.e. 20 lb/yd^2—MDOT's minimum aggregate application rate) for each of the unique combination that were generated from Table 4-4. As clarified in the preceding section, the scope of this research included the two most commonly used emulsions in the state of Michigan, and three different EARs or binder application rates (BARs) for a given combination of aggregate type, AAR, and emulsion type. The selected EARs or BARs for this study were 0.39, 0.42, and 0.46 gal/yd^2, representing MDOT's low, medium, and high limit of application rates, respectively. Table 4-5 details the experimental test program carried out in this research. Additionally, one of the objectives to be accomplished under this task (Task 2) was to evaluate whether there is an effect of chip seal substrate properties on the performance of chip seals. For this purpose, field cores provided by MDOT from a road section were also included in the testing program. Therefore, in total, 16 unique samples were included in the final sample preparation program, as shown in Table 4-4.

Table 4-4 Final Sample Preparation Matrix

Test Combination	Slag	Natural	Gerkin
Number of Aggregate Gradations	1	1	1
Number of Aggregate Application Rates	1	1	1
Number of Emulsion or Binder Types	2	2	1
Number of Emulsion or Binder Application Rates	3	3	3
Number of Laboratory-produced Samples	6	6	3
Field Cores	1		
Total Number of Unique Samples	16		

Table 4-5 Experimental Test Program

Aggregate Type	Emulsion/ Binder Type	EAR/BAR (gal/yd^2)	Abrasion Test	Bleeding Test	2D Image Analysis*	3D Image Analysis**
Slag (20 lb/yd^2)	CRS-2M	0.39	√	√	√	√
		0.42	√	√	√	√
		0.46	√	√	√	√
	CSEA	0.39	√	√	√	√
		0.42	√	√	√	√
		0.46	√	√	√	√
Natural (20 lb/yd^2)	CRS-2M	0.39	√	√	√	√
		0.42	√	√	√	√
		0.46	√	√	√	√
	CSEA	0.39	√	√	√	√
		0.42	√	√	√	√
		0.46	√	√	√	√
Gerkin (18 lb/yd^2)	PG70-28	0.25	√	√	√	-
		0.30	√	√	√	-
		0.35	√	√	√	-
		0.40	-	√	√	-

** Percent embedment, aggregate orientation and percent bleeding area ** Mean Profile Depth*

In this research, chip seal components (emulsion/binder and aggregates) were placed and seated on asphalt concrete substrates with a diameter of 150-mm and a height of 55-mm. The procedure described in a previous MDOT project (OR15-508) was followed in applying the emulsion/binder and aggregates on the substrates, with an exception to the binder and aggregate application temperatures in the case of the hot-applied chip seal specimens. The application temperatures for those specimens were 175 and 45°C for the binder and aggregate, respectively. Following the application of the chip seal components, the specimens first underwent the compaction process using a hand-kneading compactor, as specified in ASTM D 7000, for three half cycles in one direction and three half cycles in a perpendicular direction. Then, the specimens were further compacted by a servo-hydraulic Material Testing System (MTS) to simulate the cyclic pressure in the field. The pressure level used in the Superpave Gyratory Compactor (i.e., 600kPa) was exerted on the specimens in a cyclic haversine mode at a frequency of 0.1 Hz for 25 cycles. Once the compaction process was done, the specimens were conditioned at 35°C for 24 hours in an environmental chamber prior to further processing for each of the tests performed in this research. Figure 4-13 illustrates several steps of chip seal fabrication for exemplary purposes.

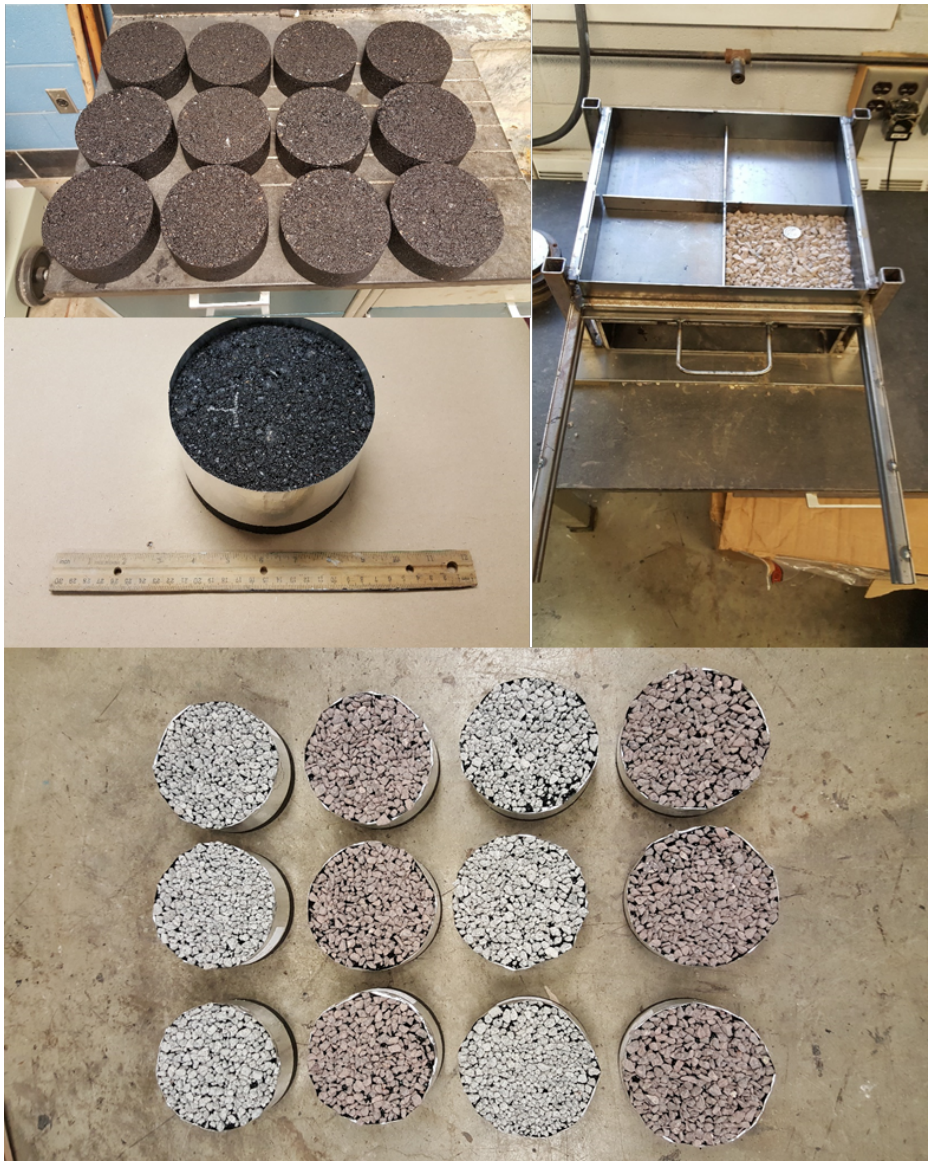

Figure 4-13 Several steps of chip seal specimen fabrication

4.3 Performance Testing

As reflected in Chapter 2 and repeatedly emphasized throughout this report, the most common distresses for a single-layer chip seal application are aggregate loss and bleeding. Hence, the research team performed bleeding susceptibility and aggregate loss tests on the chip seal samples fabricated for this study to quantify the percent embedment limits of chip seals. Chapter 2 also provided insights into emerging testing methods and equipment available for evaluating performance of chip seals in the laboratory and its relation to the field performance. A review of literature indicated that several test procedures utilizing laboratory wheel tracking devices have been developed to evaluate performance of chip seals, particularly in relation with aggregate loss, bleeding, and rutting (for multiple layer chip seals) distresses. For this research study, the equipment of choice for evaluating chip seal performance in the laboratory was a Hamburg Wheel

Tracking (HWT) device. The choice of the HWT device over any other available testing devices was due to the potential shortcomings of those devices in various aspects of testing and evaluation. The limitations of those devices include, but are not limited to, high equipment cost, feasibility issues with equipment setup, inefficiency of testing conditions, and inability to discern the expected performance among chip seals due to the nature of the applied load. Additionally, the HWT device was preferred because one of the sought scopes of this research was to quantify the aggregate loss of chip seals caused by braking/acceleration, which can be simulated by the HWT device (through modification). Additionally, the HWT device is now readily available in laboratories of many agencies as it has been widely used throughout the US to evaluate the potential rutting and moisture resistance of hot/warm mix asphalt mixtures. The information compiled by Larrain (Mendez Larrain, 2015), as shown in Table 4-6, highlights this fact. As it can be seen from the table that many Departments of Transportation in the United States now require this test as part of their mixture design specifications. Hence, the research team performed bleeding susceptibility and aggregate loss tests on chip seal samples using a modified version of Hamburg Wheel Tracking (HWT) device. Table 4-7 presents the final experiment design and testing conditions for the performance testing that were performed. The details for modifying the HWT device and each of the tests are described in the following sub-sections.

4.3.1 Modifying the Hamburg Wheel Tracking Device and Test Conditions for Chip Seal Performance Evaluation

The Hamburg Wheel Tracking (HWT) device (Figure 4-14(a)) is used to determine the susceptibility of a compacted asphalt concrete specimen to permanent deformation and moisture damage using a reciprocating steel wheel. The specimen submerged under hot water is loaded with a steel wheel at a rate of about 52 passes per minute. The load on the wheel is 158 lbs. The test method outlined in AASHTO T 324 describes a procedure for testing asphalt concrete specimens in the HWT device.

Prior to performing any tests, the research team worked on investigating the appropriate test conditions for evaluating chip seals using the HWT device. This was necessary as there is currently no standard test procedure established for testing of chip seals using the HWT device. Since the objective of quantifying the aggregate loss of chip seals caused by braking/acceleration was part of the research, the research team also investigated the fixed wheel test condition as well. For that reason, the evaluations of the test conditions were undertaken with consideration of chip seal raveling distress.

Test conditions included evaluating efficiency of steel and rubber wheels, test temperature, number of loading cycles, and wheel speed and load on abrasion of chip seals. Initial trial test results indicated that the use of a steel wheel, high-temperature testing (i.e., above 25°C), high number of loading cycles, and slow wheel speed were either too harsh test conditions to evaluate the raveling or did not show any raveling distresses on the specimens. Hence, the research team decided to modify the HWT device wherein the steel wheel was replaced with a rubber wheel, and the rubber wheel was fixed, as it was not allowed to roll while abrading. The installed rubber wheel had a tire pressure of 34 psi, and the load on the wheel was reduced to 125 lbs., which corresponds to the weight of a loaded wheel track used for assessing bleeding of micro surfacing mixtures, as described under ASTM D 6372 standard. The modified version of the HWT device is shown in Figure 4-14(b). Initial trials with the fixed rubber wheel in a dry condition at a room temperature

revealed promising results. Additionally, the visual observation of trial specimens revealed that the raveling of chip seals with the fixed rubber wheel was complete after several abrasion cycles under the HWT device at a frequency of rotation of 25 revolutions per minute (rpm). Thus, there were no more aggregates dislodged after a few cycles of abrasion. It was observed that, in general, a total of 10 HWT cycles were found to be effective enough to evaluate the raveling distress at a room temperature. It must be noted that a cycle under the HWT device corresponds to one pass in a forward direction and another pass in a backward direction, thus totaling to two passes per a cycle. The final selected HWT configurations and test conditions are described in the following sections.

Table 4-6 HWTD test conditions and limits used by DOTs (Larrin 2015)

Department of Transportation	PG grade	Number of Wheel Passes	Test Temperature (°C)	Maximum Rut Depth (mm)
California	PG58-XX	10,000	50	12.7
	PG64-XX		55	
	PG70 and higher		60	
Colorado	PG58-XX	10,000	46	4
	PG64-XX		50	
	PG70-XX		55	
	PG76-XX		60	
Illinois	PG58-XX	5,000	50	12.5
	PG64-XX	7,500		
	PG70-XX	15,000		
	PG76-XX	20,000		
Iowa	PG58-XX	20,000	50	N/A
	PG64-XX			
	PG70-XX			
Kansas	N/A	10,000	50	12.5
Louisiana	PG70-22(level 1)	20,000	50	10
	PG76-22(level 1)			6
Montana	PG58-28	Plant mix: 10,000 Mix design: 15,000	44	13
	PG64-XX		50	
	PG70-28		56	
Oklahoma	PG64-XX	10,000	50	12.5
	PG70-XX	15,000		
	PG76-XX	20,000		
Texas	PG64-XX	10,000	50	12.5
	PG70-XX	15,000		
	PG76-XX	20,000		
Utah	PG58-XX	20000	46	10
	PG64-XX		50	
	PG70-XX		54	
Level 1: Low traffic, Average Daily Traffic (ADT)<7000 Level 2: High Traffic, (ADT) >7000				

Table 4-7 Experiment design for chip seal performance testing

Test	Test Temperature, °C	Specimen Conditioning	Parameter of Interest	Number of Replicates
Hamburg Wheel Tracking (HWT)	54	Wet	Bleeding	2
	19	Dry	Aggregate loss	2

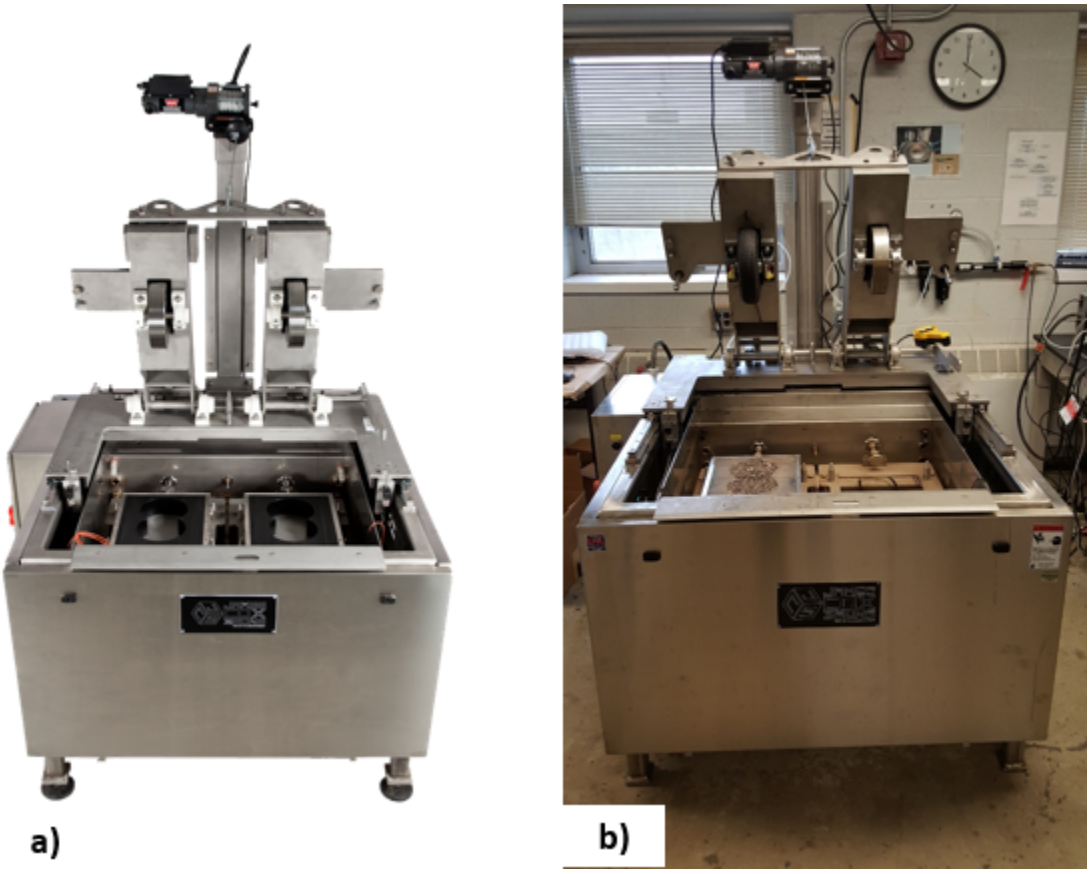

Figure 4-14 HWT device a) before modification (image from Jamescoxandsons.com) and b) after modification.

4.3.2 The HWT Device Testing for Bleeding Susceptibility

Trial tests were continued to determine number of the HWT cycles to be applied and a suitable test temperature to assess the bleeding performance of chip seals under HWT device. The use of a rubber wheel (free to roll) and the load defined above (i.e., about 125 lbs.) are maintained for the consistency purposes. The number of HWT cycles to be applied on chip seal samples was established based on the review of USDOT specifications on the HWT device and engineering judgment of the research team. Close inspection of Table 4-6 reveals that the number of HWT cycles ranges from 5000 to 20000 cycles, depending on the state and performance grade of binder being used. For example, Illinois DOT procedure calls for 5000 cycles for asphalt concrete mixtures with a high-performance grade of 58. Overall, if the average number of HWT cycles is assumed to be 10000 for evaluating asphalt concrete mixtures (considering low-volume roads) and a typical HMA pavement is designed to last 20 years, given that a typical chip seal is designed to

last about 5 years, the number of cycles in HWT should be about 1/4th of 10000, which is 2500. Hence, the number of HWT cycles to be used in chip seal bleeding assessment was selected to be 2500. Additionally, the HWT tests for the bleeding susceptibility were decided to be performed under a wet condition. A submerged/wet testing condition makes it easier to keep the test temperature constant and minimizes the potential temperature increase resulting from friction between the wheel and chip seal surface.

The test temperature at which the bleeding test to be performed was initially selected as 61°C. This selection was based on the average seven-day maximum pavement surface temperature in Lansing, MI, as recommended by NCHRP project 9-50. However, initial test results showed that the rubber wheel in the HWT device started picking-up aggregates. This was due to the fact that the binder was excessively soft at this temperature, as it was rising to the surface and sticking to the tire. Once the binder sticks to the tire, the tire lifts the aggregates attached to the binder. This can be considered as 'bleeding' or 'flow' failure. Such phenomenon can be observed in the field when excessive bleeding occurs. After consultation with the research advisory panel (RAP), it was decided to reduce the test temperature based on the interpretation of the surface temperature profile of Michigan roads which was collected from 2013 to 2015. Upon reviewing the data, the research team first selected 54°C as the HWT bleeding test temperature, which was based on 97th percentile of statewide average cumulative temperature distribution. An example of the temperature data is presented in Figure 4-15 for University region. After numerous trial tests, the aggregate picking-up was still observed at this test temperature (54°C) for some of the chip seal samples, especially towards end of HWT cycling.

It is important to note that the problem of 'aggregate pick-up' is not a failure of the testing condition, it is the failure of the specimen. This phenomenon is analogous to the tertiary flow in asphalt mixture rutting tests. During the rutting tests on asphalt mixtures, the sample first goes into an initial densification, followed by a steady plastic deformation. After certain number of cycles, the phenomenon of 'tertiary flow' occurs, where the rate of change of plastic flow increases, causing the asphalt mixture to 'flow' and fail quickly. Similarly, in chip seal bleeding test, at certain levels of binder application rates, the binder slowly comes to the surface, increasing the bleeding area. However, at some binder application rate, the binder is simply excessive and quickly rises to the surface (due to readjustment of the aggregates), sticking to the tire and causing the 'aggregate-pickup' phenomenon. For example, in Figure 4-16,emulsion application rates (EARs) of 0.39 and 0.42 gal/yd^2 did not cause 'tertiary flow' at the end of 2500 cycles of HWT loading for chip seal specimens with Slag and CRS-2M emulsion. However, at the EAR of 0.46 gal/yd^2, the emulsion residue was simply too excessive, and the tertiary flow phenomenon occurred. Therefore, the point at which the tertiary flow (which leads to aggregate pickup) phenomenon is observed can be used as the threshold of true failure of the chip seal with respect to bleeding. Further review of the literature on this specific subject revealed that aggregate pick up in the field can happen when the mean texture depth of chip seal is below 1.5 mm, and with the viscosity of emulsion is being less than 200 Pa.s. (TNZ report, 2005). Additionally, a study performed for the assessment of the bleeding potential of multilayer chip seals through accelerated testing reported that aggregate pick-up phenomenon occurred for a relatively high number of traffic cycling at a high test temperature (Lee and Kim, 2010). Although an aggregate pickup issue was not reported in the study, another study by Lee and Kim (Lee and Kim, 2008) ascertained that, the percent bleeding area of chip seal specimens prepared at various emulsion and aggregate application rates ranged from as low as 30 percent to as high as 90 percent.

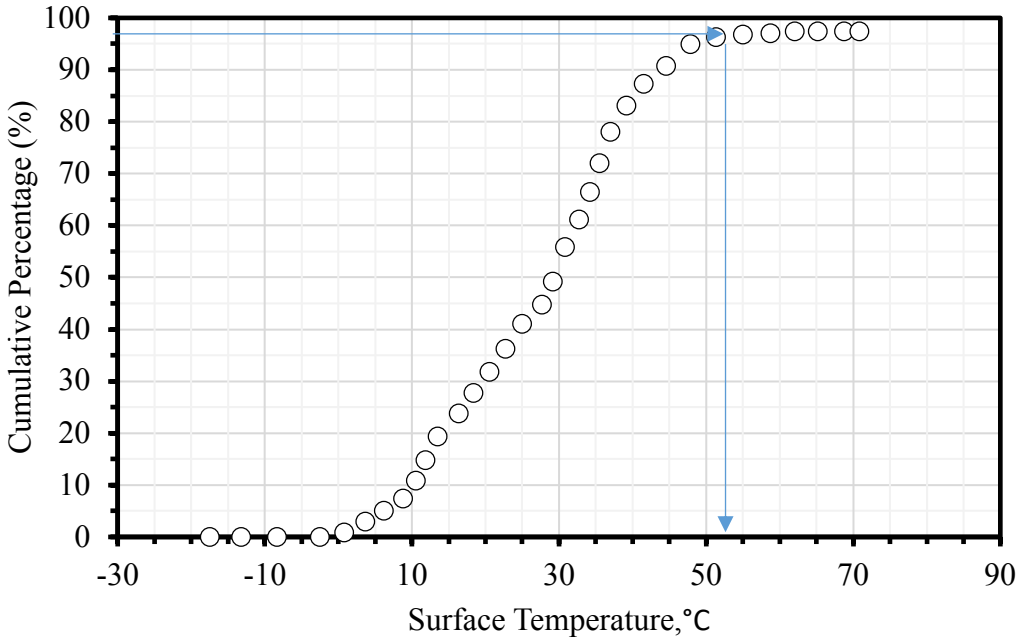

Figure 4-15 Cumulative surface temperature distribution for University region.

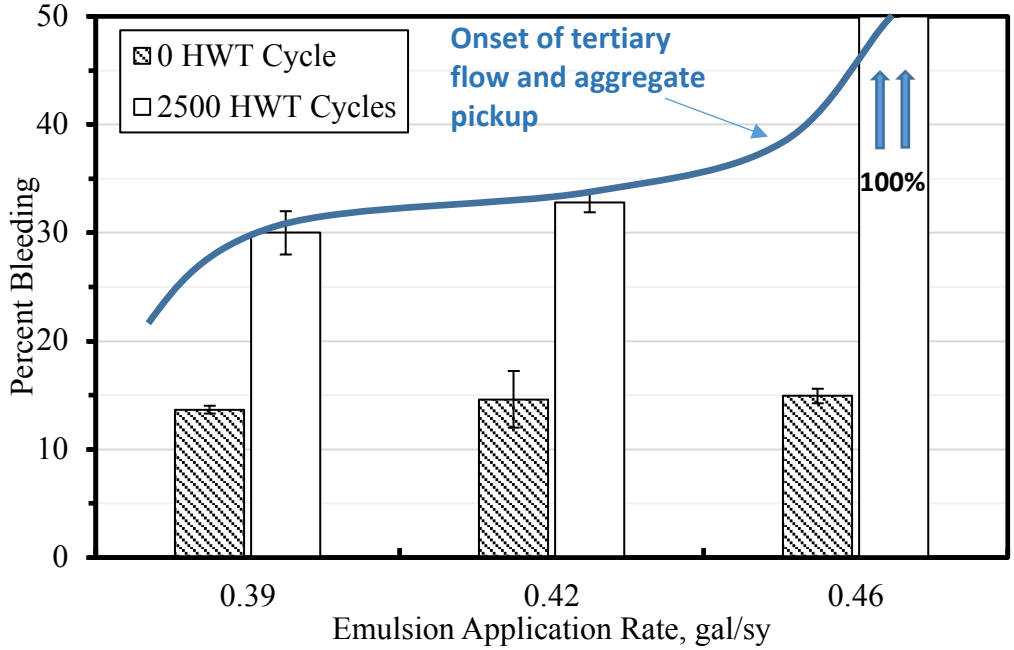

Figure 4-16 Percent bleeding area as a function of EAR for chip seal specimens with slag and CRS-2M emulsion.

One of the significant observations from that study was that the magnitude of the percent bleeding area was clustered at approximately 40 and 80 percent for the chip seal specimens, and there was no trend when transitioning from one application rate to another for a given EAR or AAR. For example, the increase in the magnitude of the bleeding area from 40 percent to 80 percent occurred suddenly when the EAR was gradually increased for a given AAR or vice versa. It is also worth mentioning that the research team tried the steel wheel to remediate the problem, but the slag aggregates were crashed down under such loading condition. Hence, the use of the steel wheel was not pursued any further. Subsequently, the research team selected 40°C as the test temperature, which was roughly the maximum average surface temperature in Michigan, as shown in the data in Table 4-8 provided by MDOT.

Table 4-8 Average surface temperature distribution for Michigan

Regions	Surface Temperature, °C
Bay	34.6
Grand	27.6
Metro	38.3
North	23.9
Southwest	39.6
Superior	19.2
University	27.1
Maximum	**39.6**

The bleeding test performed at 40°C using chip seal specimens with slag and natural aggregates at three emulsion application rates (0.39, 0.42, and 0.46 gal/yd^2) did not lead to the problem of 'aggregate pick-up' by the rubber wheel. When the research team performed the bleeding tests at 40°C, it was observed that the test was able to capture the expected trend of bleeding with respect to an increase in trafficking (i.e. HWT cycling) as well as across the variation of the emulsion application rates. The test results for these sets are presented in Figure 4-17 and Figure 4-18 for the chip seal specimens fabricated with slag and natural aggregates, using CRS-2M emulsion, respectively. However, as it can be seen from the figures, the magnitude of chip seal bleeding was not to the extent that the research team could have marked any chip seal sample as a failure. For that reason, the research team decided on the test temperature of 54°C and performed each of the bleeding tests at that temperature. Meanwhile, the HWT wheel and its threads were extensively cleaned at every interval of the HWT device trafficking (i.e. 0, 200, 300, 500, and 1500 cycles) to minimize the tire pick-up due to the stickiness of the tire. It was observed that the pick-up reduced with some instances of cleaning happening at the final interval of the HWTD trafficking (i.e. last cycle of 1500).

Because of the test results, the following configurations were used for evaluating the bleeding distress;

(i) The HWT device with a rubber wheel with a tire pressure of 34 psi and a load of 125 lbs. used,
(ii) The test temperature was selected as 54°C,
(iii) The bleeding test was performed under a wet condition,

(iv) The total number of the HWT cycles was 2500.

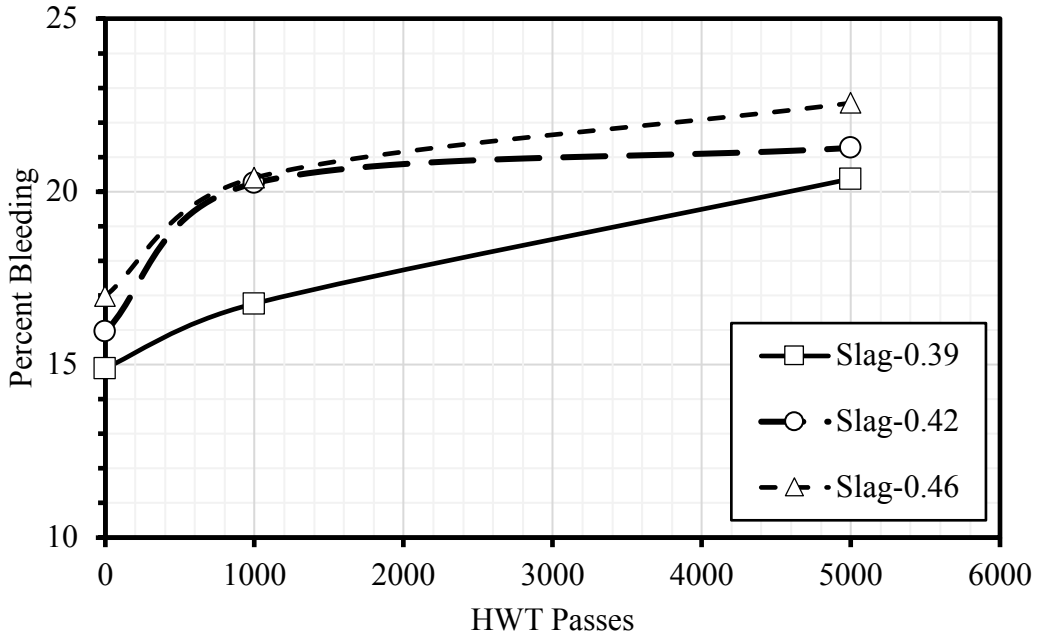

Figure 4-17 Percent bleeding area as a function of HWT passes and EAR for slag and CRS-2M emulsion tested at 40°C.

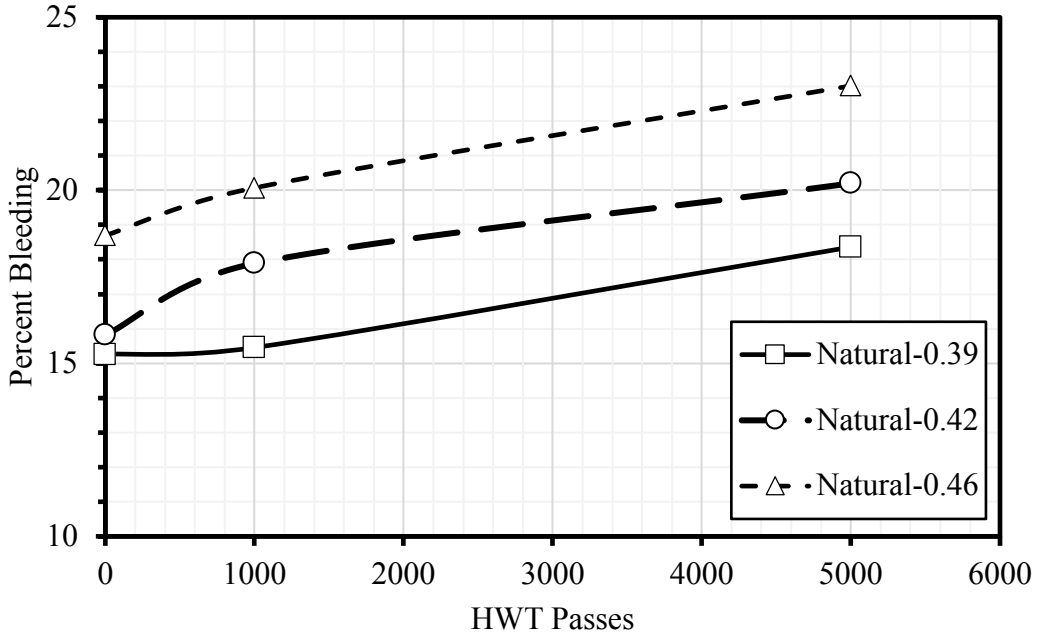

Figure 4-18 Percent bleeding area as a function of HWT passes and EAR for natural aggregate and CRS-2M emulsion tested at 40°C.

4.3.3 The HWT Device Testing for Aggregate Loss Susceptibility

Since the initial trials of the HWT device as described in Section 4.3.1 were performed for an effort to characterize the chip seal aggregate loss, the same configurations were utilized to quantify the chip seal aggregate loss in this research, but at a lower test temperature. To obtain the test temperature, the Enhanced Integrated Climatic Model (EICM) implemented in the AASHTOWare Pavement ME Design software was utilized to predict the temperatures 6 mm below the surface of a pavement. First, a Pavement ME run was performed on a typical asphalt pavement structure composed of a 4" asphalt concrete layer, followed by a 6" gravel base and a semi-infinite subgrade layer. The intermediate outputs of the Pavement ME software were extracted to obtain the hourly temperatures, which were then averaged for each month to obtain monthly average temperatures shown in Table 4-9. Assuming that aggregate loss typically occurs when the binder is relatively soft, an average of the temperatures between April and October was taken as the aggregate loss test temperature.

As a result, the following configurations were used for evaluating the aggregate loss distress;

(i) The HWT device with a fixed pneumatic rubber wheel and with a tire pressure of 34 psi, and an initial load of 125 lbs was used,
(ii) The test temperature was selected as 19°C,
(iii) The aggregate loss test was performed under dry condition,
(iv) The total number of the HWT cycles was 10.

Table 4-9 Average monthly air and pavement surface temperatures of Lansing, MI

Month	Temperature °C	
	Air	6mm below surface
January	-5.78	-4.20
February	-6.25	-4.37
March	-1.60	0.48
April	7.36	**10.86**
May	14.87	**19.93**
June	17.42	**22.17**
July	21.04	**26.70**
August	19.90	**24.37**
September	17.21	**20.79**
October	9.89	**11.81**
November	3.22	4.49
December	-1.50	-0.34

Since the HWT device test is an abrasive test, which is performed under dry conditions through the fixed wheel, the effect of the generated heat due to the friction during the HWT device

testing had to be considered. For that reason, the dummy chip seal specimens were prepared and conditioned at 16°C in an environmental chamber for at least 3 hours prior to the HWT device aggregate loss testing. Following the conditioning period, the specimens were subjected to the HWT test, and the surface temperature profile of the specimens were monitored through a hand-held thermometer. It must be noted that the total test duration, including removing the test specimens (already housed in the HWT molds) from the chamber and installing them to the HWT device, took less than a minute to complete. Figure 4-19 shows the variations in the surface temperature of chip seal specimens, measured from the center of the specimens. As it can be seen from the figure that the test with the generated heat is, on average, performed within a reasonable variation of the targeted test temperature of 19°C. Hence, the chip seal test specimens prepared for the aggregate loss susceptibility test were conditioned at 16°C in an environmental chamber for at least 3 hours before being tested under the HWT device. The test procedure was precisely maintained the same for each of the specimens tested for this purpose.

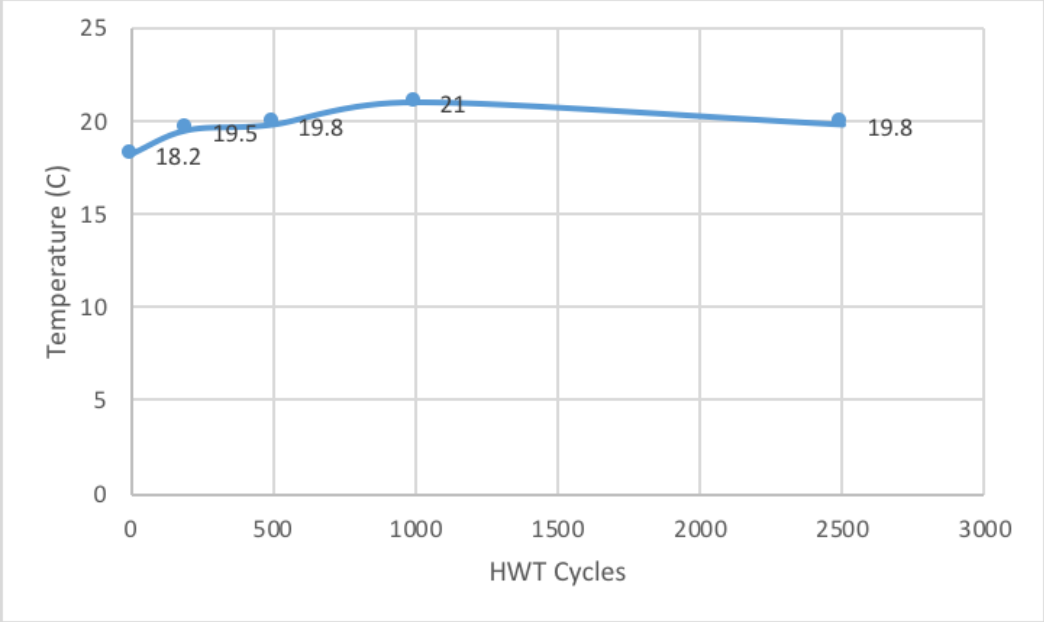

Figure 4-19 Variations in surface temperature during the HWT device abrasion test.

5. IMAGE ANALYSIS RESULTS

This chapter details the efforts toward quantifying the microstructure (i.e., percent embedment and orientation) and surface profile (i.e., mean profile depth) of the chip seal specimens through 2D and 3D image analysis techniques. This chapter also reflects upon the effects of the variables tested in this research on the quantified properties. The included variables were emulsion and aggregate types, as well as emulsion/binder application rates.

5.1 2D Image Analysis for Percent Embedment and Orientation

5.1.1 Percent Embedment of Chip Seal Aggregates

The procedure and the software (CIPS) developed in a previous MDOT project (OR15-508) were utilized to compute the percent embedment of aggregates for the specimens fabricated in this study. The percent embedment of the aggregates retained on sieves no.4 and above was quantified using each aggregate method, the details of which can be found in the previous project. As indicated previously, the emulsion-based chip seal specimens consisted of a single aggregate application rate (AAR) and three different emulsion application rates (EARs), whereby the hot-applied chip seal specimens were prepared at a single AAR and four different binder application rates (BARs) for a given source of aggregate and emulsion/binder.

Figure 5-1 presents the percent embedment of the emulsion-based chip seal specimens at a range of EARs. It should be noted that two replicate specimens were prepared for each combination of the chip seals thereof. Unless otherwise stated, the whisker bars presented in the figure as well as in other figures throughout this report represent one standard deviation around the mean. For the percent embedment, the maximum coefficient of variation (COV) observed among all data was 5.9 percent, which indicates the versatility of each aggregate method. The magnitude of the percent embedment for the emulsion-based chip seal specimens prepared in this study was ranged from about 58 to 73 percent. As shown in Figure 5-1, regardless of the aggregate source and emulsion type, there is, overall increase in the magnitude of percent embedment with an increase in the EAR, as expected.

The close inspection of Figure 5-1 further indicates that the chip seal specimens prepared with natural aggregates attains higher embedment depths than the chip seal specimens prepared with slag aggregates for a given EAR and emulsion type. This observation can be attributed to the flakiness ratio of the aggregates. As presented in the preceding chapter, natural aggregates are flakier than slag aggregates. Aggregate overlapping, which is highly related to an excessive AAR can also impact such trend. Even though the same AAR of 20 lbs/yd2 was used for both aggregate sources, as shown later in the report, this application rate was more than the optimal AAR (i.e. amount that forms one stone-thick layer) for slag. This excessive AAR could have resulted in aggregate overlapping for the chip seals specimens with slag, thereby introducing another factor for the lesser percent embedment depth that was observed. Additionally, the binder absorption level of slag aggregates is higher than natural aggregates, which results in a relative increase of binder absorption into the aggregate. This might also be a cause of lower percent embedment depths for slag aggregates.

Another observation from Figure 5-1 is that the level of the percent embedment for a given aggregate source is not considerably changed when the emulsion type (CRS-2M vs. CSEA) is changed. This observation was further evaluated by conducting a statistical analysis of the means at a confidence level of 95 percent. The test results confirmed that, for a given aggregate source, the percent embedment was not significantly varied where a change in the emulsion type was recorded. It should be noted that both emulsions had approximately the same residual asphalt content (69.1 vs. 69.5 percent), as presented earlier.

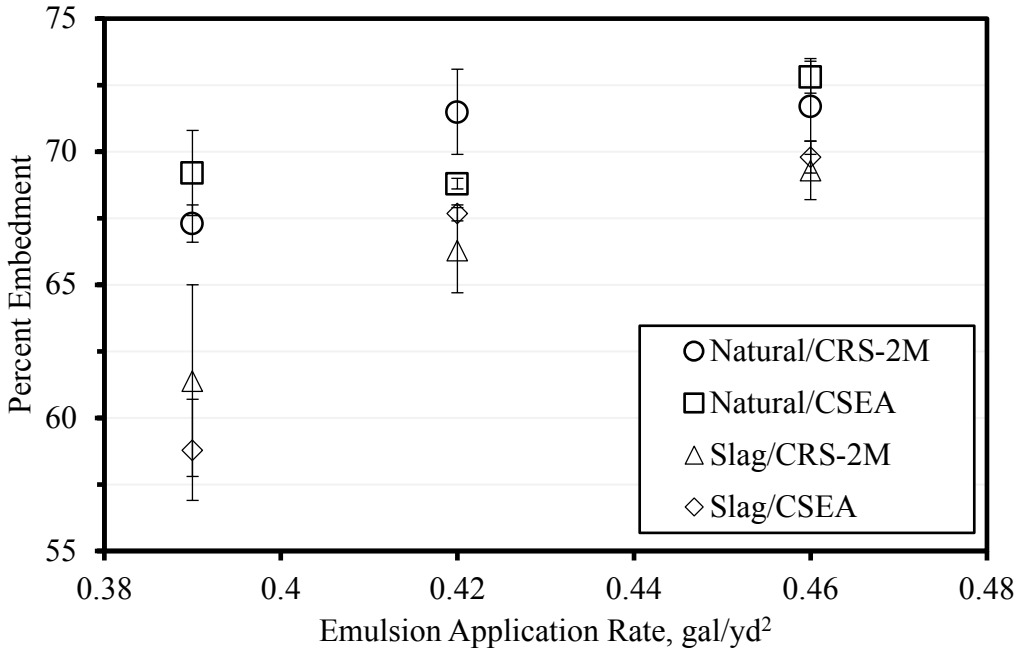

Figure 5-1 Percent embedment of the emulsion-based chip seals as a function of EAR.

Figure 5-2 shows the percent embedment of the hot-applied specimens, prepared with Gerkin aggregates and PG 70-28 binder, as a function of binder application rate (BAR). The magnitude of the percent embedment was in the range of about 72 to 83 percent, a range higher than that observed for the emulsion-based chip seals. The conversion method suggested by Epps et al. (Epps, Chaffin and Hill, 1980) was used to equate the BARs to the EARs. The BARs of 0.25, 0.30, 0.35, and 0.40 gal/yd^2 were corresponded to the EARs of 0.30, 0.36, 0.42, and 0.48 gal/yd^2, assuming 69.3 percent binder residue in the emulsion. The difference in the observed percent embedment range between the two forms of chip seals cannot be explained from the perspective of the applied emulsion volume. However, it should be noted that the aggregates used for the hot-applied chip seals are flakier than the aggregates used for the emulsion-based chip seals. Additionally, the AAR used for the hot-applied chip seals was at an optimum rate of 18 lbs/yd^2, which could have potentially impacted the observed range. Furthermore, the differences in the interaction mechanism between the chip seals components for the two forms of chip seals could have also contributed to the differences in the observed range. Nevertheless, as shown in Figure 5-2, there is a general increase in the magnitude of percent embedment with an increase in the BAR. The percent embedment increase rate seems faster than the increase rate observed for the emulsion-based chip seals, however, the scatter in Figure 5-2 could be a reason for such observation.

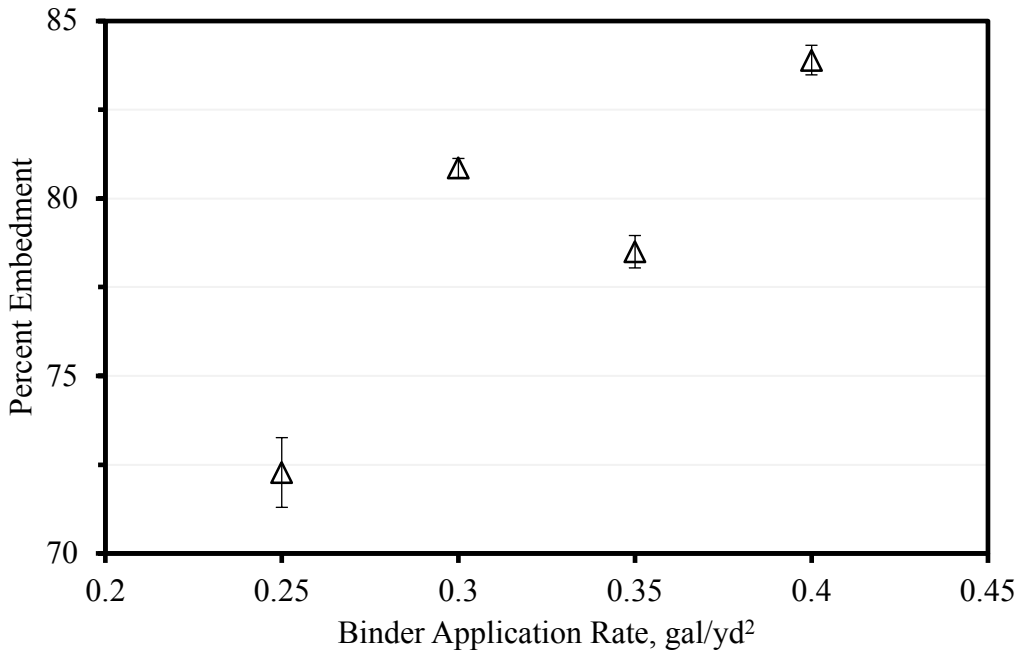

Figure 5-2 Percent embedment of the hot-applied chip seals as a function of BAR.

5.1.2 Orientation Distribution of Chip Seal Aggregates

The algorithms in the CIPS software were further improved to quantify orientation distribution of chip seal aggregates. Figure 5-3(a) displays a screen shot of the chip seal analysis software (CIPS). The extent of aggregate orientation on the flat side is a critical indicator for satisfactory chip seal performance. Chip seals with a uniformly distributed aggregate orientation would perform better than that of chip seals forming a distribution of aggregate orientation to the lesser extent. The orientation angle of aggregates can be defined as the angle between major axis and the horizontal axis as shown in Figure 5-3(b). In this research, the orientation angle of 20º was marked as a threshold angle for quantifying aggregates lying on their flattest side. In other words, aggregates with angle of 20º and less are considered aligning on their flattest side on the pavement substrate. It must be stated that, to the best knowledge of the research team, there is no literature available in quantifying aggregate orientation in chip seals nor defining a threshold limit for such purpose. However, it has been frequently stated that all or most of the aggregates should align on their flattest side and form a one-stone thick layer for satisfactory performance of chip seals.

The cumulative percentage of aggregates lying on the flattest side (CPAF) was determined by Equation 5.1.

$$\text{CPAF} = \frac{\sum_0^{20} N_\theta}{N} \tag{5.1}$$

where N_θ is the number of aggregates with orientation angle θ, and N is the total number of aggregates on the specimen.

The more well distributed the aggregates on their flat side, the higher the CPAF. For example, if all aggregates align on their flattest sides, the CPAF would be equal to 100%, indicating a well compacted chip seal.

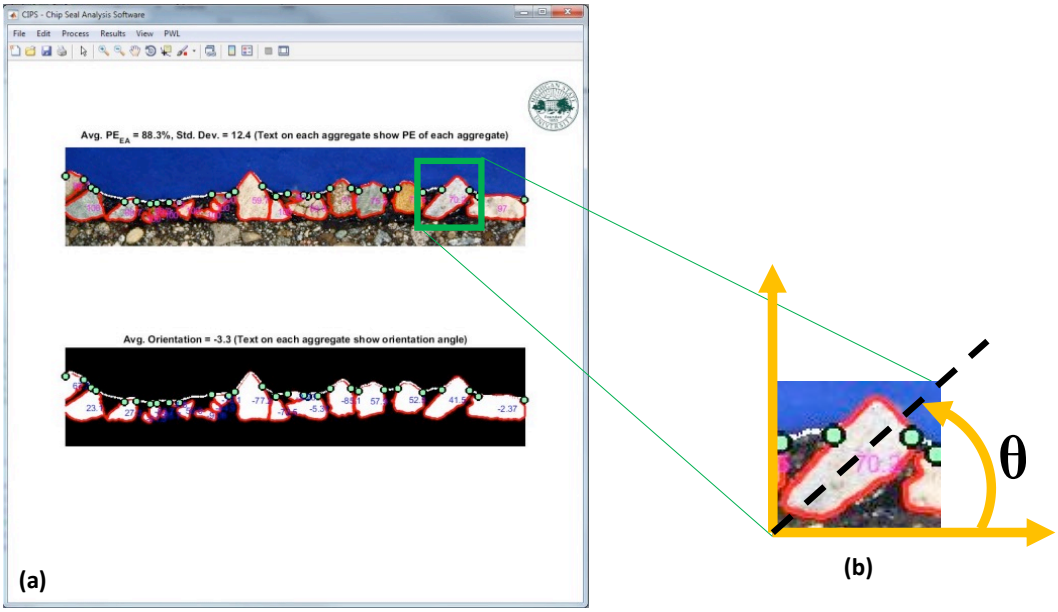

Figure 5-3 (a) Screenshot of the CIPS software illustrating the computation of percent embedment using each aggregate method, (b) illustration of orientation of the aggregates.

Figure 5-4 shows the CPAF for the emulsion-based chip seal specimens at a range of EARs. The COVs observed among all specimens did not exceed 8.1 percent, except for two sets. The COVs for the specimens fabricated with slag aggregates and CRS-2M emulsion at the EARs of 0.39 and 0.46 gal/yd^2 were 14.2 and 20.8 percent, respectively. The extent of such variation in the observed data is deemed very reasonable and acceptable, given the high variability of commonly utilized test methods in the paving industry such as the dynamic modulus testing of asphalt concrete. The magnitude of the CPAF was ranged from as low as 37 percent to as high as 54 percent for the emulsion-based chip seals. The figure indicates that, regardless of the aggregate source and emulsion type, there is a sudden decrease in the magnitude of the CPAF when the EAR increases from 0.39 to 0.42 gal/yd^2. However, the magnitude of the CPAF is, overall, slightly reduced with an increase in the EAR from 0.42 to 0.46 gal/yd^2.

Figure 5-4 also shows that, for a given aggregate source, the CPAF is not noticeably changed when the emulsion type (CRS-2M vs. CSEA) is changed, except with regards to the specimens with natural aggregates at the EAR of 0.39 gal/yd^2. The statistical analysis of the mean values performed at a confidence level of 95 percent also indicated that the emulsion type did not influence the aggregate orientation distribution of chip seals, except with regard to the specimens with natural aggregates at the EAR of 0.39 gal/yd^2. It is postulated that such difference is within the experimental variability, and it can be assumed that the emulsion type does not influence the orientation distribution of aggregates. It should be noted that the conclusions provided on emulsion types as related to the percent embedment and aggregate orientation are only applicable to the materials included in this study. Further studies are needed to validate this finding for other emulsion types.

Like the trend observed for the percent embedment of aggregates, the chip seal specimens prepared with natural aggregates overall result in higher CPAF values than the chip seal specimens prepared with slag aggregates for a given EAR and emulsion type, as shown in Figure 5-4. Again,

the flakiness ratio, aggregate application rate, and absorption level as well as their interaction are among the factors leading into such observation, as discussed previously.

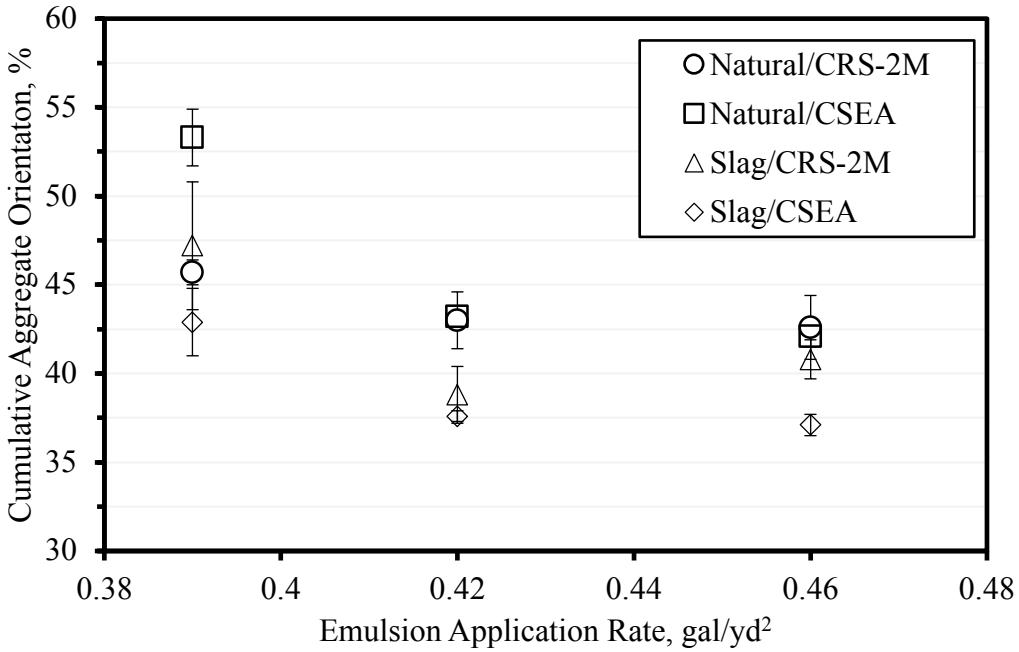

Figure 5-4 CPAF for the emulsion-based chip seals at a range of EARs.

Figure 5-5 presents the CPAF for the hot-applied chip seal specimens as a function of binder application rate (BAR). The magnitude of the CPAF was in the range of about 47 to 70 percent for the hot-applied chip seals, a range higher than that observed for the emulsion-based chip seals. As seen from the figure, the trend observed in this case is opposite of what is observed for the emulsion-based chip seals. The CPAF increases up to a point with an increase in the BAR, and then is followed by a sharp decrease. One potential reason for such observation could be related to the viscosity and density of asphaltic component of chip seals. Emulsions are less viscous and denser than binders. Hence, when aggregates are spread over emulsion, they can be readily penetrated and subsequently meet the substrate with their self-weight, even before compaction. In this case, the orientation of aggregates is relatively less affected by the viscosity of the emulsion but is dominated more by aggregate-to-aggregate interlock, the extent of which depends on the physical properties of aggregates such as size and shape. In the case of hot-applied chip seals, after spreading, the aggregates are initially "floated" on the binder due to the denser medium, and then they are also pushed into the substrate through compaction. At this stage, the binder acts as more of a lubricant compared to the emulsion, thus aggregates are more prone to align on their flat side while being compacted. Further research is recommended to better understand the aggregate-binder microstructure of hot-applied chip seals.

5.2 3D Image Analysis for Determining Mean Profile Depth of Chip Seals

One of the primary functions of chip seals is to improve surface texture properties of the existing pavements. The surface texture of chip seals is evaluated by microtexture and macrotexture characteristics. Frictional properties of the aggregates used contribute to the microtexture characteristics of chip seals, whereby the macrotexture characteristics are dominated

by aggregate size, shape, and gradation (Guirguis and Buss, 2017). Additionally, the macrotexture characteristics are also affected by aggregate type, application rates of chip seal components, and traffic volume (Adams and Kim, 2010; Aktaş *et al.*, 2013; Praticò, Vaiana and Iuele, 2016). While the microtexture characteristics are of a great importance for chip seals, the macrotexture characteristics are often used as a key indicator of assessing the common chip seal distresses as well as for evaluating construction quality of chip seals (Roque, Anderson and Thompson, 1991; Adams and Kim, 2010; Aktaş *et al.*, 2011; Shuler *et al.*, 2011; Gürer *et al.*, 2012; Chaturabong, Hanz and Bahia, 2015). For example, the macrotexture depth of 0.9 mm is defined as a threshold point for retreating New Zealand's chip seal projects which accommodate speeds greater than 70 km/h (43 mi/h) (TNZ report, 2005; Gransberg, 2007). The percent macrotexture loss shows a correlation with chip seal aggregate loss and bleeding distresses (Adams and Kim, 2010; Chaturabong, Hanz and Bahia, 2015). Also, macrotexture along with average least dimension of aggregates is used for calculation of the percent embedment depth of chip seals (Shuler *et al.*, 2011).

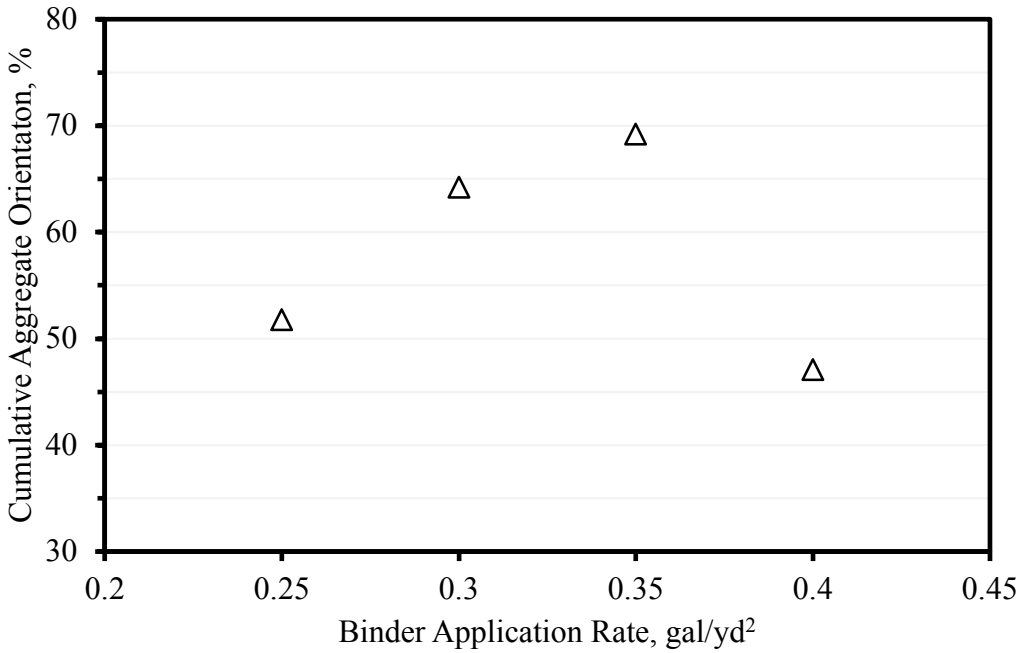

Figure 5-5 CPAF for the hot-applied chip seals at a range of BARs.

Pavement surface macrotexture is usually quantified through a volumetric test method, known as a sand-patch test (ASTM E965, 2015). In this procedure, a known volume of specified sand is spread over a pavement surface by forming a circular shape, and then average diameter of the area covered by the sand is determined. Subsequently, the average pavement macrotexture depth is determined by dividing the volume of the sand with the covered area. The resulting quantity is defined as the mean texture depth (MTD) of pavement macrotexture.

There are also other methods that are used to quantify the chip seal macrotexture such as volumetric-based methods, profile meters, and visualizing techniques (Uz and Gökalp, 2017). The volumetric methods, other than the sand patch test, are outflow meter test (ASTM-E2380, 2015)

and New Zealand's sand circle test (TNZ report, 2005). The examples of profile meters are various commercially available laser profilers and a circular track meter (ASTM-E2157, 2015). The examples of visualizing methods are X-ray tomography scanning and photogrammetry methods (Uz and Gökalp, 2017). The methods other than the volumetric ones determine the mean profile depth (MPD) from a profile of pavement macrotexture. Then, a linear regression equation provided in ASTM-E1845 (2015), also presented in Equation 5.2, is used to translate the MPD into an estimated texture depth (ETD), which is closely related to the MTD measured from ASTM E965.

$$ETD = 0.2 + 0.8 \times MPD \tag{5.2}$$

where MPD and ETD are expressed in mm.

In this research, 3D photogrammetric software (3DF Zephyr) was utilized to construct the surface topography of chip seal specimens. This task was performed to investigate the effect of chip seal macrotexture on the performance. To this end, a series of images taken around a chip seal specimen surface by a smartphone was uploaded to the software package in order to generate an artificial 3D surface texture of the chip seal specimen. Figure 5-6 illustrates an image of the 3D surface texture of a chip seal specimen. Then, the generated 3D image was uploaded to another software (Autodesk Netfabb) to extract the 3D coordinates (mesh). A screenshot of the software is shown in Figure 5-7. Finally, the obtained mesh was processed by a MATLAB-based algorithm developed during this research for calculation of the mean profile depth as described in ASTM E1845.

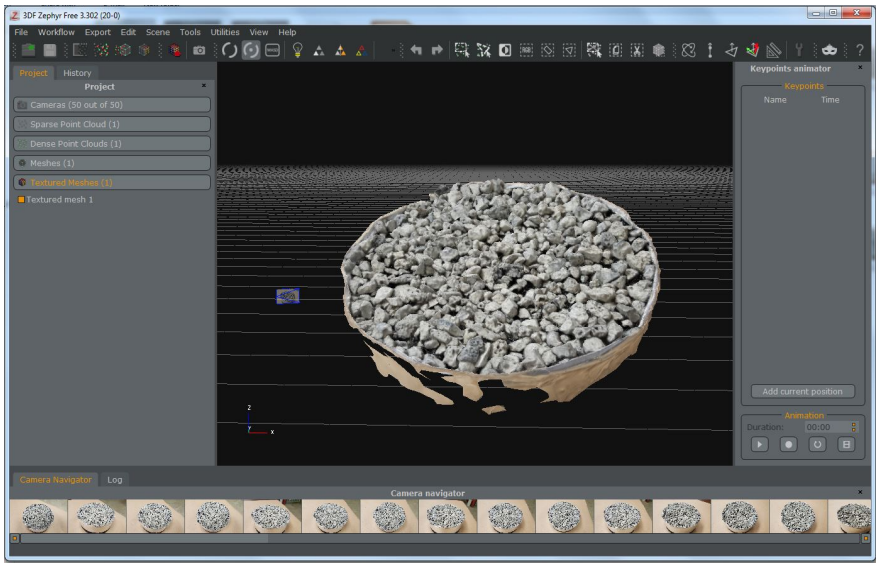

Figure 5-6 Example of the reconstructed 3D surface texture of a chip seal specimen.

Since the MPD of the specimens used in this research was to be calculated at every HWT device cycle of interest (i.e. 0, 200, 300, 500, and 1500), the target cross-sectional area for the MPD calculations was the HWT device wheel path. Thereby, once the 3D mesh of a chip seal specimen was obtained, the wheel path was cropped from the 3D mesh. Then, a total of 30 lines in the longitudinal direction (the HWT device trafficking direction) were obtained at every 1-mm intervals through the transverse direction within the wheel path. The MPD for each line was calculated in accordance with ASTM E1845. The final MPD for a given specimen was calculated

by averaging the MPDs of the all lines incremented in the wheel path. Figure 5-8 shows a plot of the MPD values for each line before the HWT device loading and after the total of 2500 HWT device cycles. Finally, the estimated mean texture depth (ETD) was calculated from Equation 5.2.

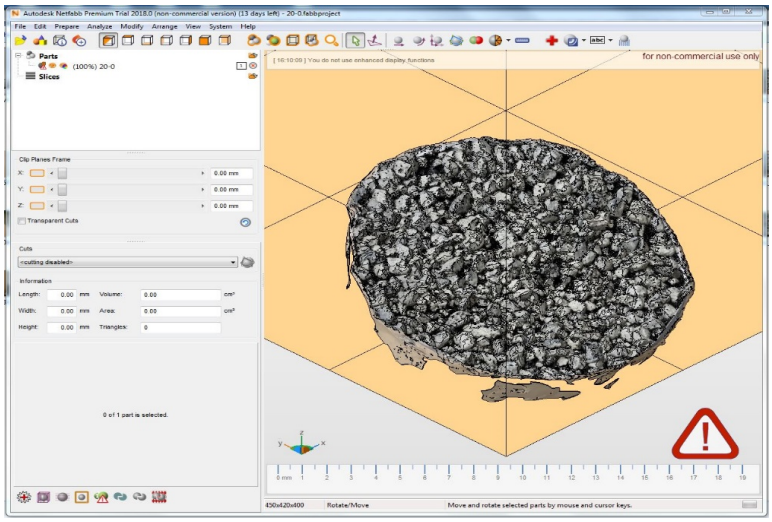

Figure 5-7 Screenshot of the chip seal mesh extraction software.

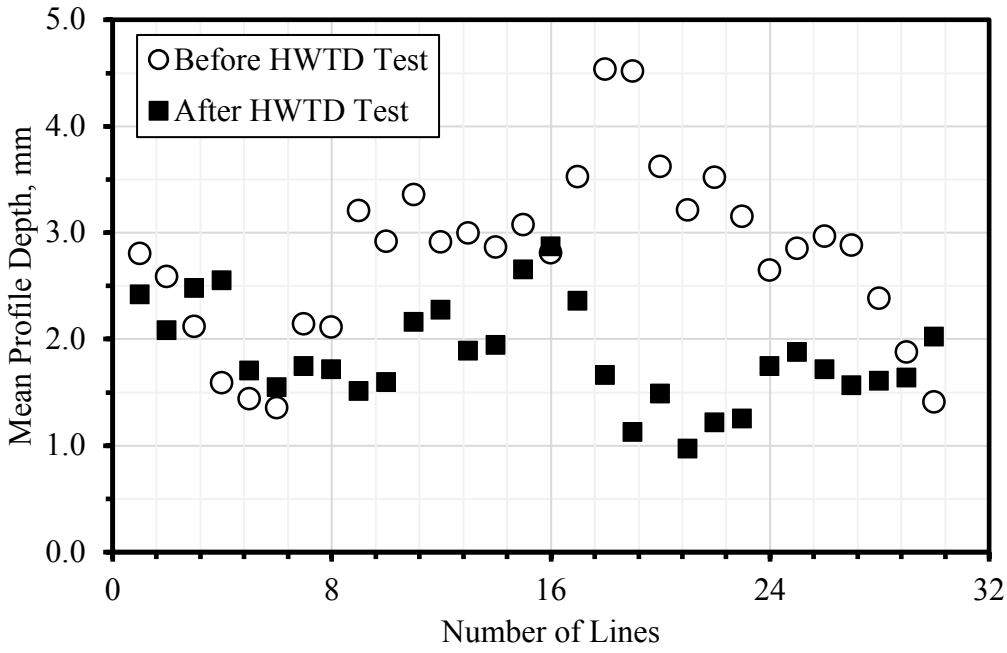

Figure 5-8 Mean profile depth variations across the wheel path before and after the HWT device test.

A pilot study was conducted to explore the relationship between the MPDs calculated from the 3D imaging method and a laser texture scanner. A series of chip seal specimens was fabricated by varying aggregate application rates to produce chip seals with different macrotexture profiles. A laser texture device, the Ames model 9300, was used to measure the macrotexture of the chip seal surfaces. The test results are plotted in Figure 5-9. As shown in the figure, the MPDs measured from both methods are highly correlated as manifested by the very high coefficient of

determination value of 97 percent. It can be also seen from the figure that the MPDs of the specimens are slightly under those predicted by the 3D imaging method as compared to that of the MPDs measured from the laser scanner. Additionally, the variability of the data from both methods was low, except at one data point for the 3D imaging method. The COV for the data point was 16.9 percent. It must be noted that the specimens were not subjected to any forms of loading when the MPDs were measured from both methods.

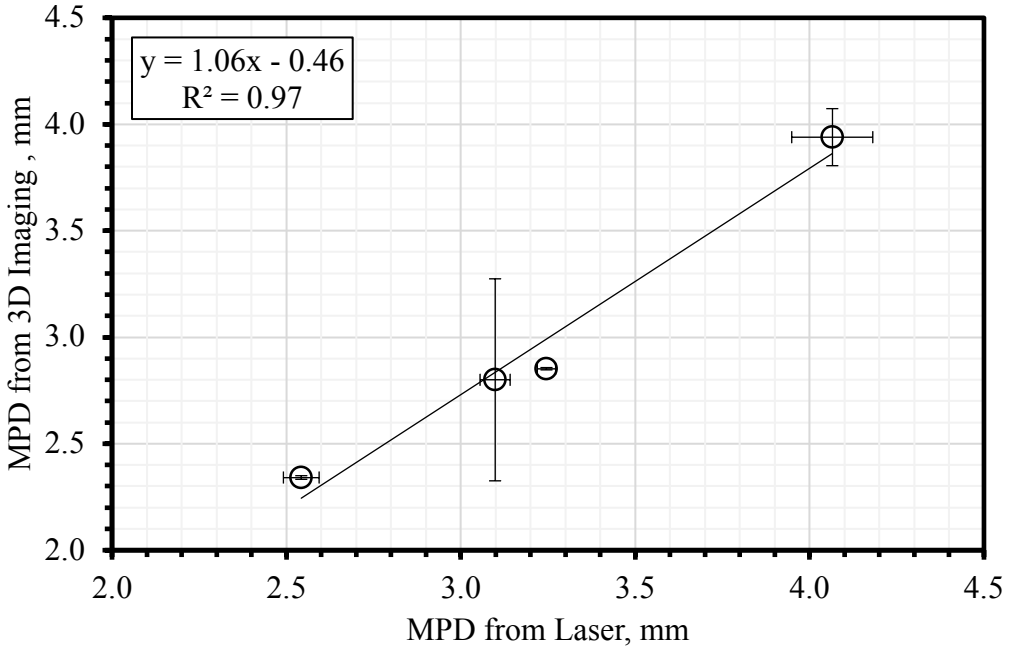

Figure 5-9 Comparison of the MPD via 3D image-based method and laser-based method.

Once again, the 3D imaging procedure was applied to the chip seal specimens fabricated in this study to determine the MPD, leading to 180 individual data points generated during the research. Then, the estimated texture depth (ETD) was calculated from Equation 5.2 for each specimen. During the analysis of the test results, it was recognized that the variation in the ETD values was very high between the two replicate specimens, especially after the HWT device cycles. The maximum coefficient of variation (COV) found among all specimens was 24.4 percent before the HWT device cycling, with an overall average COV of 12 percent. However, the maximum COV observed for the data points after the HWT device cycles were applied was as high as 57 percent, with an overall average COV of 20 percent including all HWT device cycles.

Figure 5-10 shows the change in ETD as a function of EAR for each aggregate source and emulsion type before the HWT device loading. The ETD values are scattered to a considerable extent with no discernable pattern with respect to neither the EAR nor aggregate and emulsion types. The confounding effects of the AAR, RAR, and aggregate orientation could have contributed to such observation. Despite the high variability, Figure 5-11 and Figure 5-12 are plotted to show overall change in ETD as a function of the HWT device cycles for the chip seals specimens prepared with natural and slag aggregates at a range of EARs, respectively. As it can be seen from the figures, the ETD of chip seals generally show a relatively rapid drop after initial HWT device loading and then followed by a steady decrease with further loading. This indicates

that aggregates typically align on their flat side immediately after initial traffics and then continue to align towards the flat side at a slower rate through further traffic influences. This observation is consistent with the reported literature (Aktaş *et al.*, 2013; Adams, 2014). The figures show that, for a given aggregate type, there are no overall, no distinct differences in the ETDs of chip seals made with the two emulsions (CRS-2M and CSEA). This suggests that the emulsion types studied in this research did not affect the macrotexture of chip seals.

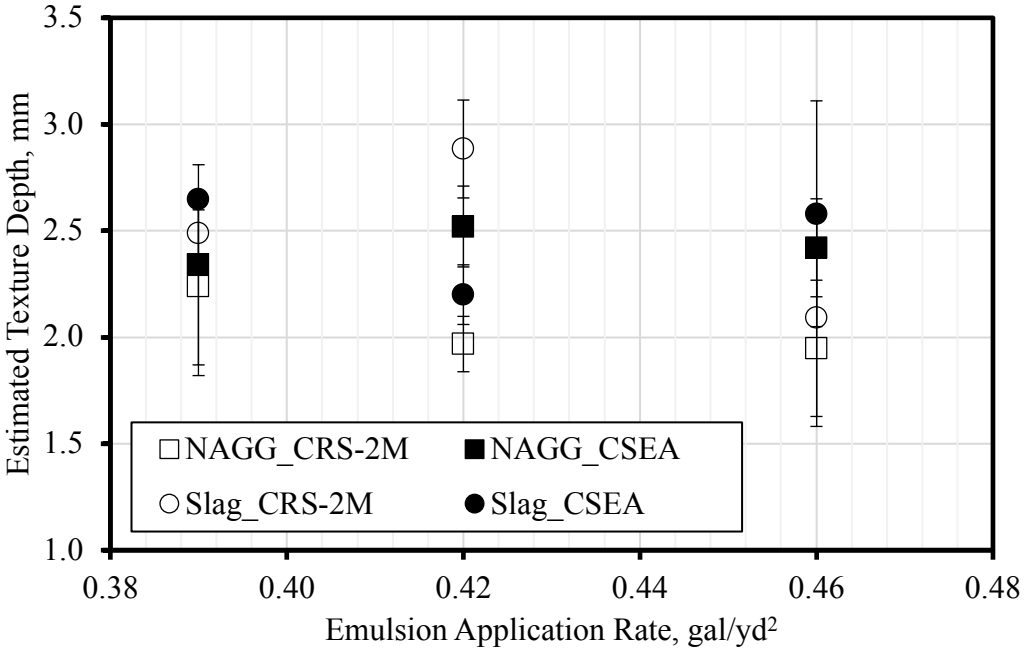

Figure 5-10 Change in ETD as a function of EAR for before HWT device loading.

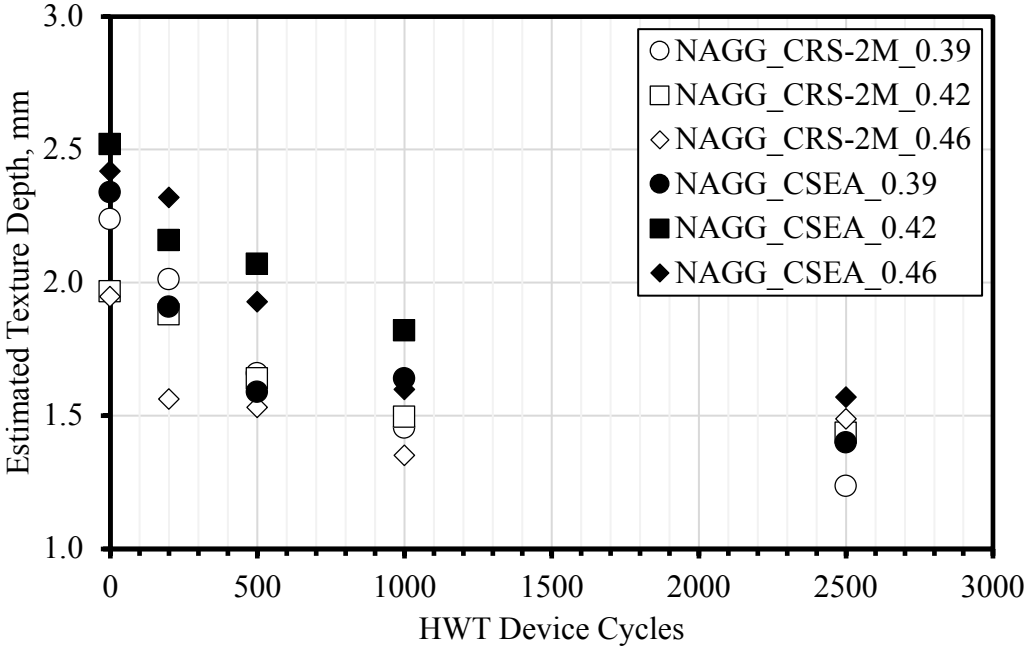

Figure 5-11 Change in ETD as a function of HWT device loading for chip seals with natural aggregates.

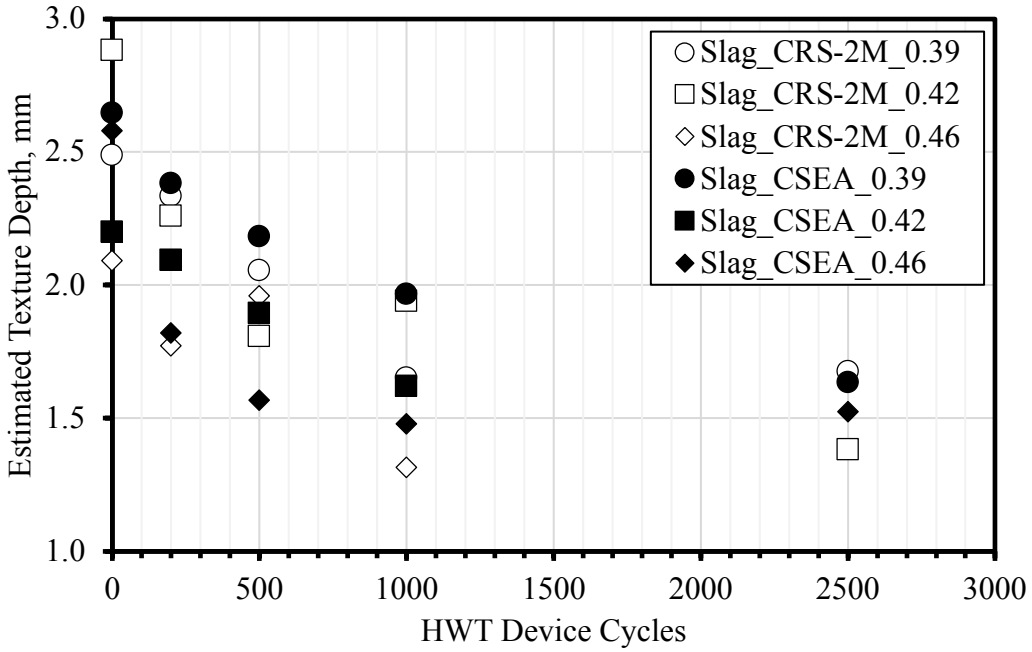

Figure 5-12 Change in ETD as a function of HWT Device loading for chip seals with slag aggregates.

5.2.1 *Chip Seal Aggregate Application Rate*

In the preceding sections, the AAR as well as variations in the RAR due to the increase in the EAR were listed among the factors affecting the variations in the observed trends. This section provides the relevant data to show how the used AAR was excessive, and that there was a change in the RAR due to an increase in the EAR.

Chip seal aggregates should form a one-stone thick layer for satisfactory performance. Excessive or insufficient aggregate rates affect aggregate-binder microstructure to a considerable extent, and result in premature failures of chip seals (Lee and Kim, 2008; Kumbargeri, Boz and Kutay, 2018). The aggregate rate at which a one-stone thick layer is achieved is defined as an optimal aggregate application rate (design rate). In practice, an additional amount of aggregate (up to 10 percent, as recommended in AASHTO PP 82) is suggested to help reduce the potential for aggregates to be picked up by pneumatic rollers during construction. The amount of aggregates retained on the chip seal surface after sweeping off in the field is defined as the residual aggregate rate (RAR). The RAR can be thought of an effective aggregate application rate as it is the rate at which the performance of chip seals takes part in the field. In the laboratory, the chip seal specimen at the end of conditioning time is turned vertically and any loose aggregate is removed by slight hand brushing of the specimen surface without applying any remarkable amount of force. The amount of the remaining aggregates on the surface is calculated as the RAR. In an ideal case, the ratio of the optimal AAR to the RAR should be close to 1.1, including the extra 10 percent aggregates accounted for the potential pick-up during the construction.

During the initial phase of the research project, a series of the chip seal specimens using Slag and CRS-2M emulsion was prepared at the aggregate application rates of 20, 19, and 16 lbs/yd^2 with the emulsion application rate of 0.39 gal/yd^2. The emulsion application rate was

selected to minimize formation of aggregate overlapping. The residual aggregate rates (RAR) were 16, 15.3, and 14.2 lbs/yd^2 for the aggregate application rates of 20, 19, and 16 lbs/yd^2, respectively. The ratio of the AAR to the RAR was calculated as 1.25, 1.24, and 1.13 for high, medium, and low AARs, respectively. The results indicate that the optimal AAR is around 16 lbs/yd^2 for Slag aggregates. A set of chip seal specimens was also prepared with natural aggregates and CRS-2M emulsion at application rate of 20 lbs/yd^2 and 0.39 gal/yd^2, respectively. The resultant ratio of the AAR to the RAR was 1.18, implying that the AAR for natural aggregates is approximately around the optimal value. The design aggregate application rate of 18 lbs/yd^2 for Gerkin aggregates was determined through a performance-based design process prior to the start of this project.

The design application rates for the aggregates used in this study were also determined using the board test as specified in AASHTO PP 82. In this test, aggregates are placed on a board, measuring three feet by one and half feet, until every gap is filled, and a one-stone thick layer is formed (Figure 5-13). The quantity of the aggregates placed is selected as the design application rate. The measured design aggregate rates, including a 10 percent whip-off factor, based on the board test were 20, 17.8, and 18.7 lbs/yd^2 for natural, slag, and Gerkin aggregates, respectively. The board test generally, confirmed the conclusions about AARs found in the preceding paragraph. After consultation with MDOT research panel, it was decided to utilize an AAR of 20 lbs/yd^2 (MDOT's minimum limit) for the chip seal specimens made with natural and slag aggregates.

Figure 5-14 presents the variations in the RAR as a function of the EAR for the emulsion-based chip seal specimens fabricated in this study. The increase in the RAR is clearly shown with an increase in the EAR for both aggregate sources. Also, the ratio of the AAR to the RAR for the specimens with natural aggregates was 1.17, 1.12, and 1.11 for the EARs of 0.39, 0.42, and 0.46 gal/yd^2, respectively. Likewise, the ratio of the AAR to the RAR for the specimens with slag aggregates was 1.30, 1.23, and 1.18 for the EARs of 0.39, 0.42, and 0.46 gal/yd^2, respectively. This outcome and the results presented in the preceding paragraph indicate that the AAR of 20 lbs/yd^2 was a reasonable application rate for natural aggregates, but not for slag aggregates.

Figure 5-13 Board Test for determining design AAR for natural, slag, and Gerkin aggregates (left to right).

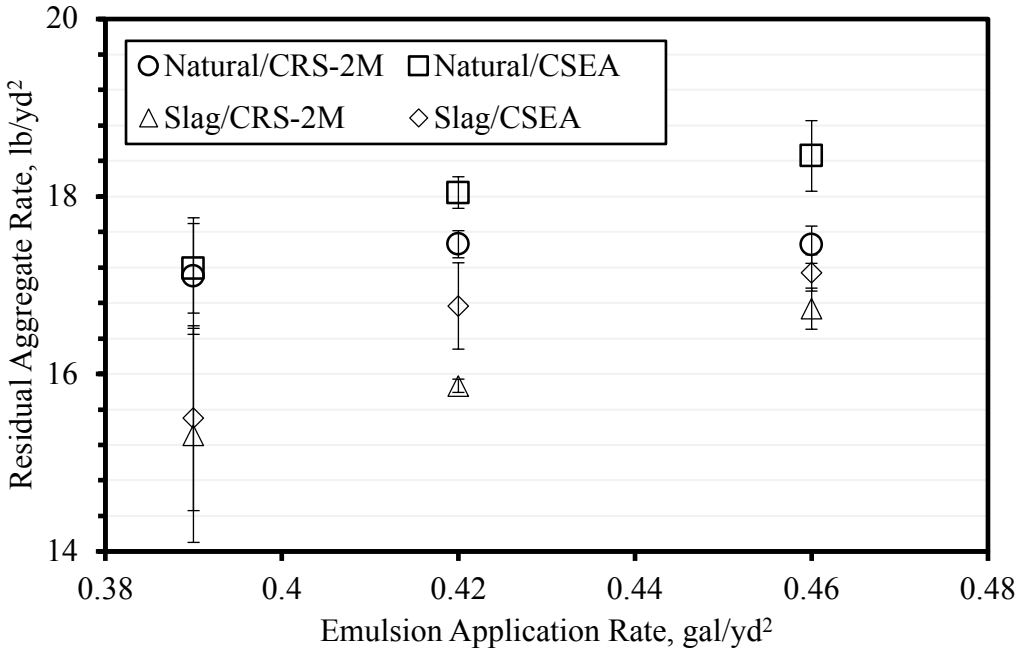

Figure 5-14 Change in RAR as a function of EAR for emulsion-based chip seals.

The variations in the RAR as a function of the BAR for the hot-applied chip seal specimens are plotted in Figure 5-15. The increase in the RAR is also evident for the hot-applied chip seals with an increase in the BAR, but the increase rate was lower than those with emulsified chip seals. The ratio of the AAR to the RAR was 1.13, 1.13, 1.08, and 1.07 for the BAR of 0.25, 0.30, 0.35, and 0.40 gal/yd^2, respectively. The results confirmed that the AAR used in this chip seal was appropriate.

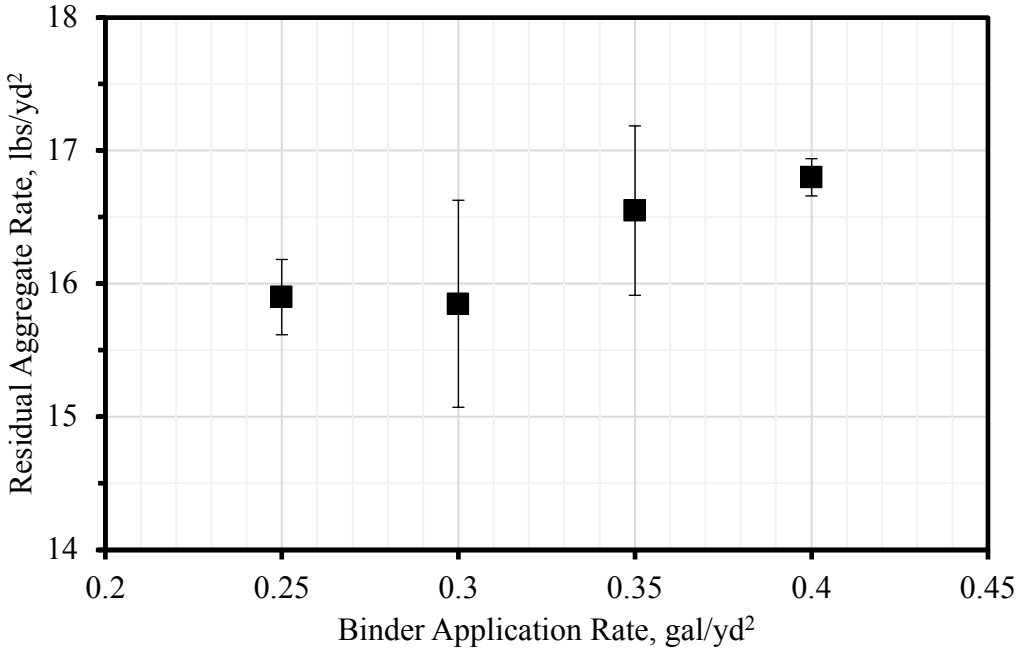

Figure 5-15 Change in RAR as a function of BAR for hot-applied chip seals.

6. EVALUATION OF AGGREGATE LOSS

In this chapter, the experimental work conducted to evaluate the effects of substrate types, emulsion types, emulsion application rates, and percent embedment of aggregates on the susceptibility of chip seals to aggregate loss is described. The analysis performed to establish a percent embedment threshold limit based on aggregate loss for each aggregate source used is also described. Additionally, the numerical analysis to investigate the effects of the percent embedment and aggregate flakiness on the susceptibility of chip seals to aggregate loss is documented in this chapter as well.

6.1 Quantifying Aggregate Loss

The specimens prepared in this research were subjected to the HWT device abrasion test at 19°C to evaluate the effects of chip seal characteristics in terms of aggregate loss. The details of the HWT device abrasion test is provided in Chapter 4. Starting from the end of the curing phase of chip seals to the end of the abrasion test, the aggregate loss was quantified using three different types of aggregate loss indices. The details of each indices are provided below.

6.1.1 Aggregate Loss by Hand Brushing

At the end of the curing time, each test specimen was turned vertically, and any loose aggregate was removed by slight hand brushing of the specimen surface without applying any remarkable amount of force. This procedure replicates the process of sweeping off after the compaction of chip seals in field. The percentage of aggregate loss by hand brushing (ALB) was calculated from Equation 6.1.

$$ALB = \frac{A}{B} \times 100 \tag{6.1}$$

where, A is the weight of the aggregates lost due to the hand-brushing, B is the weight of the aggregates retained on the chip seal specimen surface after the curing period.

6.1.2 Aggregate Loss by Abrasion

Aggregate loss by abrasion is the aggregate loss that occurred after the HWT device test. The percentage of aggregate loss by abrasion (ALA) was computed using Equation 6.2.

$$ALA = \frac{C}{D} \times 100 \tag{6.2}$$

where, C is the weight of aggregates lost due to the abrasion and D is the weight of aggregates retained on the chip seal specimen surface after the hand-brushing.

6.1.3 Cumulative Aggregate Loss

The cumulative aggregate loss (CAL) is the combined loss of the hand brushing and the abrasion and was calculated using Equation 6.3.

$$CAL = \frac{C \times \mathrm{m} + A}{B} \times 100 \tag{6.3}$$

where, m equals 2.62 ($m = A_{total}/A_{wheelpath}$, see Figure 6-1) to account for the specimen surface area as the HWT wheel does not abrade over the entire area. Other parameters were defined in previous equations.

6.2 Effect of Substrate Properties on Chip Seal Aggregate Loss

One of the objectives to be accomplished under Task 2 of this research was to evaluate whether there is an effect of chip seal substrate properties on the performance of chip seals. Hence, prior to the start of any chip seal mixture tests in this research, a series of tests were conducted on chip seals with the same characteristics (i.e., aggregate and emulsion application rates) placed on asphalt mixture substrates obtained from field and prepared in laboratory. For this purpose, aggregate loss was chosen as a performance indicator for evaluating the chip seals. The extent of aggregate loss was quantified through the HWT device.

Towards this goal, emulsion-based chip seal specimens were prepared on laboratory-fabricated (lab cores) and field substrates, using one source of aggregate (natural) and emulsion (CRS-2M). The aggregate and emulsion application rates (AAR and EAR) for both substrate types were 18 lb/yd^2 and 0.39 gal/yd^2, respectively. It must be noted that this task was performed before the research advisory panel's recommendation on utilizing an aggregate application rate of 20 lb/yd^2 for the chip seal specimens prepared throughout the research. The specimen preparation and testing procedures for the HWT aggregate loss test as described in Chapter 4 were closely followed for both sets, except with some differences in the testing conditions. The initial idea of the research team was to capture the change in loading magnitude during the HWT device abrasion cycles. For that reason, the HWT device was coupled with a load cell and a portion of the HWT device weight was lumped on the load cell, as shown in Figure 6-1, for this part of the study. The magnitude of the load on the load cell was 75 lbs, this, resulting in less than 125 lbs of the initial load on the specimens. The load of 125 lbs is the load established for assessing the bleeding and aggregate loss potential of the chip seals in this study, as described in Chapter 4. Additionally, the test was conducted at a temperature of 25°C to achieve the objective of this task.

The specimens were abraded in a dry condition under the HWT device at an initial loading rate of 75 lbs on the load cell. Figure 6-2 presents the percent aggregate loss by abrasion (ALA) for each substrate type. The test results indicate that the chip seals prepared with the field substrates showed less aggregate loss compared to that of the chip seals prepared with laboratory-fabricated substrates. However, a statistical analysis conducted at a 95 percent confidence interval indicated that there was no statistically significant difference between the two chip seals. Based on the results obtained from this preliminary study, the research team recommended using laboratory-fabricated substrates to meet the objectives of the research project.

Before closing the discussion on this task, it must be noted that the research team abandoned the idea of capturing the impact of change in loading magnitude during the abrasion cycles. This was because of the difficulty involved in precise measurement of the vertical and horizontal forces acting on the specimens because of the dynamic loading as well as the time and budget constraint of the project.

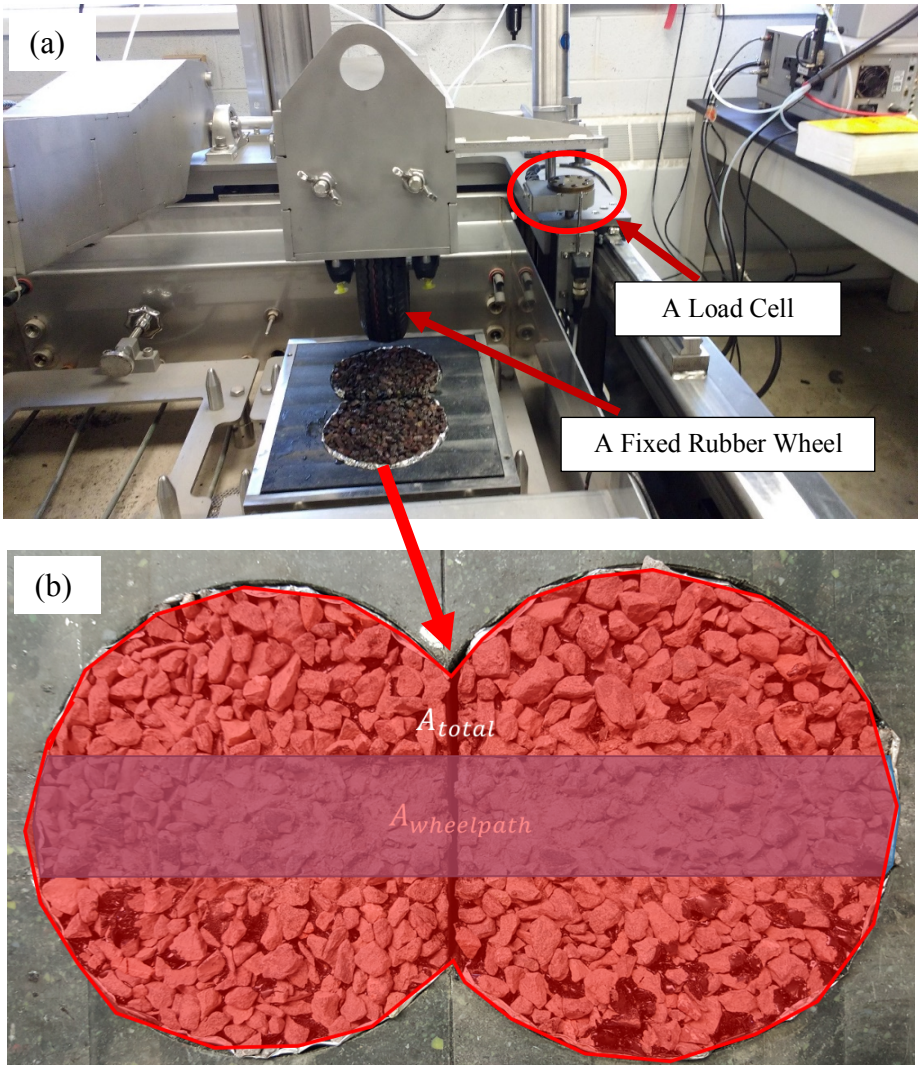

Figure 6-1 Illustration of (a) HWT device test set-up for evaluating the effect of substrate types, (b) area of the tire loading.

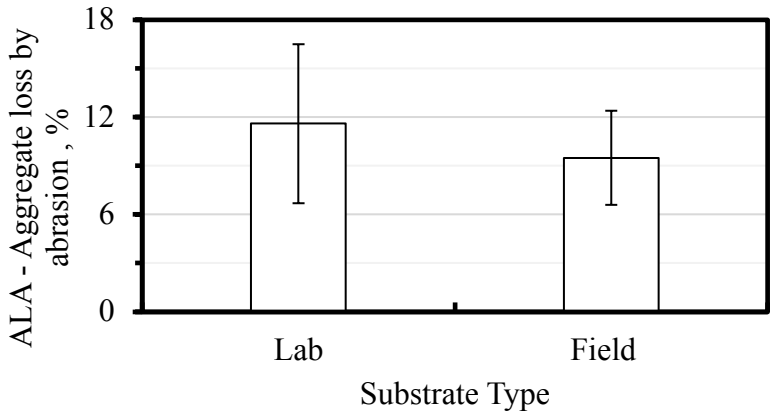

Figure 6-2 Effect of substrate type on aggregate loss.

6.3 Effects of Chip Seal Components on Aggregate Loss

The percentage of aggregate loss by hand brushing (ALB) as a function of the EAR is depicted in Figure 6-3 for the emulsion-based chip seals. The percent ALB is nearly identical for the specimens prepared with Natural aggregates across the EAR, and the ALB corresponded, on average, to 3.9 percent. In the case of the specimens made with slag, the percent ALB decreased as the EAR increased from 0.39 to 0.42 gal/yd^2, then nearly stayed constant (about 8 percent) with any further increase in the EAR. The overall average for the ALB was 9.9 percent. The observed trend in the ALB implies that once a certain EAR is achieved, or a certain percent embedment value is reached, any further increase in the EAR would have no apparent effect on the bond between the aggregates and the emulsion binder, and accordingly on aggregate loss by hand brushing. Additionally, considering the scattered trend and the variability in the data shown in Figure 6-3, the effect of the emulsion type on the percent ALB is not evident. Furthermore, Figure 6-3 also shows that the magnitude of the percent ALB for the specimens with slag is higher in comparison to the counterpart specimens, which was as a result of the excessive AAR used for the chip seals with slag aggregates.

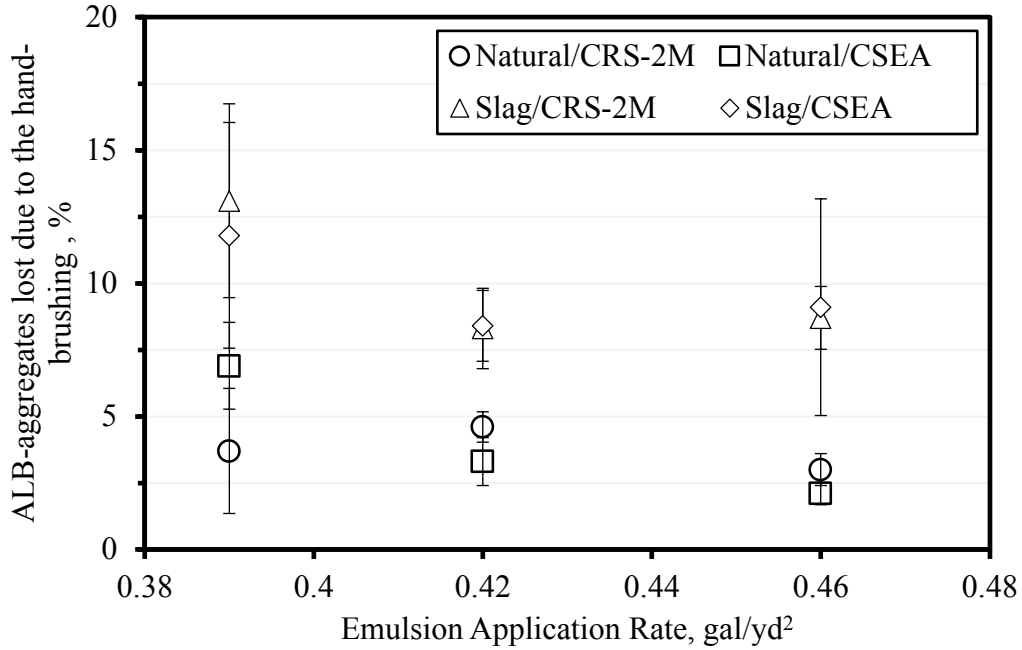

Figure 6-3 Aggregate loss by hand brushing for the emulsion-based chip seals.

Figure 6-4 presents the percentage of aggregate loss by abrasion (ALA) as a function of the EAR for the emulsion-based chip seals. It must be noted that the HWT device abrasion test and associated procedure developed for this research were one of the first-kind used in simulating the abrasion effect on chip seals and was a very harsh test compared to other tests used for quantifying chip seal aggregate loss. Relatively low specimen to specimen variability of the data shows a promise for this test. The overall average COV observed for the chip seal specimens was 14 percent for this test, with a maximum COV of 37.3 percent. It should be indicated that only three data points out of twelve observations resulted in a COV that was higher than 20 percent. Such outcome showed the suitability of the HWT device abrasion test for chip seals, but further

studies are needed to confirm this outcome and to investigate the repeatability and reproducibility of the test.

Nevertheless, the percent ALA for the emulsion-based chip seals was ranged from 15.7 to 37.3 percent. As it can be seen from Figure 6-4, in general, the percent ALA is decreased while the EAR is increased, owing to the increase in the level of percent embedment. The figure also indicates that the emulsion type does not show a discernable pattern with respect to the percent ALA. In other words, the emulsion types used in this research do not have an impact on the chip seal performance with respect to the aggregate loss susceptibility. Another reading from the figure indicates that the specimens with natural aggregates perform better than the specimens with slag when the aggregate loss is of concern. The chip seals with natural and slag aggregates exhibited an overall average ALA of 22.4 and 31.5 percent, respectively. It is commonly believed that chip seals with cubical aggregates (i.e., slag) perform better than the chip seals with flaky aggregates (i.e. natural), however the results presented here show otherwise. Several factors could have contributed to such outcome. First, since the aggregate types used were not the same type, the aggregate-emulsion compatibility could have played a role in such observation. Also, the gradation distributions of the aggregates were different. Moreover, the possible variations in the aggregate-binder microstructure (i.e. orientation, percent embedment, as well as aggregate interlock) between the two chip seals possess a great potential for the observed trend. The numerical study addressed one aspect of this trend, as presented later in this chapter.

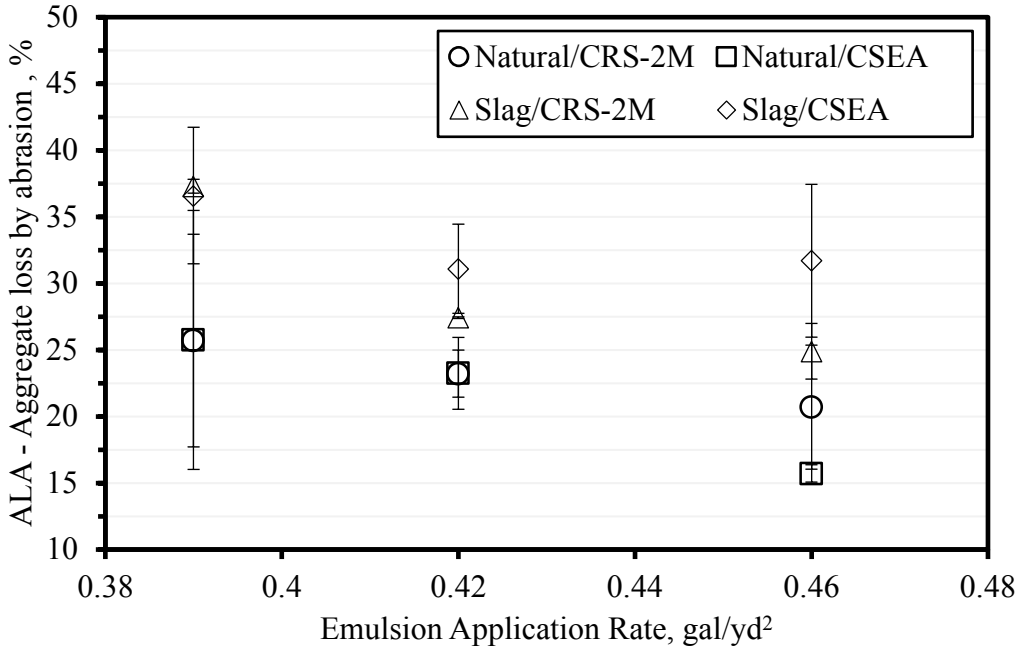

Figure 6-4 Aggregate loss by abrasion for the emulsion-based chip seals.

The cumulative aggregate loss (CAL) for the emulsion-based chip seals is presented in Figure 6-5. The trends and discussion made for the ALB and ALA hold for the CAL as well. This is an expected outcome as the CAL is the combined loss of the two indices. On an average basis, the CAL was 24.9 and 37.4 percent for the chip seals with natural and slag aggregates, respectively. This shows that the aggregate loss for chip seals with natural aggregates was 33.4 percent less than that the aggregate loss for the chip seals with slag aggregates.

Figure 6-6 through Figure 6-8 present the aggregate loss indices for the hot-applied chip seals. As shown in Figure 6-6, the change in the magnitude of the percent ALB with respect the BAR is nearly identical to that of the emulsion-based chip seals, with an overall average ALB of 5.6 percent. This trend suggests that the optimal percent embedment for the hot-applied chip seals was reached as well.

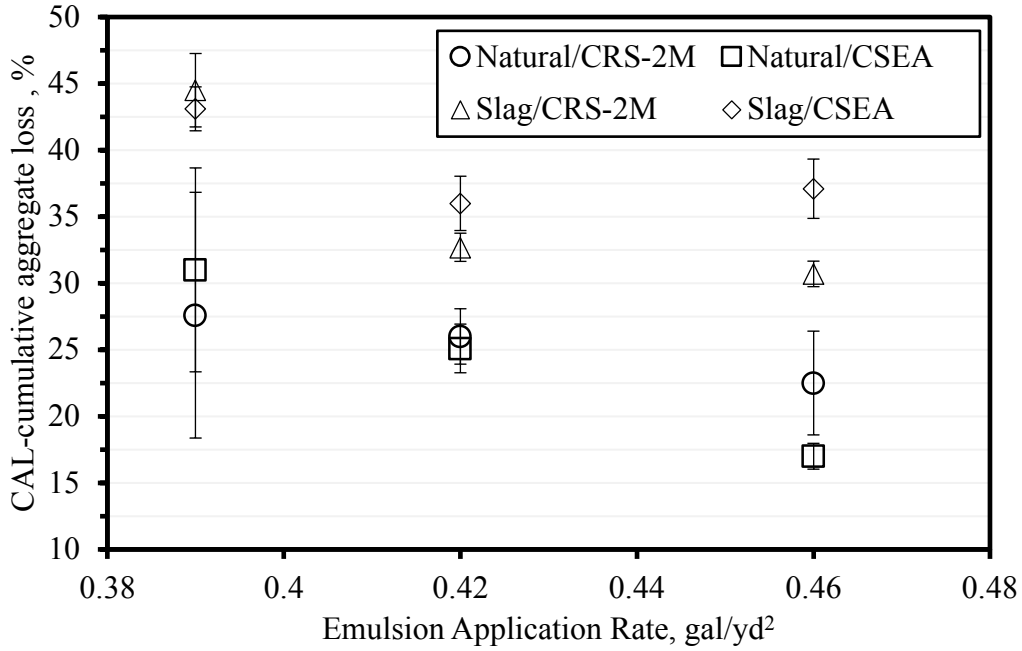

Figure 6-5 Cumulative aggregate loss for the emulsion-based chip seals.

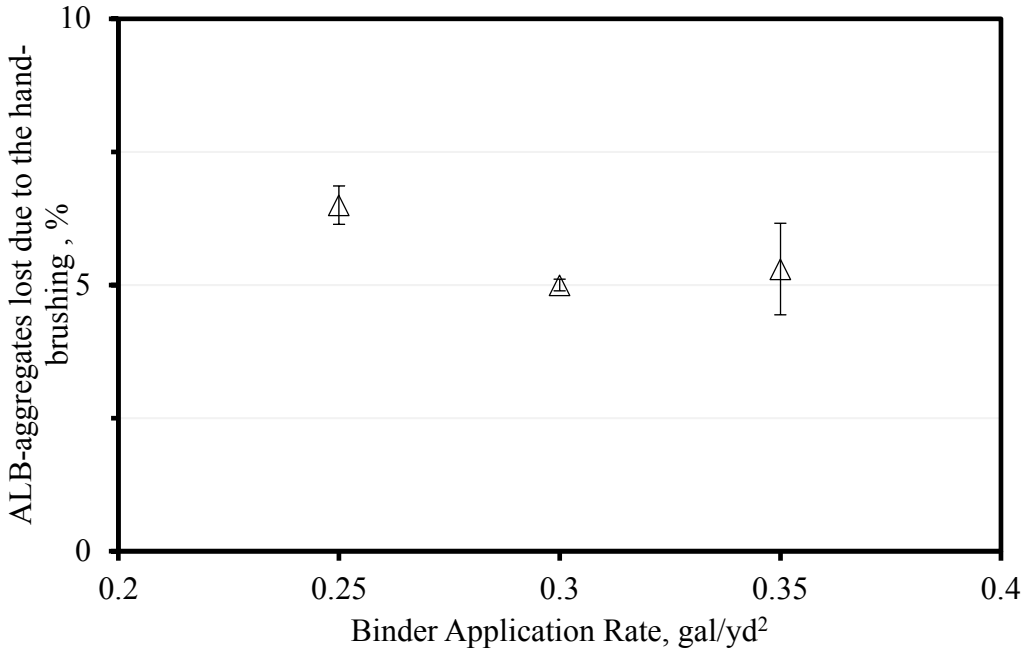

Figure 6-6 Aggregate loss by hand brushing for the hot-applied chip seals.

Figure 6-7 depicts the percent ALA for the hot-applied chip seals. The percent ALA ranged from 25.5 to 39.4 percent, with an overall average of 30.6 percent. As shown in the figure, the percent magnitude loss of the ALA is minimal when the BAR is increased from 0.30 to 0.35 gal/yd^2, suggesting that, on the basis of the available BAR range, a threshold of BAR or percent embedment value is reached. The cumulative aggregate loss (CAL) for the hot-applied chip seals is presented in Figure 6-8. Similarly, the trend in CAL is similar to trends observed for the other two indicies, as expected. The overall average CAL was 33.5 percent for the hot-applied chip seals.

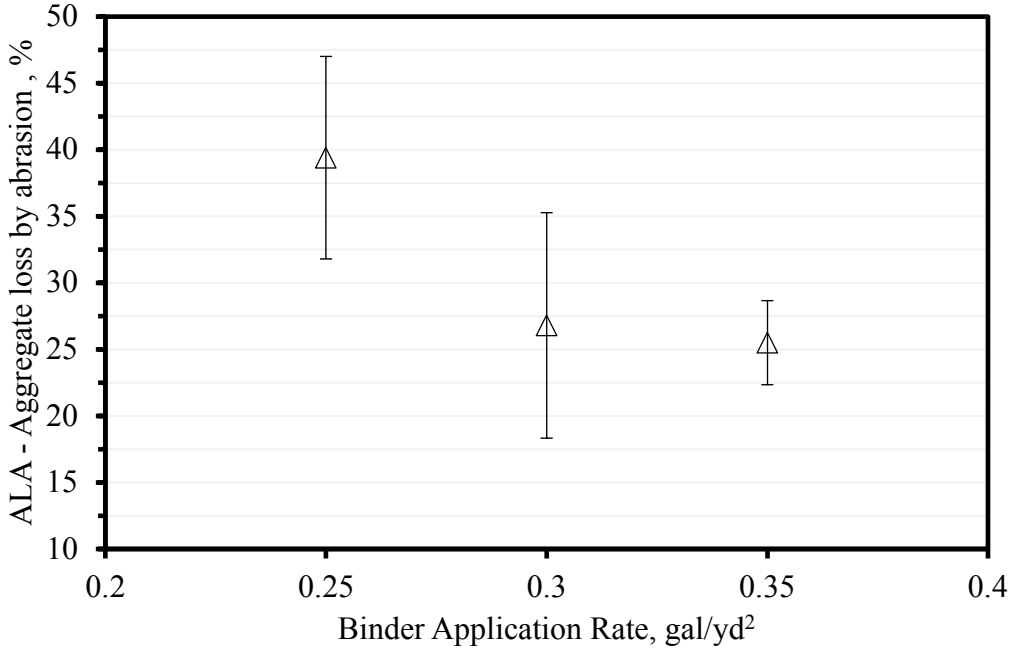

Figure 6-7 Aggregate loss by abrasion for the hot-applied chip seals.

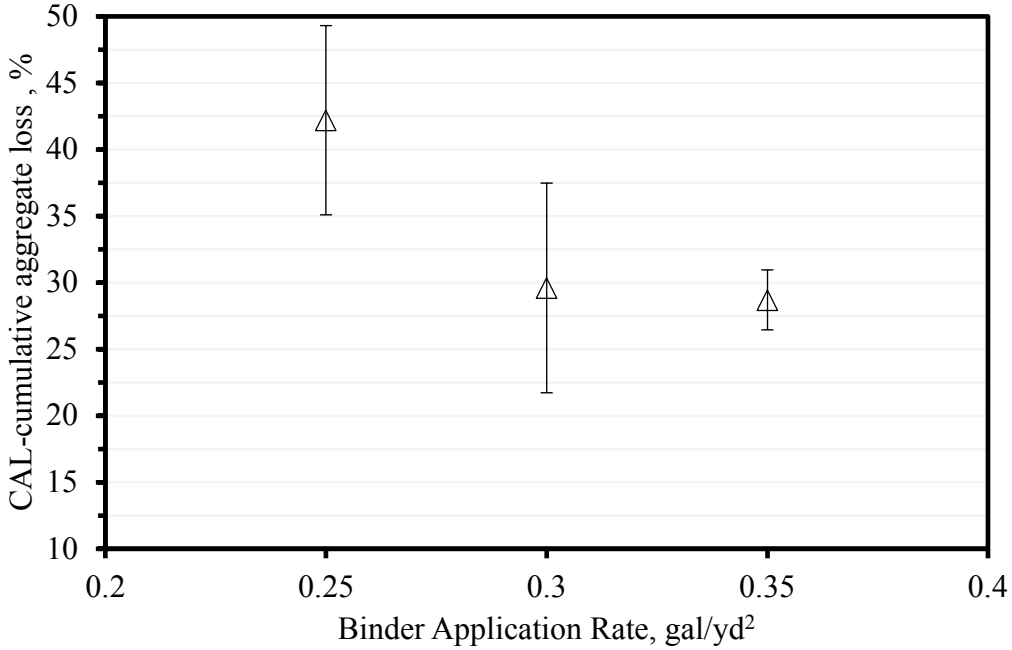

Figure 6-8 Cumulative aggregate loss for the hot-applied chip seals.

In light of the percent average CAL values, the laboratory performance rank of the chip seals analyzed in this research from the perspective of chip seal aggregate loss would be as follows; emulsion-based chip seals with natural aggregates, hot-applied chip seals, and emulsion-based chip seals with slag aggregates. This is if they were to be placed in the same location. However, it should be noted that a typical practice for the hot-applied chip seals is that the aggregates are pre-coated for better retention. Thus, the magnitude of percent loss would have been lower for the hot-applied chip seals if the aggregates were pre-coated. This statement is not meant to endorse the hot-applied chip seals. The results of a comparative life-cycle cost analysis would be able to properly rank the chip seals for their performance.

A study by Adams and Kim indicated that there is generally, an increase in the amount of aggregate loss with respect to the increase in the initial macrotexture magnitude of chip seals (Adams and Kim, 2014). However, despite a moderate trend in one direction, the data presented in the cited reference showed a considerable scatter. The possible relationship between the initial estimated texture depth (ETD) and the aggregate loss was also investigated in this study. As indicated previously, the initial estimated texture depth of the emulsion-based chip seals was obtained from the 3D image analysis. Figure 6-9 presents the aggregate loss by abrasion with respect to the initial estimated texture depth. As shown in the figure, there is no definitive relationship between the initial ETD and the aggregate loss. Such a high scatter in data implies that the initial ETD is not a proper parameter for the performance evaluation of chip seals when the aggregate loss is of concern.

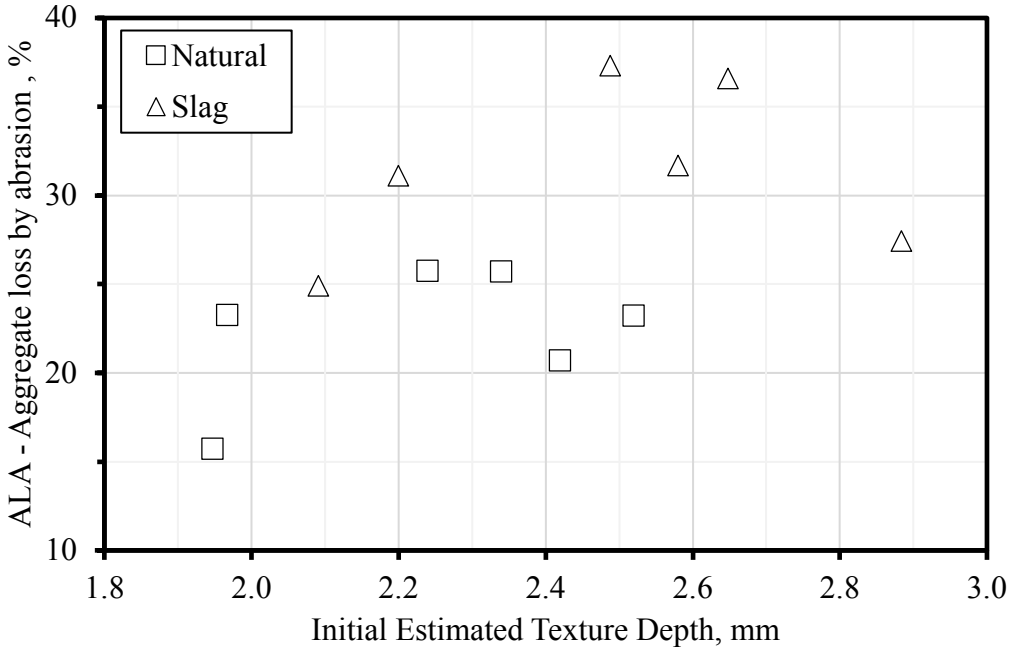

Figure 6-9 Relationship between the aggregate loss by abrasion and the initial estimated texture depth.

However, from a theoretical point of view, the initial ETD should have provided a relationship with the aggregate loss. This is because, in the case of idealized chip seals which form a one-stone thick layer, the macrotexture captures the accurate level of percent embedment of

aggregates. The results shown in Figure 6-9 suggest that the macrotexture did not capture the entire aggregate-binder microstructure properly. This was evidenced by investigating the relationship between the aggregate loss and the percent embedment calculated from the macrotexture as well as the percent embedment measured from the image-based 'each aggregate method'. The percent embedment (PE) of aggregates can be measured from the macrotexture (ETD) and average least dimension (ALD) of aggregates using Equation 6.4 (Shuler *et al.*, 2011).

$$PE = \frac{ALD - ETD}{ALD} \times 100 \quad (6.4)$$

The percent embedment of aggregates was calculated from Equation 6.4 and plotted against the corresponding aggregate loss value for each of the chip seal specimen fabricated in this study. The results are presented in Figure 6-10.

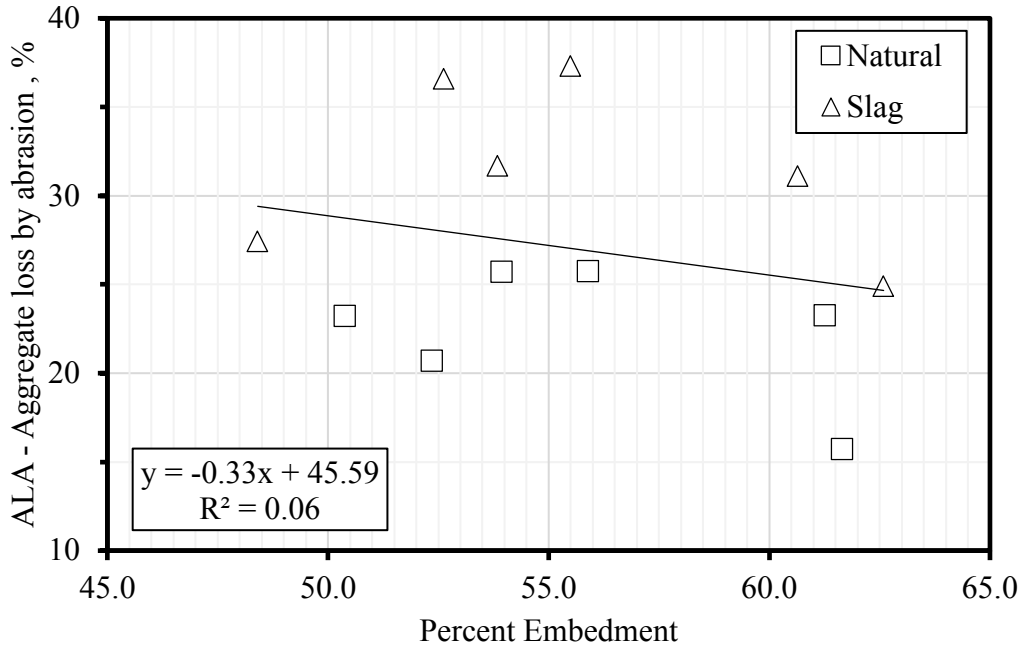

Figure 6-10 Relationship between the aggregate loss by abrasion and the percent embedment measured from the initial ETD.

As shown in Figure 6-10, the percent embedment computed from Equation 6.4 did not produce a clear trend or relationship with the chip seal aggregate loss, as also evidenced by a very low coefficient of determination (R^2) value at 6 percent. This conclusion strongly supported the study objective of the previous and this MDOT project, which was aimed at developing a standard test procedure to directly and accurately calculate the aggregate percent embedment. As stated in the previous report, the percent embedment calculated from the macrotexture measurements is heavily dependent on major assumptions which do not reflect the field conditions. As also shown in this research, the chip seal aggregates do not fully align on their flat side right after construction. However, the macrotexture measurement assumes that the aggregates are aligned on their least dimension. Additionally, the macrotexture-dependent percent embedment does not account for aggregates that are overlapping on each other in the chip seal aggregate-binder structure. Also, it

does not capture the penetration of aggregates into the existing pavement, nor the surface variations of the existing pavement, all of which can impact the performance of chip seals to a great extent.

Figure 6-11 displays the relationship between the percent embedment calculated from the image-based 'each aggregate method' and the aggregate loss for the emulsion-based chip seals. As shown in Figure 6-11, the relationship between the percent embedment and the aggregate loss is much stronger as compared to the texture-based percent embedment (R^2 = 74%). The results clearly show the power and versatility of the developed procedure for determining the percent embedment of aggregates.

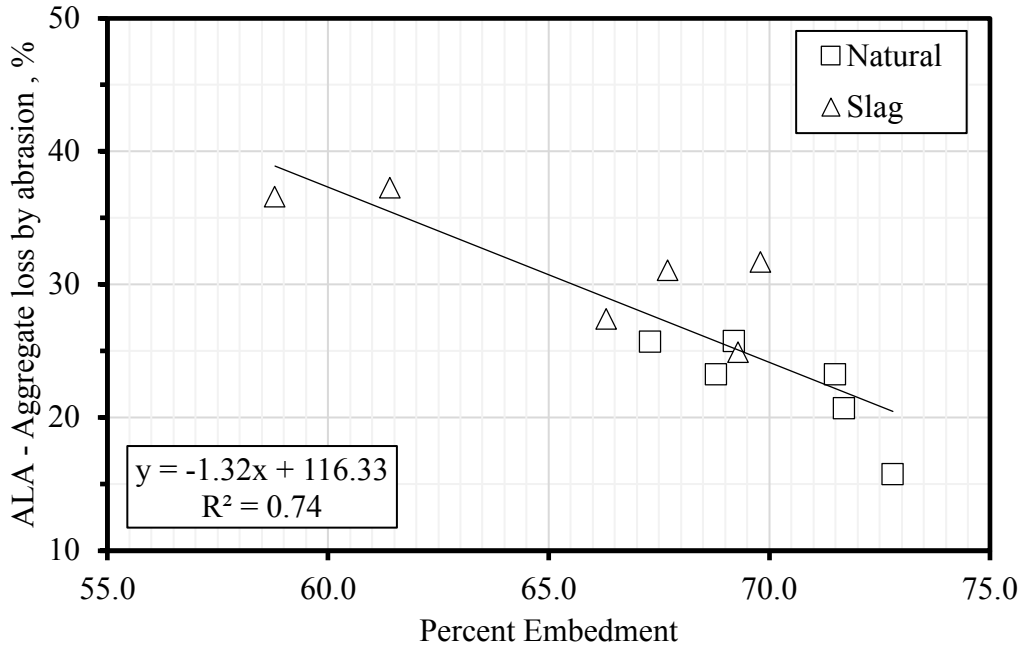

Figure 6-11 Relationship between the aggregate loss by abrasion and the percent embedment measured via the digital image analysis.

6.4 Establishing Percent Embedment Limit for Aggregate Loss

The main objective of this research was to establish performance-based minimum and maximum limits of the percent embedment of aggregates in chip seal treatments considering the aggregate loss and bleeding distresses, respectively. To that end, the threshold for the pass-fail criteria of the percent aggregate loss was needed to be able to select a limiting percent embedment value.

The review of literature indicated that an aggregate loss of 10 percent is consistently used for ranking performance of chip seals based on the laboratory testing(Lee and Kim, 2008, 2010; Miller, Arega and Bahia, 2010; Johannes, Mahmoud and Bahia, 2011; Wasiuddin *et al.*, 2013). This failure limit of 10 percent is usually used for the test results obtained from the sweep test as described in ASTM D7000. The sweep test is intended to evaluate the curing characteristics of emulsion-based chip seals to determine the time required for the chip seal to sufficiently cure before traffic is allowed. The curing time is determined on the basis of the 10 percent limit (Shuler *et al.*, 2011). This test method has also been utilized (with modifications) by several researchers

to investigate the effect of several other variables on performance characteristics of chip seals using the reference aggregate loss value of 10 percent (Miller, Arega and Bahia, 2010; Johannes, Mahmoud and Bahia, 2011; Aktaş *et al.*, 2013; Wasiuddin *et al.*, 2013; Rizzutto *et al.*, 2015; Howard *et al.*, 2017). However, such limit was not applicable to the HWT device abrasion test. The resultant aggregate loss in the HWT device abrasion test, even with a relatively high EAR, was always more than 10 percent. This is because of the significant differences in the nature and magnitude of the applied load in the HWT device test as opposed to the sweep test. In sweep test, a nylon strip brush with an attached weight of 3.3 pounds (1500 gr) and with the capability of a free-floating vertical movement is used to exert the load on the chip seal surface for a duration of 60 seconds. On the other hand, the initial load on the wheel in the HWT device is 125 pounds, and the fixed rubber wheel is abraded through the specimen surface.

In the NCHRP Report No.837, the researchers utilized the *Vialit* test to quantify aggregate loss to establish the emulsion performance-grade specifications. The aggregate threshold limit for low-volume traffic was established at 35 percent based on the known performance of an emulsion on low-volume traffic in a -19°C region. The aggregate threshold limits for medium and high-volume traffics were set at 30 and 25 percent, respectively, which were determined on the basis of the observed abrupt aggregate loss results with the decrease in temperature (Kim *et al.*, 2017). Even though the aggregate loss threshold limits were somewhat reasonable for the magnitude of aggregate loss observed in this research, they were subjectively derived based on a specific chip seal performance and the trend observed through experimental data. Additionally, the climatic region (-19°C) of the chip seal with known performance is also different than the climatic region of Michigan.

The MDOT chip seal specification (12SP505 (A)) defines a chip seal application as a failure when the loss of cover aggregate exceeds 40 percent of a segment length of 528 feet (which is based on a consensus decision of industry partners and MDOT staff). As per the specification, the allowable threshold limit of 40 percent is a linear measurement and not dependent on the area of the aggregate. However, personal communication with MDOT research panel indicated that even though the aggregate loss is taken as a linear measurement, the aggregate loss usually occurs across the entire pavement width. Hence, the research team decided to set the allowable threshold limit as 40 percent for aggregate loss. It should be noted that, for a given aggregate type, the area-based aggregate loss of 40 percent equates to the weight-based aggregate loss of 40 percent.

The correlation between the percent embedment and aggregate loss by abrasion is plotted for the emulsion-based and hot-applied chip seals in Figure 6-12 and Figure 6-13, respectively. It is evident from the figures that none of the chip seals tested in this study exhibited aggregate loss more than the allowable limit of 40 percent. To determine the percent embedment limit for a given aggregate source, a linear regression fit was first applied to each data set to establish the relationship between the parameters of interest. Then, the percent embedment intercept point with the aggregate threshold limit was determined and set as a minimum percent embedment limit for the chip seal resistance to the aggregate loss.

As it can be determined from the regression equations in Figure 6-12, the minimum allowable percent embedment limit for chip seals with natural aggregates is 58.4 percent, whereas it is 55.7 percent for the chip seals with slag aggregates. Similarly, the percent threshold limit for the hot-applied chip seal is 71.6 percent, as illustrated in Figure 6-13.

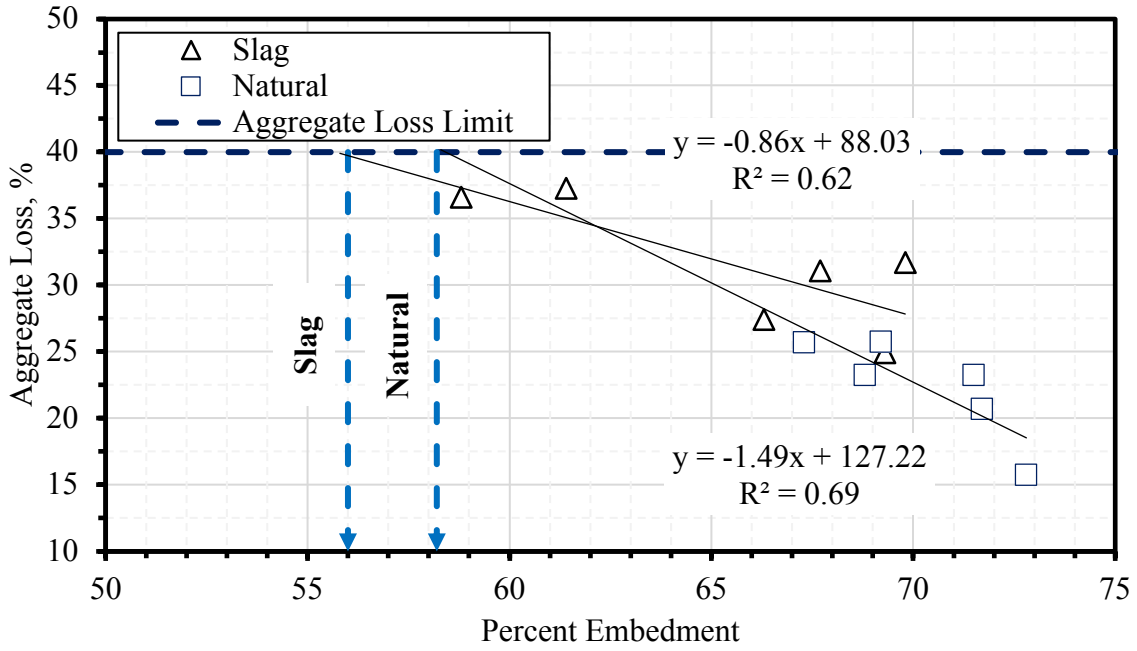

Figure 6-12 Minimum percent embedment limits for the emulsified chip seals used in this study.

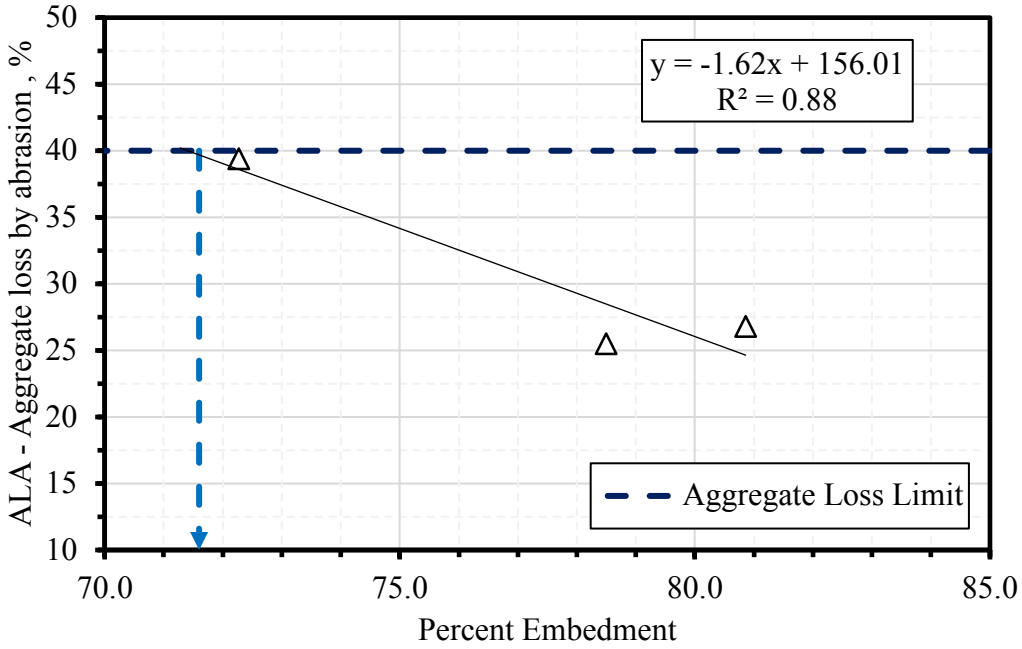

Figure 6-13 Minimum percent embedment limit for the hot-applied chip seal used in this study.

6.5 Evaluating the Effect of Aggregate Shape on Aggregate Loss via Finite Element Analysis

It has been observed from laboratory testing and analysis that flaky (natural) aggregates have been performing better than that of cubical(slag) aggregates. It has been argued that, although shape attributes better potential performance to cubical aggregates, the complex aggregate to aggregate interaction and aggregate interlocking effect yields better performance to flaky aggregates. To verify the hypothesis, 2D finite element (FE) analysis was performed on chip seals to understand this phenomenon through mechanistic approach.

This part of the study was performed in two (2) phases:

- In phase I, finite element (FE) models were developed from actual 2D images of these chip seal specimens and analyzed to compute tensile strains at aggregate-binder interface. Tensile strain was chosen to be the parameter for explaining and characterizing chip seal aggregate loss behavior.

- In phase II, the 2D images of chip seal samples were artificially processed to create multiple percent embedment (PE) conditions ranging from 25% to 94%. The main objective of this phase was to study the effect of PE on comparative performance of both the aggregate types.

6.5.1 Phase I: Finite Element Model development

In phase I, chip seal specimens (Figure 6-14(a)) prepared for imaging were cut using a small tile saw and slices were obtained for image analysis (Figure 6-14(b)). In addition, a blue playdough was applied on the top of slices for the purpose of creating a color contrast and followed by taking images of the vertical cross section of each side of the slices using a document camera (Figure 6-14 (c)). These images were further processed to specify certain pixel intensities to the different zones of the cross section (Figure 6-14 (d)). The images were then converted into a finite element mesh as shown in Figure 6-14(e), using an in-house algorithm developed in MATLAB®. Material properties for the finite element mesh were assigned based on the pixel intensity shown in Figure 6-14(d). Aggregate is represented by the white color. The asphalt binder layer is represented by black color and substrate hot mix asphalt (HMA) pavement by a dark grey color. Aggregate is modelled as an elastic material, whereas asphalt binder and substrate HMA were assigned viscoelastic properties using Prony series coefficients. Table 6-1 shows the relaxation times (τ_i) and dimensionless elastic coefficients (g_i) or the generalized Maxwell model (Prony series). All these images were converted into finite element meshes for further analysis (tensile strains). The traffic/tire loading function used in this study was based on the recommendation from previous researchers (Huurman, 2010). Figure 6-15 shows the stress functions, which are based on actual stress measurements from a moving tire. The loading pulse was a combination of two individual functions: 1) a step function characterizing the vertical load variation, 2) a sinusoidal function fitting lateral load pattern. Further details and equations regarding the loading functions can be found in other research (Huurman, 2010).

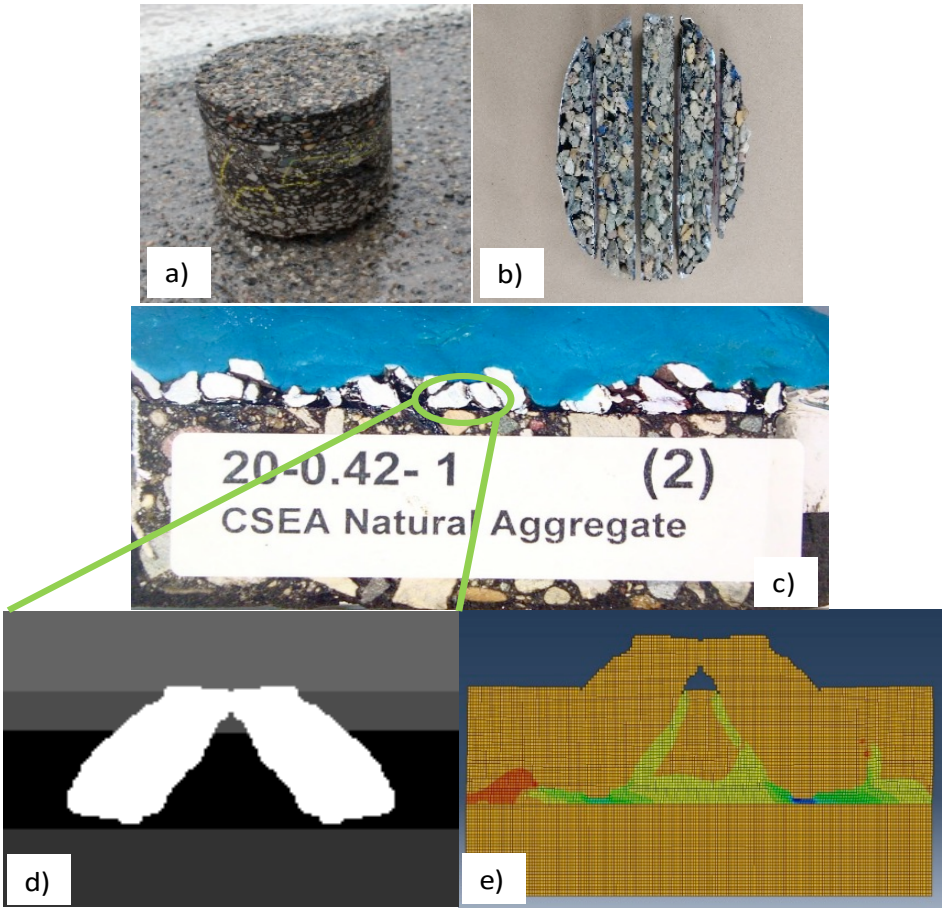

Figure 6-14 Stepwise procedure for FE mesh creation

Table 6-1 Prony series coefficients for asphalt binder and substrate HMA

Asphalt Binder		Asphalt Mixture (substrate)	
G_o (Pa) =	11.9E+06	G_o (Pa) =	6.90E+09
τ_i (s)	g_i	τ_i (s)	g_i
1.000E-03	0.4009	1.000E-07	0.1344
4.642E-03	0.2462	1.668E-06	0.1212
2.154E-02	0.1731	2.783E-05	0.1683
1.000E-01	0.0984	4.642E-04	0.1845
4.642E-01	0.0505	7.743E-03	0.1676
2.154E+00	0.0205	1.292E-01	0.1172
1.000E+01	0.0075	2.154E+00	0.0624
4.642E+01	0.0019	3.594E+01	0.0268
2.154E+02	0.0005	5.995E+02	0.0092
1.000E+03	0.0001	1.000E+04	0.0071

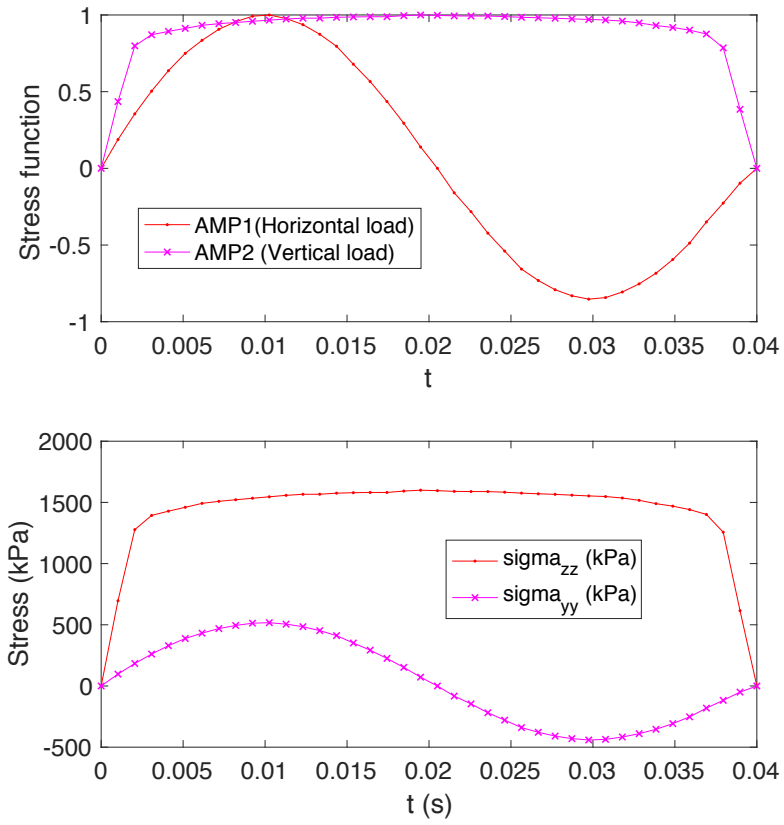

Figure 6-15 Illustration of the horizontal and vertical stress functions applied to the top of the chip seals: Top graph is the normalized shape functions; bottom graph is the actual stresses applied (after Huurman 2010)

Screen shots of the FE models with tensile strain results are shown in Figure 6-16. As shown, the magnitudes of tensile strains (in red color) developed at the interface of aggregate and binder in case of cubical aggregate type are significantly higher as compared to the flaky aggregate. Maximum tensile strain (ϵ_T^{max}) at the aggregate-binder interface was thought to relate to the aggregate loss and selected as a parameter for comparison of different aggregates. Figure 6-17 shows the ϵ_T^{max} results for both the aggregate types. It can be observed that the ϵ_T^{max} value in case of flaky aggregate type is significantly lower than that of cubical aggregate. The flaky aggregates 'lean' and support each other leading to a stronger aggregate network through interlocking. This network of aggregates helps resist the traffic loads (especially transverse component) thus leading to a better resistance to aggregate loss. This proves that the aggregate interlocking and complex aggregate to aggregate interaction plays an important role in aggregate loss behavior of chip seals. Owing to these reasons, the natural aggregates show better performance than the slag aggregates.

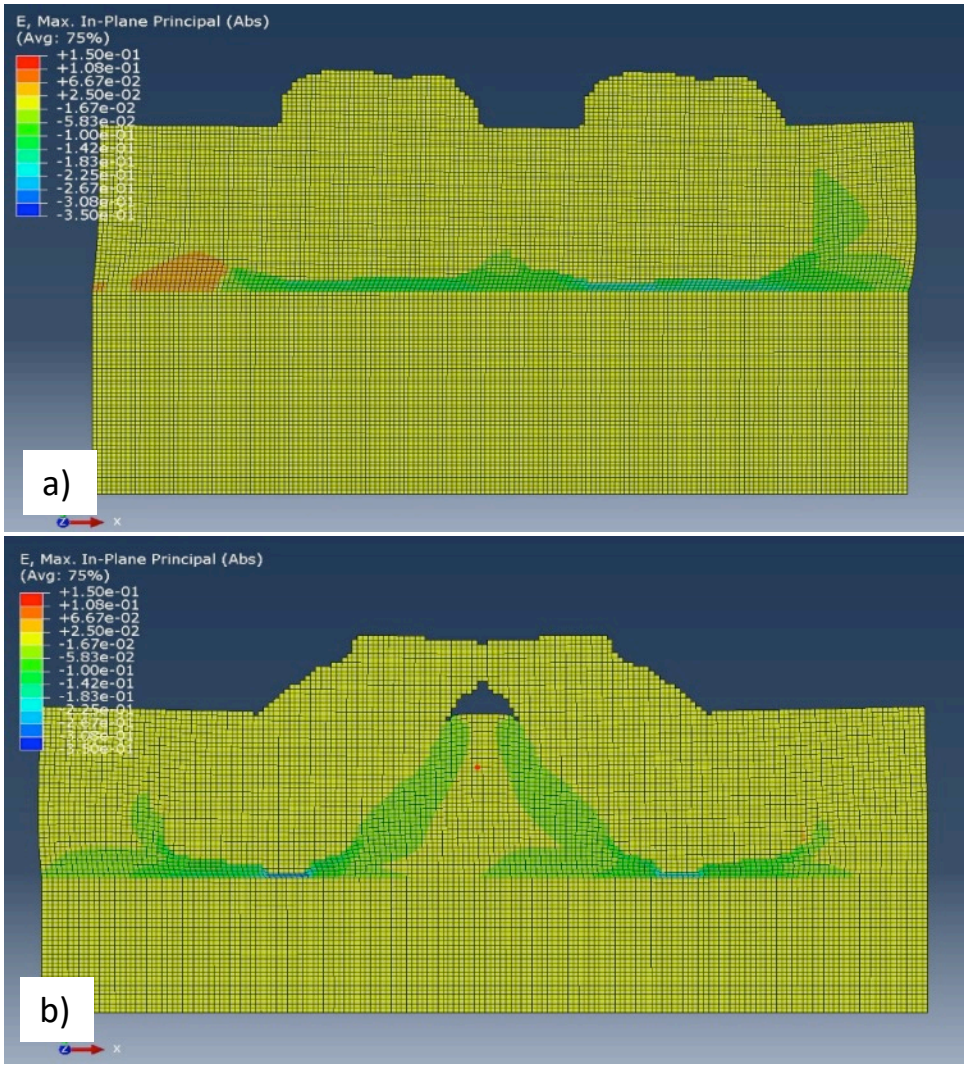

Figure 6-16 Screen shots of tensile strain results for FE models

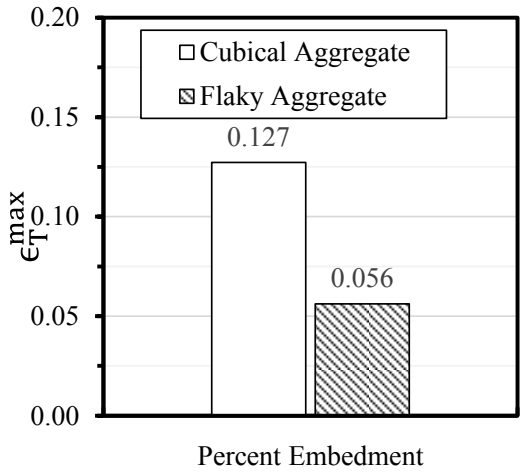

Figure 6-17 ϵ_T^{max} results

6.5.2 Phase II: Study of Effect of Percent Embedment on Aggregate loss

In phase II, the actual images of chip seal samples were artificially processed to create multiple percent embedment (PE) conditions: 25, 50, 72 and 94%. This exercise was performed for both the aggregate types. Further, procedure described for phase I was also followed to convert these images to FE mesh patterns. These FE meshes were further analyzed to compute tensile strains at the aggregate-binder interface. Figure 6-19 and Figure 6-19 show the principal strain profiles for the FE model simulations at different PEs for cubical and flaky aggregate type respectively. Figure 6-20 depicts the ϵ_T^{max} results at all three temperatures, for specimens with different PEs for cubical and flaky aggregate type respectively. ϵ_T^{max} decreased with increase in PE. For PE of 25%, comparatively higher values of tensile strains can be observed (at interface) in both the cases. The tensile strains lead to loss of bond between aggregate and binder, which eventually result in aggregate loss. With increase in PE, more surface area of aggregate comes into contact with the asphalt binder. This results in the aggregates getting braced and supported from all the sides by asphalt binder. The overall matrix thus attains higher strength, resulting in lower aggregate loss. Furthermore, at all the PE conditions, the tensile strain values are comparatively lower in the instance of flaky aggregate type, making it a stronger chip seal type with respect to aggregate loss susceptibility.

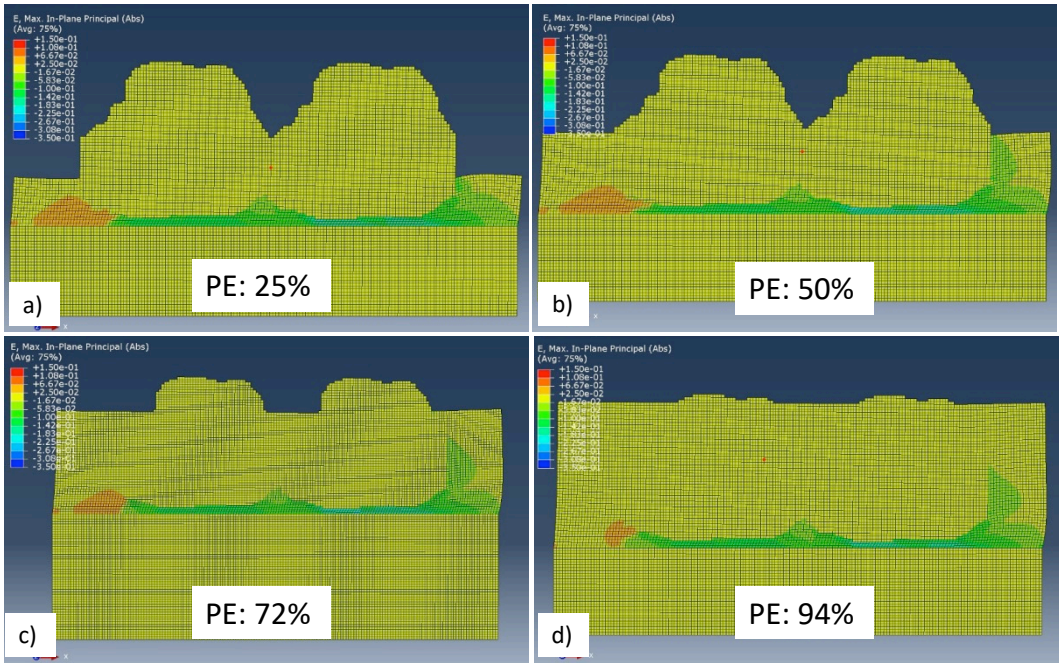

Figure 6-18 Principal strain distribution at for different PEs for cubical aggregate type

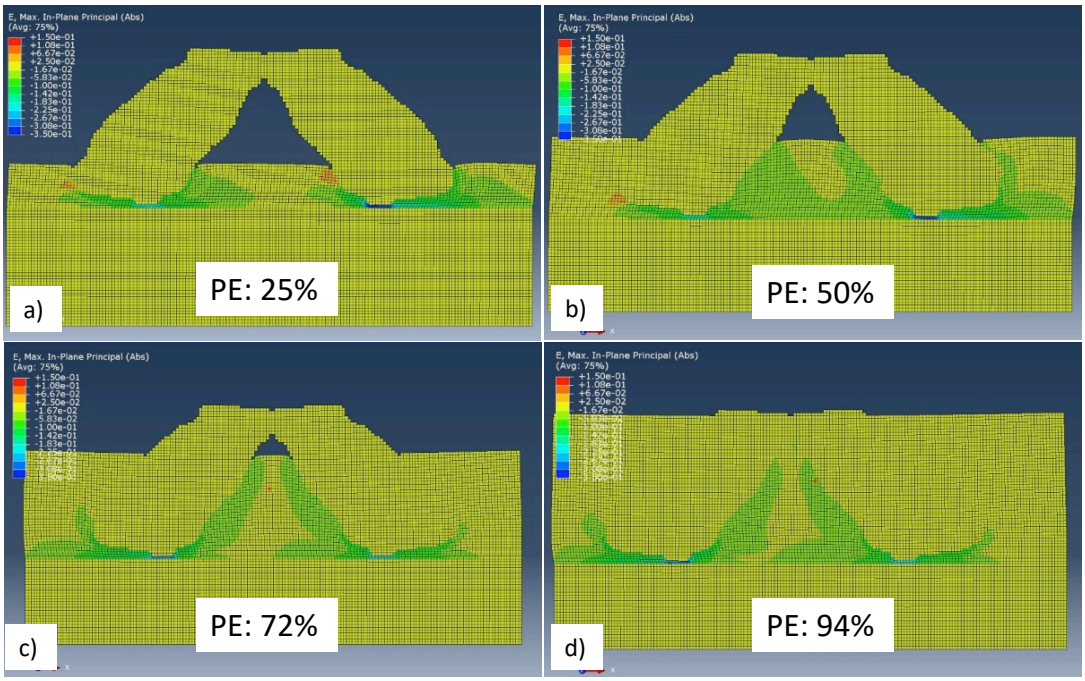

Figure 6-19 Principal strain profiles for different PEs for flaky aggregate type

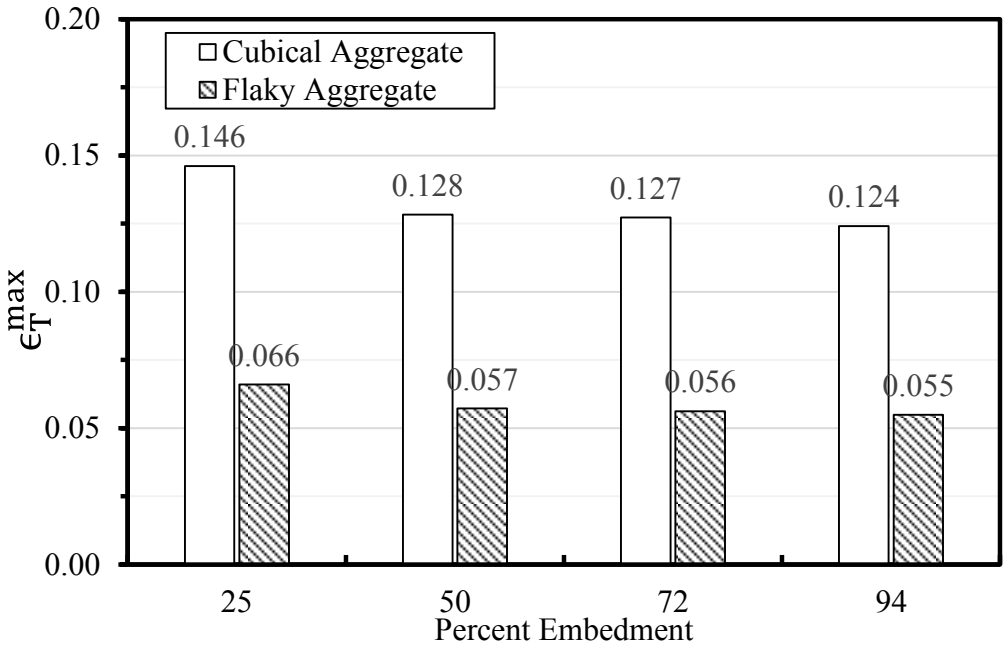

Figure 6-20 Maximum strain (ϵ_T^{max}) results at different percent embedments for cubical and flaky aggregate types

7. EVALUATION OF BLEEDING

In this chapter, the effects of emulsion application rates, emulsion types, aggregate types, and percent embedment of aggregates on the susceptibility of chip seals to bleeding are presented. The amount of bleeding was quantified through 2D digital image analysis. Additionally, the chip seal macrotexture at each of the HWT device trafficking intervals was obtained from the 3D image analysis and was correlated to the bleeding potential of the chip seals to explore the relationship between macrotexture and the bleeding of chip seals. Based on the test results, the percent embedment threshold limit was established for each aggregate source used in this study. The methodology, results, and discussion are presented in the following subsections.

7.1 Quantifying Bleeding

The modified HWT device test, the details of which are provided in Chapter 4, was utilized to run the bleeding tests. The chip seal specimens prepared in this study were subjected to reciprocating wheel loads of the HWT device. A total of 2500 wheel cycles were applied on each specimen at a temperature of 54°C under wet conditions. The amount of bleeding was quantified before the start (no loading) and after the end (final loading) of the HWT device test for each specimen used in this study. Additionally, the extent of bleeding was also determined at 200, 500, and 1000th cycles for the emulsion-based chip seals. This was done to evaluate the progression of bleeding in chip seals due to traffic. Hence, it yielded a set of five observations for emulsion-based chip seals, consisting of 0, 200, 500, 1000, and 2500th cycles.

As described previously, the 3D surface profile of each specimen was constructed by photogrammetric software (3DF Zephyr) to obtain the macrotexture of the chip seals. Additionally, the top plane view of the 3D surface at each HWT device test interval was cropped to obtain the portion of wheel path to determine the percent binder area. The images were further processed by the revised CIPS software developed by the research team and converted to binary images. An example of the screenshot of the image acquisition and processing phase using 3DF Zephyr software and the corresponding binary image is illustrated in Figure 7.1. The percent binder area (referred to as 'percent bleeding (PB)' in this report) for each specimen was determined from the binary images using Equation 7.1.

$$PB = \frac{A_{black}}{A_{total}} \times 100 \quad (7.1)$$

where A_{black} is the area covered by black pixels (representing the binder), and A_{total} is the total area of the image. For the data presented in this chapter, a total of 128 images were generated and processed to determine the amount of percent bleeding using Equation 7.1.

It should be noted that the early attempts of obtaining 2D images from the plan view by simply taking a picture did not reveal images with sufficient contrast between the aggregates and the binder. In addition, the glare on the binder, due to its glossy nature, created artificial 'white' spots leading to incorrect determination of binder area. Since the 3DF Zephyr software generates the 3D surface profile using multiple images taken from different views, the glare from the surrounding light sources can be eliminated. The final 2D plan-view image, as shown in Figure 7.,1 is free from any glare, leading to accurate results of PB.

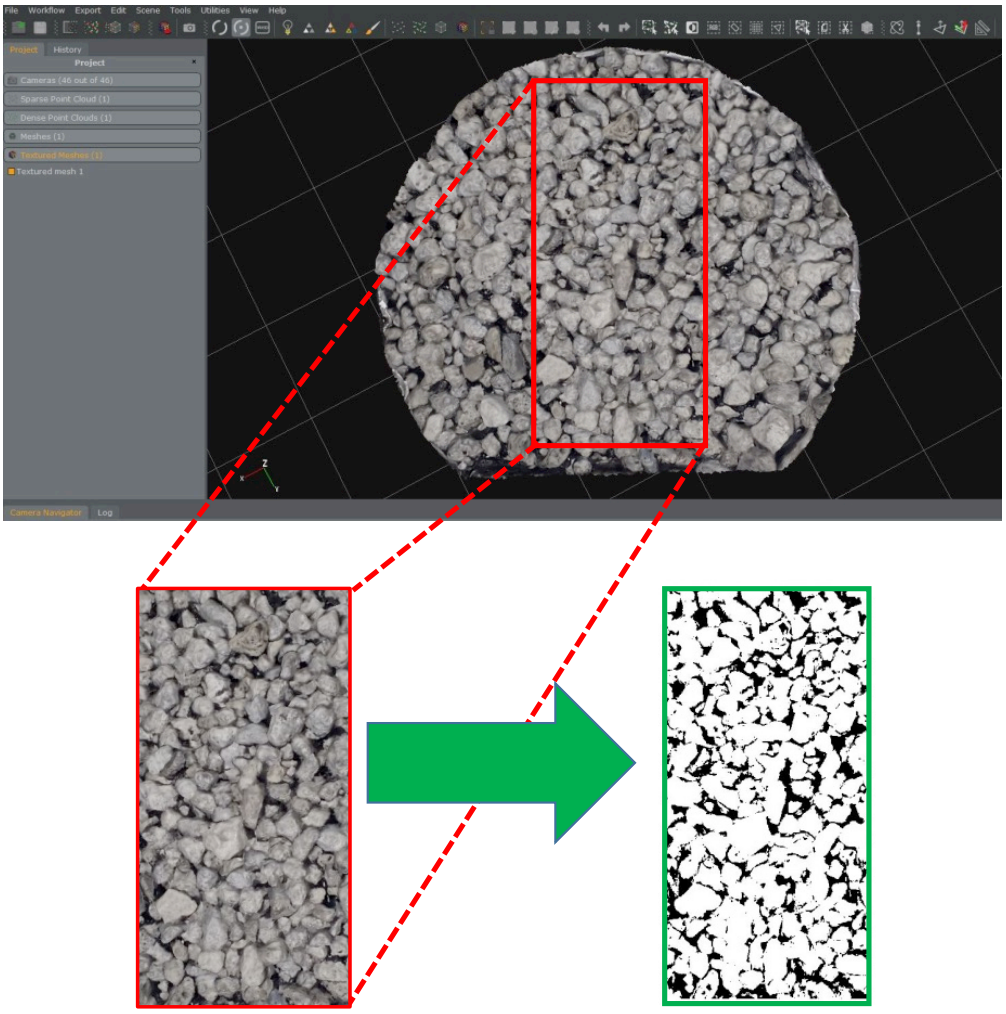

Figure 7-1 Illustration of image processing for calculating the percent binder area.

7.2 Effect of Traffic and Chip Seal Component Variables on Bleeding

The progressions of bleeding under the HWT device loading at a range of emulsion application rates (EARs) are shown in Figure 7-2 through Figure 7-5 for the emulsion-based chip seals. Before presenting the observations from the figures, it must be stated that the specimen to specimen variability observed under the HWT device bleeding test was very low, indicating the great potential for a test to be standardized for assessing the susceptibility of chip seals to bleeding. The maximum value of the coefficient of variation (COV) among all data generated was 19.7 percent, with an average COV of 7.5 percent. As for the abrasion test, additional studies are also needed to validate the repeatability and to investigate the reproducibility of the bleeding test. Figure 7-2 through Figure 7-5 indicate that, generally, the percent bleeding increases steeply after initial traffic and then transitions into a steady phase. Confounding effects of traffic and visco-elasto-plastic behavior of the binder at relatively high-test temperature lead to re-alignment of the aggregates and the initial increase in the percent bleeding.

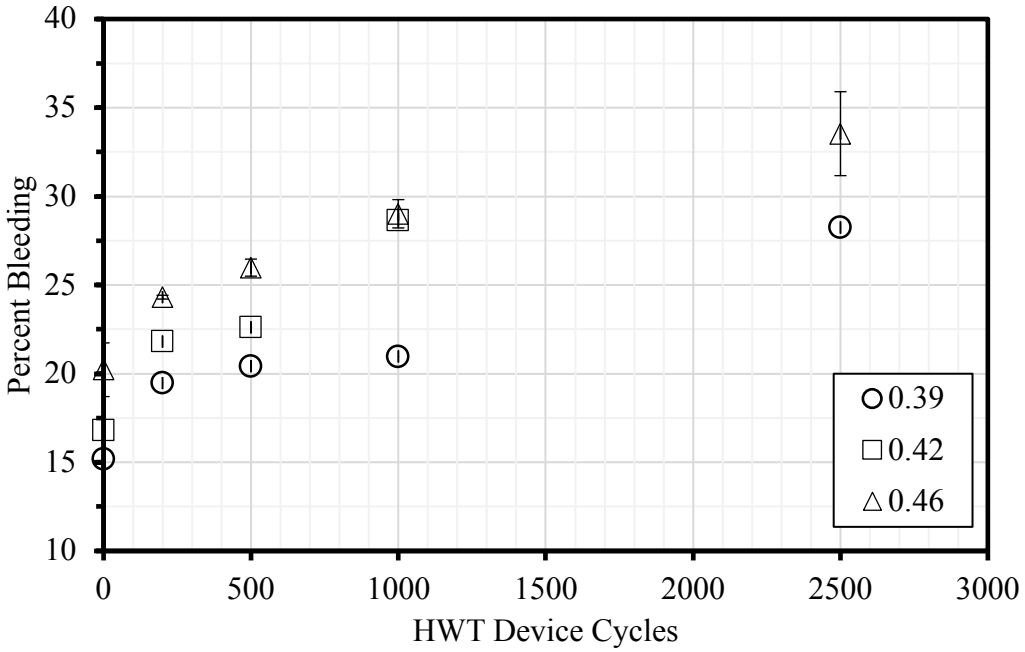

Figure 7-2 Progression of the bleeding under the HWT device loading for the chip seals with natural aggregates and CRS-2M emulsion at a range of EARs.

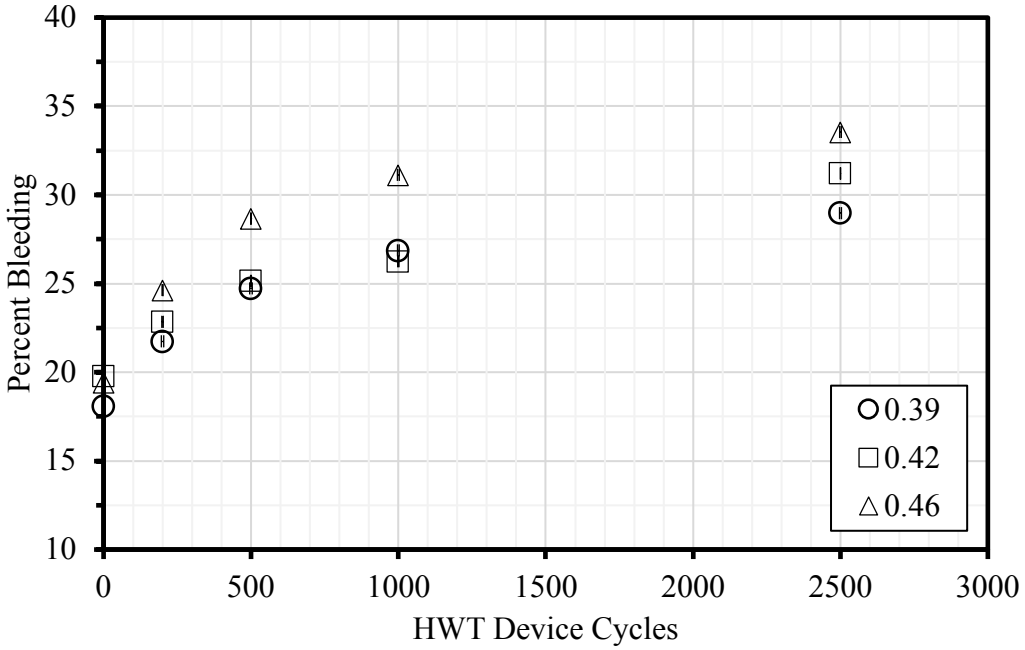

Figure 7-3 Progression of the bleeding under the HWT device loading for the chip seals with natural aggregates and CSEA emulsion at a range of EARs.

It is postulated that the percent bleeding after the transitioning point is mostly dominated by the rheological properties of the binder. With the effect of additional traffic, the rate of change of plastic flow starts increasing, and eventually reaches the 'tertiary flow' stage, where the rate of change of plastic flow increases, causing the chip seal to 'flow' and fail quickly, as explained earlier in Chapter 4. The data points indicating the abrupt change of the trend in the figures are

indications of those chip seals approaching the tertiary flow stage (i.e. natural aggregates and CRS-2M at the EAR of 0.42 gal/yd^2).

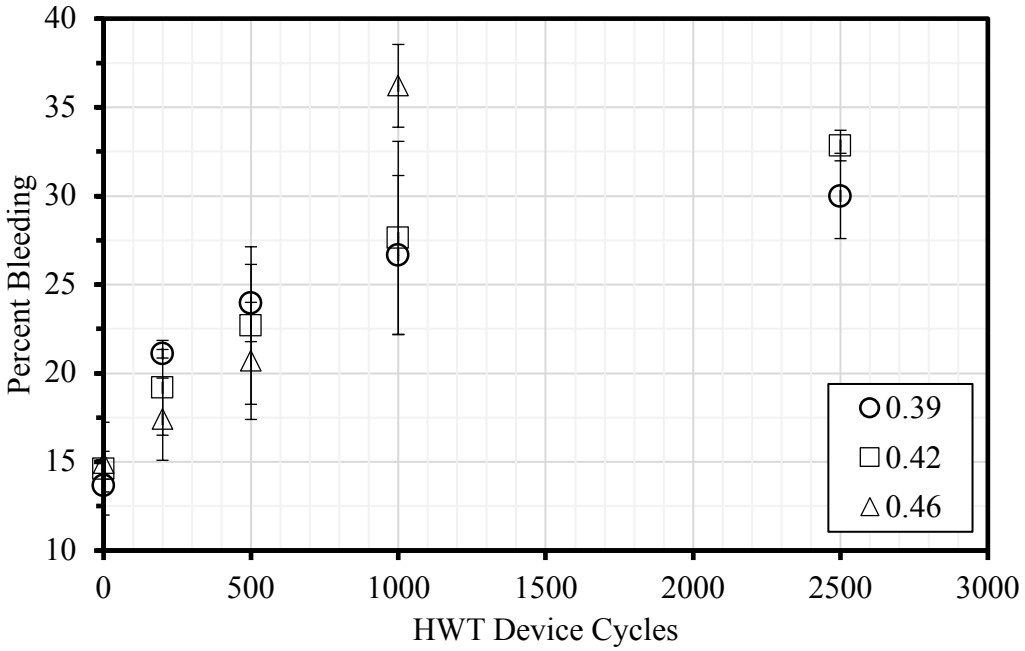

Figure 7-4 Progression of the bleeding under the HWT device loading for the chip seals with slag aggregates and CRS-2M emulsion at a range of EARs.

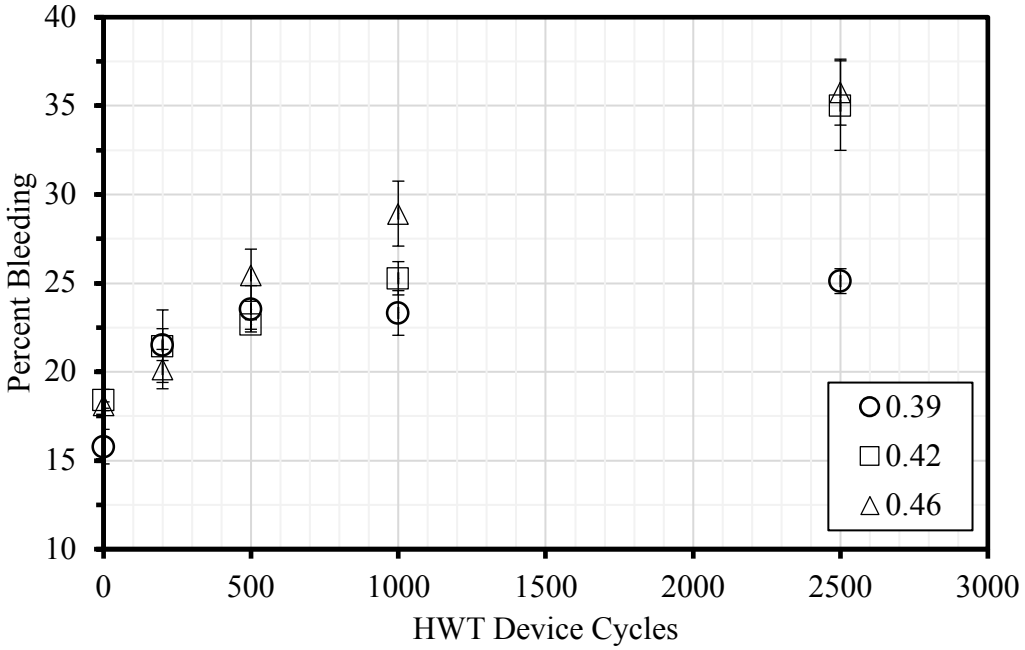

Figure 7-5 Progression of the bleeding under the HWT device loading for the chip seals with slag aggregates and CSEA emulsion at a range of EARs.

Figure 7-6 displays the percent bleeding as a function of EAR for the emulsified chip seals, calculated after the final cycle of the HWT test. Figure 7-6 indicates that there is little or no

difference in the bleeding performance of chip seals for different emulsion types. However, it is worth noting that the specimens that went into tertiary flow were prepared with CRS-2M emulsion. One important, but unexpected observation from Figure 7-6 is that the chip seal specimens with natural aggregates and CRS-2M emulsion at the EAR of 0.46 gal/yd^2 did not bleed, but the same chip seal specimens with the EAR of 0.42 gal/yd^2 showed bleeding. The fact that percent embedment values for the two EARs were within the close range, and (as shown later in this chapter) the two chip seals were around the percent bleeding failure threshold, might have led to such behavior. Figure 7-6 also indicates that the chip seals with slag aggregates, overall, exhibited a higher percent bleeding potential compared to that of the chip seals with natural aggregates. This is consistent with the relative magnitudes of percent embedment of chip seals made with natural and slag aggregates.

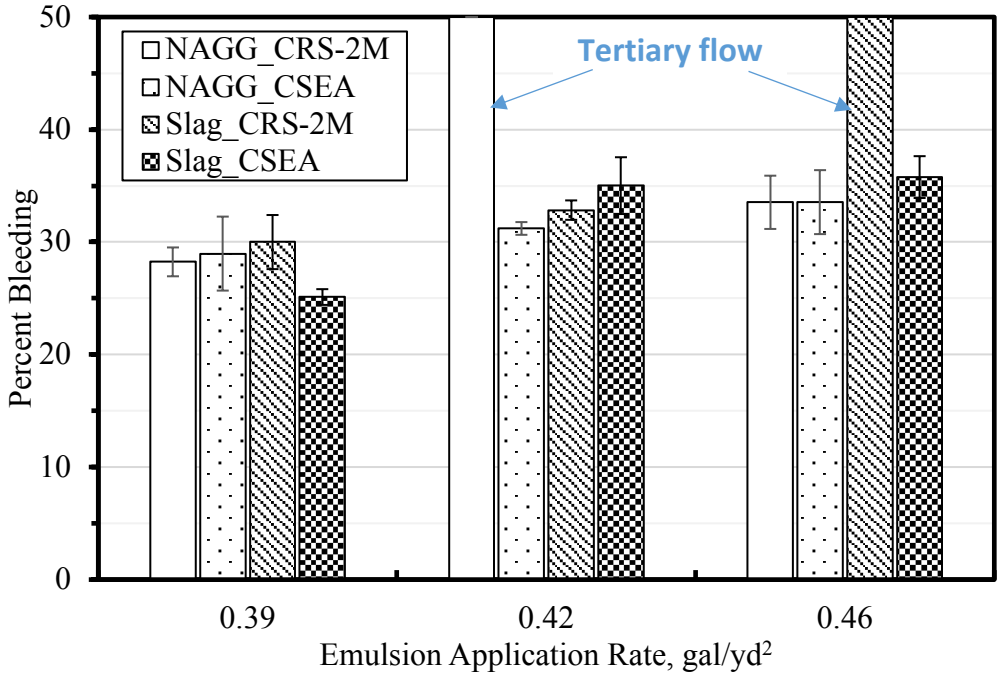

Figure 7-6 Percent bleeding at the end of HWT device test for the emulsified chip seals.

The relationship between the percent embedment and percent bleeding is presented in Figure 7-7 for the chip seals with natural and slag aggregates. It must be noted that the specimens that went into tertiary flow were purposely excluded from Figure 7-7 in order to show the correlation between the two parameters, at least up to the point where full bleeding was occurring. Nevertheless, the strong correlation between the two parameters is manifested by the very high value of the coefficient of determination (R^2). It can be clearly viewed in Figure 7-7 that, for a given percent embedment (e.g., 68%), the chip seal specimens with natural aggregates show less percent bleeding potential than the chip seals with slag aggregates. The chip seals with natural aggregates exhibit about 16.2 percent less bleeding at 68 percent embedment. Better performance of chip seals with natural aggregates could be attributed to the observation that the aggregate-binder microstructure for chip seals with natural aggregates exhibited a more stable structure under the traffic loading. This could be due to better aggregate orientation (more aggregates lying on their flattest side) and a lower level of re-alignment of aggregates under traffic.

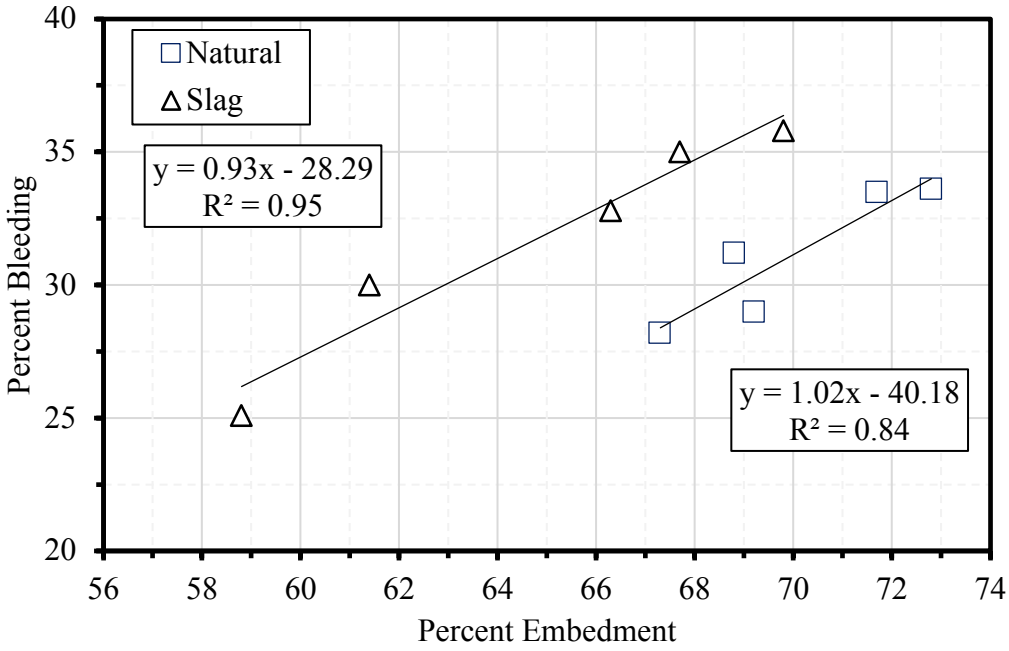

Figure 7-7 Relationship between percent embedment and percent bleeding for the emulsified chip seals.

The percent bleeding as a function of binder application rate (BAR) is presented in Figure 7-8 for the hot-applied chip seals. Like the observation seen in the emulsified chip seals, there is an increase in the percent bleeding with an increase in the BAR, as expected. Additionally, the sudden failure of the hot-applied chip seal at the BAR of 0.4 gal/yd^2 is also evident from the figure. It can be also interpreted from the figure that the bleeding occurs past to 30 percent bleeding region, as observed for the emulsified chip seals. In fact, a linear regression fit applied to the data in the figure (excluding the data point with tertiary flow) indicates that the percent bleeding at the BAR of 0.4 gal/yd^2 corresponds to 33 percent.

The relationship between the percent embedment and percent bleeding is presented in Figure 7-9 for the hot-applied chip seals. Even though there is a relationship between the two parameters for this form of chip seals, it is not as strong as the ones established for the emulsified chip seals, possibly due to the limited data points available for the hot-applied chip seals. Nevertheless, one interesting observation from Figure 7-9 is that the hot-applied chip seals show less bleeding potential even with the higher level of percent embedment when to the emulsified chip seals. For example, the hot applied chip seals with a 75 percent embedment level results in a 26 percent bleeding area. On the other hand, the emulsified chip seals with the same embedment level indicate a bleeding failure for both aggregate sources, as shown in the following section.

7.3 Establishing Percent Embedment Limit for Bleeding

Once again, the main objective of this research was to establish performance-based minimum and maximum limits of the percent embedment of aggregates in chip seal treatments considering aggregate loss and bleeding distresses, respectively. To that end, the threshold for the pass-fail criteria of the percent bleeding was needed to establish a maximum limiting percent embedment value.

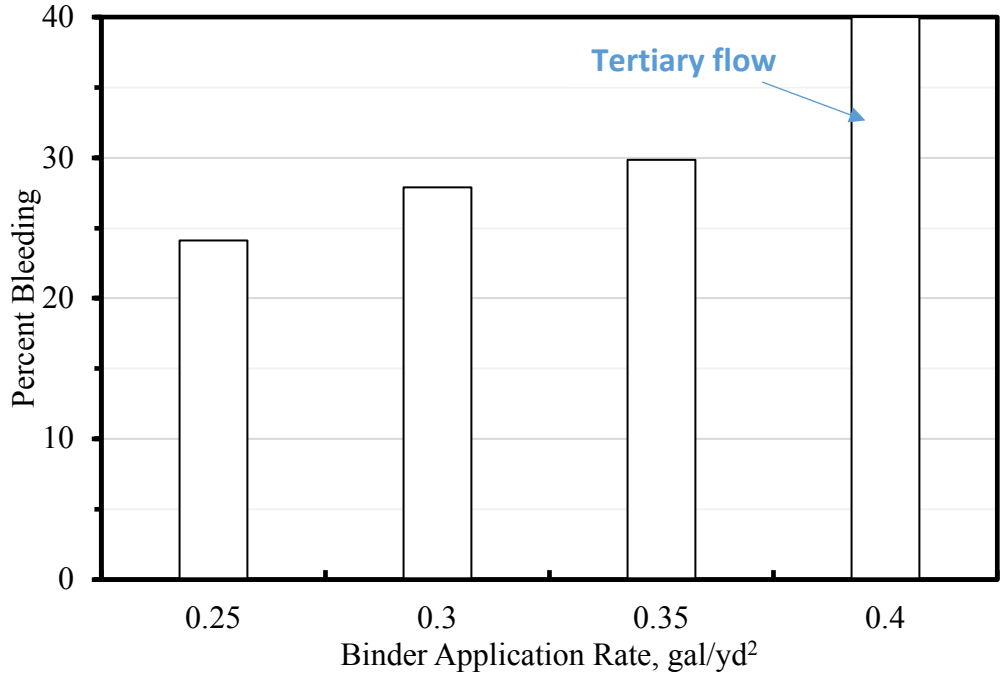

Figure 7-8 Percent bleeding as a function of BAR for the hot-applied chip seals.

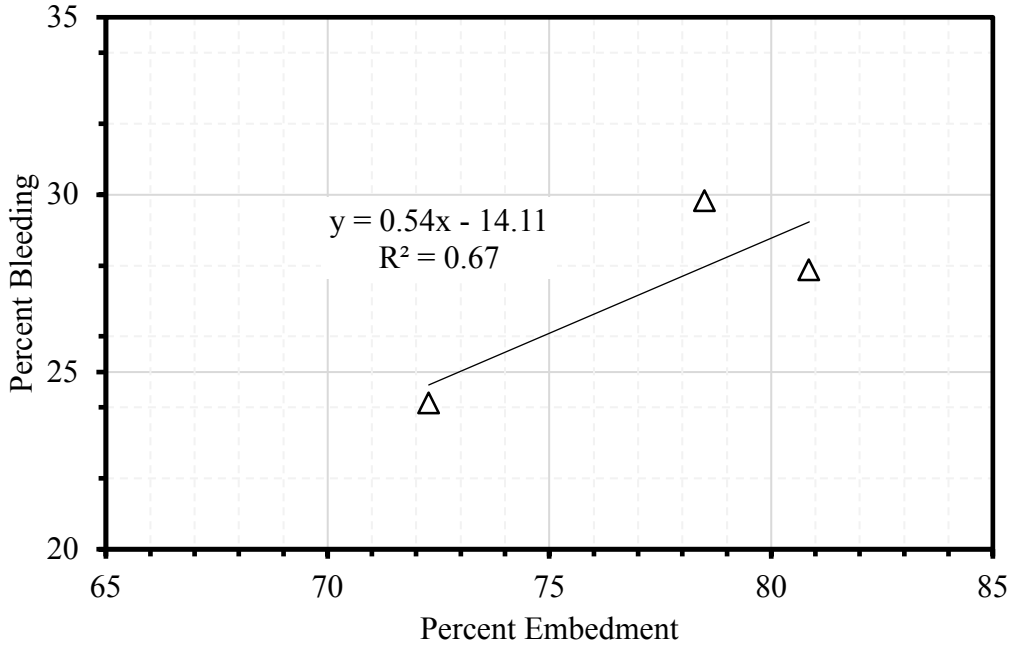

Figure 7-9 Relationship between percent embedment and percent bleeding for the hot-applied chip seals.

Similar to the aggregate loss, there is no unified methodology to define the allowable threshold limit for the bleeding in chip seals. The review of literature indicated that the chip seal macrotexture is a key indicator for evaluating the chip seal bleeding failures, and the most

commonly used macrotexture criteria is the one specified by the New Zealand road authorities. The macrotexture depths of 0.9 and 0.7 mm are defined as a threshold point for retreating New Zealand's chip seal projects accommodating speeds above and below 70 km/h (43 mi/h), respectively (TNZ report, 2005; Gransberg, 2007). Kim et al. (Kim *et al.*, 2017) utilized the MMLS3 test to quantify bleeding in chip seals to establish the emulsion performance-grade specifications. The threshold limit was set to 80 percent for that purpose. As indicated earlier in this report, in a study by Lee and Kim (Lee and Kim, 2008), the percent bleeding area of chip seal specimens prepared at various emulsion and aggregate application rates using an unmodified emulsion was ranged from as low as 30 percent to as high as 90 percent. It was observed that the magnitude of the percent bleeding area was clustered at approximately 40 and 80 percent for the chip seal specimens, and there was not a visible trend when transitioning from one application rate to another for a given EAR or AAR. Even though there is no clear statement in NCHRP Report No. 837 as to why the threshold of 80 percent was selected, the research team believes that the threshold limit of 80 percent was chosen on the basis of the observation in the study by Lee and Kim (Lee and Kim, 2008). Like the aggregate loss failure criteria, the MDOT chip seal specification (12SP505 (A)) defines a chip seal application as a failure when the percent bleeding exceeds 40 percent of a segment length of 528 feet. This allowable threshold limit of 40 percent is a linear measurement and not dependent on the area of the bleeding. However, the personal communication with MDOT research panel indicated that even though the measurement is taken as a linear measurement, the bleeding is usually observed within the entire wheel path. Therefore, it is presumed that the allowable threshold limit of a linear measure of 40 percent for the bleeding is equivalent to the area-based measurement.

In this study, the macrotexture depths of the chip seals did not drop below 1.24 mm. This is because two sets of the chip seals generated in this study showed failure at 1.5 mm texture depth on average. Also, the 0.9 mm criterion is used for assessing chip seals in the field, which may not be applicable to laboratory-produced chip seals that were subjected to accelerated testing at a high temperature. Based on the test results obtained in this research and the research team's experience, it is strongly believed that the bleeding threshold limit of 80 percent is not a reasonable limit for chip seals. A close inspection of the data in NCHRP Report No.837 revealed that the magnitude of the percent bleeding area was around 40 percent with the emulsions having the non-recoverable creep compliance (Jnr) values close to the Jnr values of the emulsions used in this study. The threshold limit of 40% in the MDOT specification is somewhat reasonable value as a failure criterion. However, the chip seal sets that experienced tertiary flow had less than 40 percent bleeding area.

As stated earlier in Chapter 4, the review of New Zealand's chip seal design manual indicated that the aggregate pick up-related bleeding observed in this laboratory study can also happen in the field when the mean texture depth of chip seal is below 1.5 mm and when the viscosity of emulsion is less than 200 Pa.s. (TNZ report, 2005). The relationship between the estimated texture depth and the percent bleeding was plotted to see if the 1.5 mm texture depth had been the reason for the aggregate pick up-related bleeding. The relevant plots are presented in Figure 7-10 and Figure 7-11 for the chip seals with natural and slag aggregates, respectively. As it can be seen from the figures that the relationship between the macrotexture and percent bleeding shows moderate to good correlation for the chip seals with natural and slag aggregates, respectively. Given the variability observed in the macrotexture measurements, the extent of the correlation was very promising, and ensured the soundness of the data generated in this study.

Another important observation from the figures is that when the estimated texture depths are extrapolated using the regression equations (given inside the figures) for both aggregate sources, the resultant curves (shown as a dashed line) were often within reasonable limits. For example, the estimated texture depths corresponding to 0 and 100 percent bleeding levels for the chip seals with natural aggregates are 3.65 and 0.18 mm, respectively. Likewise, the maximum and minimum estimated texture depths for the chip seals with slag aggregates are 3.75 and 0.21 mm, respectively. Those values are within proximity of theoretical values.

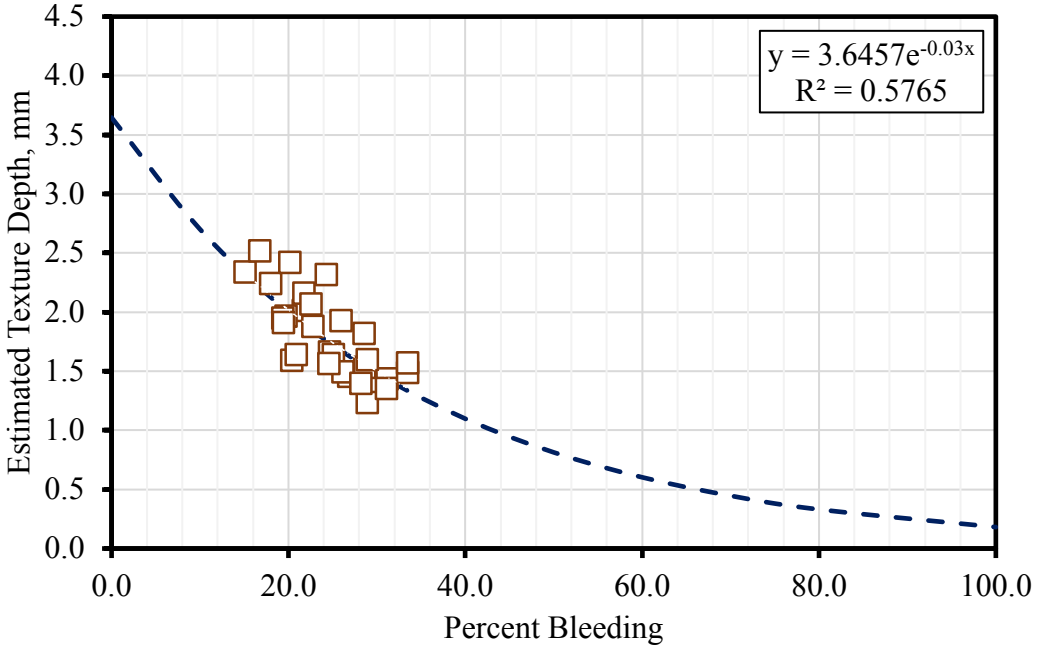

Figure 7-10 Relationship between estimated texture depth and percent bleeding for the chip seals with natural aggregates.

Through the use of the regression equations provided in Figure 7-10 and Figure 7-11, the percent bleeding areas that correspond to a 1.5 mm estimated texture depth were determined for both aggregate sources. The predicted percent bleeding area for the chip seals with natural aggregates was found to be 29.5 percent, slightly higher than the percent bleeding area of 28.6. This was the percent bleeding area observed at 1000th HWT device cycle before the chip seals with natural aggregates and CRS-2M emulsion went into tertiary flow under the HWT device. Likewise, the predicted percent bleeding area for the chip seals with slag aggregates and CRS-2M emulsion was found to be 31.7 percent. Even though this value was less than the failure bleeding area of 36.2 percent for the chip seals of interest, the predicted results overall, coincided with measured or observed laboratory test results, which confirmed that the chip seals failed in this study because they were experiencing the bleeding phenomenon. The research team designated the percent embedment points, at which the full bleeding took place for the chip seals with natural and slag aggregates using CRS-2M emulsion, as maximum percent embedment limits. The maximum allowable threshold percent embedment limit for the chip seals with natural aggregates is 71.5 percent, whereas it is 69.3 percent for the chip seals with slag aggregates. Similarly, the percent embedment threshold limit for the hot-applied chip seal is 83.9 percent. The percent bleeding corresponding to the threshold percent embedment was determined for each aggregate source. For that reason, the correlation between the percent embedment and percent bleeding is first plotted

for the emulsion-based and hot-applied chip seals in Figure 7-12 and Figure 7-13, respectively. Then, a line was drawn from the threshold percent embedment limit until it intercepted with the regression line, as shown in the figures referenced. Then, a horizontal line was drawn to determine the percent bleeding area for each aggregate source. The results indicated that the percent bleeding area was 32.7 and 35.9 percent for the chip seals with natural and slag aggregates, respectively. The percent bleeding area was 31.2 percent for the hot-applied chip seals. The percent bleeding magnitudes indicate agreement with the percent bleeding magnitudes that were observed before the failure of each chip seal in this study.

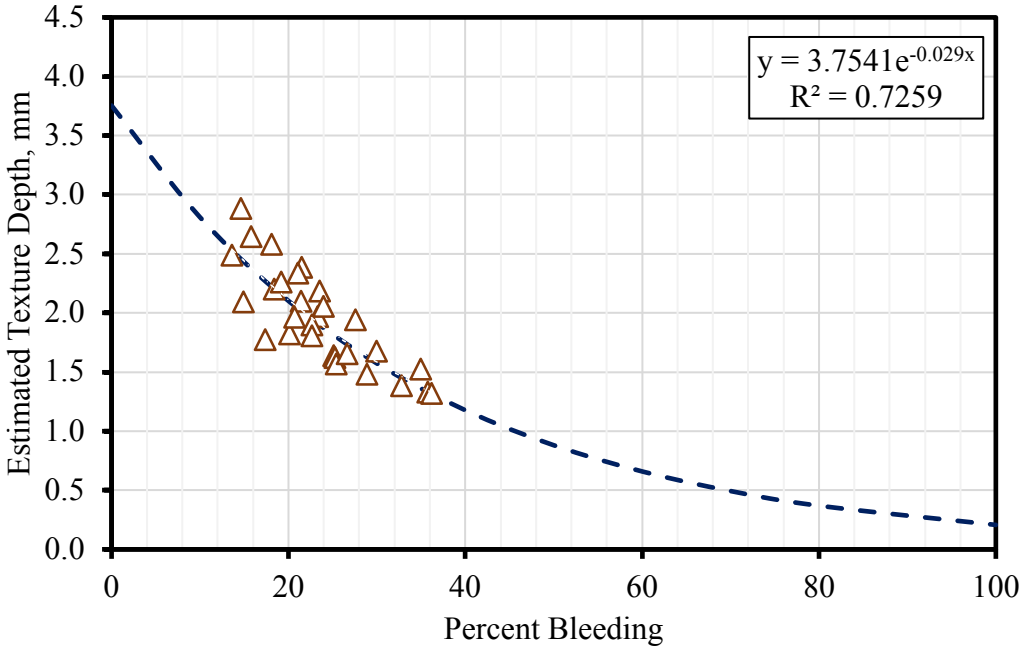

Figure 7-11 Relationship between estimated texture depth and percent bleeding for the chip seals with slag aggregates.

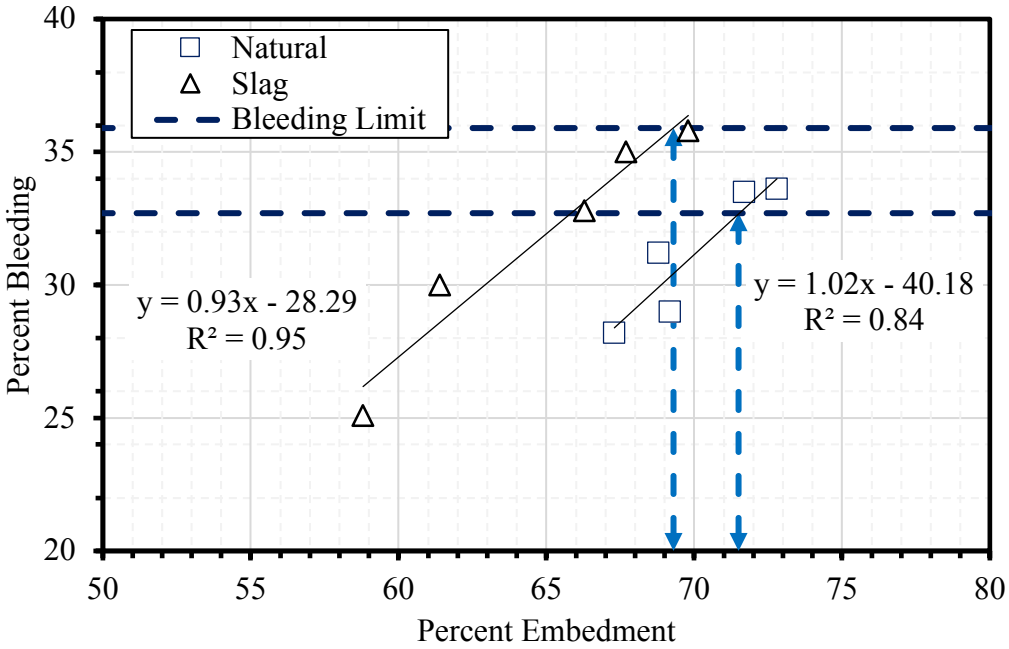

Figure 7-12 Maximum percent embedment limits for the emulsified chip seals used in this study.

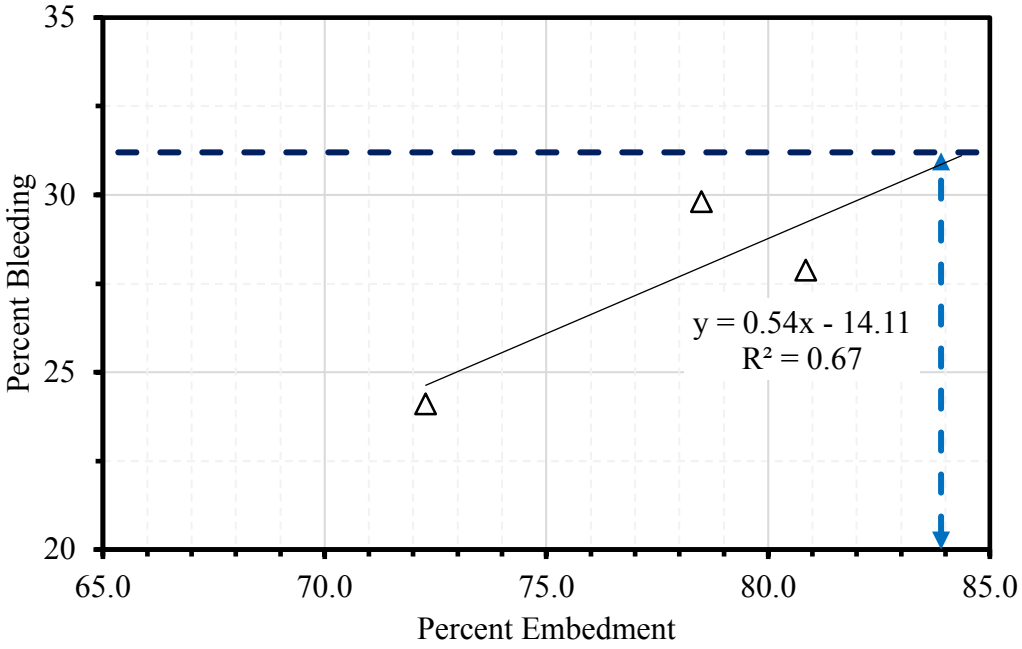

Figure 7-13 Maximum percent embedment limit for the hot-applied chip seal used in this study.

8. ESTABLISHING PAY ADJUSTMENT FACTORS AND PROCEDURES

Quality assurance specifications that specify end product quality have often been used by highway agencies for assuring construction quality. In addition, agencies are increasingly incorporating performance-related specifications (PRS) in construction contracts to specify quality in terms of parameters related to desired long-term performance. These PRS also provide a means to account for the value lost or gained by variances in these parameters from the specified target values. Although such PRS have seen limited use in the construction of new pavements, their use for pavement preservation treatments (e.g., chip seals) has been generally non-existent. If adopted, PRS would provide a means for agencies to insure quality pavement preservation treatments are delivered while creating a fair bid environment for contractors.

There are no widely accepted guidelines for PRS for pavement preservation treatments that correlate key engineering properties to treatment quality and long-term performance. Therefore, research is needed to develop guidelines to facilitate developing PRS for pavement preservation treatments that provide a direct relationship of key material and construction acceptance quality characteristics (AQC) to expected treatment performance. These guidelines will help highway agencies develop and incorporate PRS in preservation treatment contracts. In this manner, agencies would be able to specify an optimum level of quality that represents a balance of cost and performance, and accordingly establish quality-related pay adjustment factors (if desired).

The development of a PRS is based on desired outcomes and user needs which define end-product performance. This provides the rationale for pay adjustments to the contractor through the measurement and evaluation of key performance parameters. Additionally, multiple construction methods can be used to achieve the desired results of PRS. The contractor has the freedom to innovate in construction methods but simultaneously accepts the risks associated with it. This can motivate a contractor to be more conscious of providing high quality work that can exceed expectations and reduce the agency costs associated with construction inspection. In addition to higher risk for the contractor, the adoption of a PRS also requires the agency to relinquish control over some aspects of the work. Successful implementation of a PRS is beneficial to all parties involved, promoting innovative construction methods to achieve a high-quality end-product aligned with the needs of roadway users. Essentially, the following needs should be addressed for PRS development for preservation treatments:

1. Evaluation of pre-existing pavement conditions for determining the suitability of a specific preservation treatment for a given project. The effectiveness of preservation treatment depends on the treatment selection and timing. However, the timing and treatment type are significantly impacted by the pre-existing condition of the pavement surface to which the preservation treatment is to be applied. Therefore, quantifying the pre-existing conditions in terms of remaining service life (based on existing distresses) or structural integrity (e.g., based on deflection testing) is a key element for successful implementation of the PRS. Therefore, selection, timing and location of a preservation treatment are the key components for its success (Peshkin, Hoerner and Zimmerman, 2004; Peshkin and Hoerner, 2005; Anderson *et al.*, 2014). In this report, it was assumed that preservation treatments are selected considering the pre-existing conditions and

optimum timing. The details of such investigation can be found elsewhere (Peshkin, Hoerner and Zimmerman, 2004; Tenison, 2009; Rada *et al.*, 2013).

2. Identification of quality characteristics (i.e., material properties and construction variables) that are related to expected performance. The construction materials and methods may be unique to a specific preservation treatment. Similarly, the performance measures may be more functional in nature i.e., only addressing the non-load related surface conditions (e.g., ravelling, texture, and bleeding etc.).
3. Development of a quality assurance and management program that incorporates sampling and statistical procedures to link variability in quality characteristics to expected performance and pay factor adjustments. The existing procedures can be modified to account for performance limits unique to preservation treatments.

This chapter describes a concise but comprehensive procedure for developing pavement preservation PRS guidelines for chip seals treatment. While the relationships between quality characteristics and performance measures can be established using empirical, mechanistic-empirical, and performance-based laboratory and field test properties, the example shows an application of the empirical approach. Relationships were further developed between quality measures, service life, and pay adjustment factors. The expected pay curves were developed based on quality measures and were used to establish acceptable and unacceptable quality levels. The pay adjustment factors were evaluated to ensure fair payments for the quality of work produced. Although the demonstrative example presented was based on the relationships developed in the laboratory and engineering judgement, those can be further validated and improved by collecting field data. The focus of this section is to document general guidelines for the development of PRS for chip seals. The proposed procedure for the PRS development for preservation treatments contains the following steps (Chatti *et al.*, 2017):

1. Select a preservation treatment
2. Select candidate material, construction characteristics (i.e., quality characteristics) and performance measures
3. Establish relationships between quality characteristics and performance measures
4. Determine AQC limits and performance thresholds
5. Specify tests methods to measure the selected characteristics
6. Establish a sampling and measurement plan
7. Select quality measurement methods
8. Develop pay adjustment factors for incentives and disincentives

The steps presented above were followed to develop general PRS development guidelines for chip seals in flexible pavements.

8.1 Select Preservation Treatment

In this project, the preservation treatment of interest was in regard to chip seals, therefore the first step above is not applicable.

8.2 Select Candidate Material and Construction Characteristics and Performance Measures

The material and construction variable that can be used as AQCs for chip seals is the percent embedment (PE). PE of aggregate particles into the thin bituminous layer is one of the most significant parameters affecting the performance of asphalt chip seals. Bleeding or aggregate loss may be encountered in chip seal applications depending on the aggregate percent embedment. Therefore, PE just after construction is used as an AQC while aggregate loss and bleeding after about 5 years of service life are considered as performance measures for chip seal applications.

8.3 Establish AQC-Performance Relationships

An agency can develop an AQC-performance relationship if PE can be related to expected percentages of aggregate loss or bleeding. Relationships between PE and percent aggregate loss, and PE and bleeding were developed based on the laboratory evaluations of chip seals as discussed in Chapters 6 and 7. These relationships are shown again in Figure 8-1 and Figure 8-2 for natural and slag aggregates, respectively. Equations (8.1) and (8.2) show the relationships for aggregate loss and bleeding:

$$AL = -1.49 \times PE + 127.22 \quad (8.1)$$

$$B = 1.02 \times PE - 40.18 \quad (8.2)$$

where:

PE = percent embedment, AL = percent aggregate loss, and B = bleeding area, %

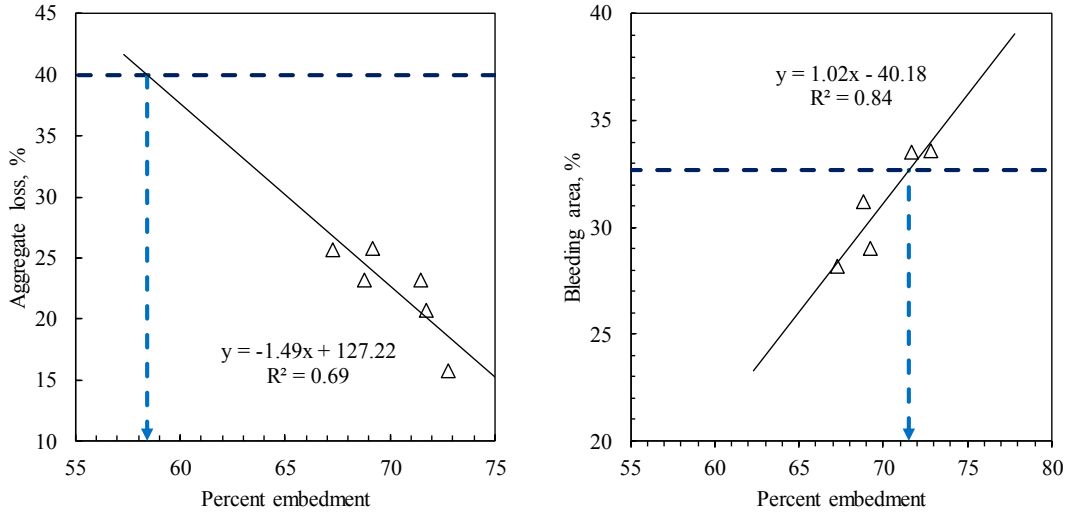

(a) Aggregate loss (b) Bleeding

Figure 8-1 Relationships between PE and chip seal performance — natural aggregates

The relationships above were developed in the laboratory by testing different chip seal samples. Since field monitoring data was not available, a series of pavement sections with varying aggregate loss and bleeding deterioration rates over time were established based on typical PE ranges identified in Figure 8-1. The simulated aggregate loss and bleeding over time are shown in Tables 8-1 and 8-2, respectively.

Threshold values of 40% and 33% were used as the failure criteria for aggregate loss and bleeding, respectively for each types of aggregates. Based on Equations (8.1) and (8.2), the service lives to threshold values for each of the sections listed in Tables 8-1 and 8-2 were estimated for both performance measures. The PE and service lives based on aggregate loss and bleeding were related to establish regression models as shown in Figure 8-3.

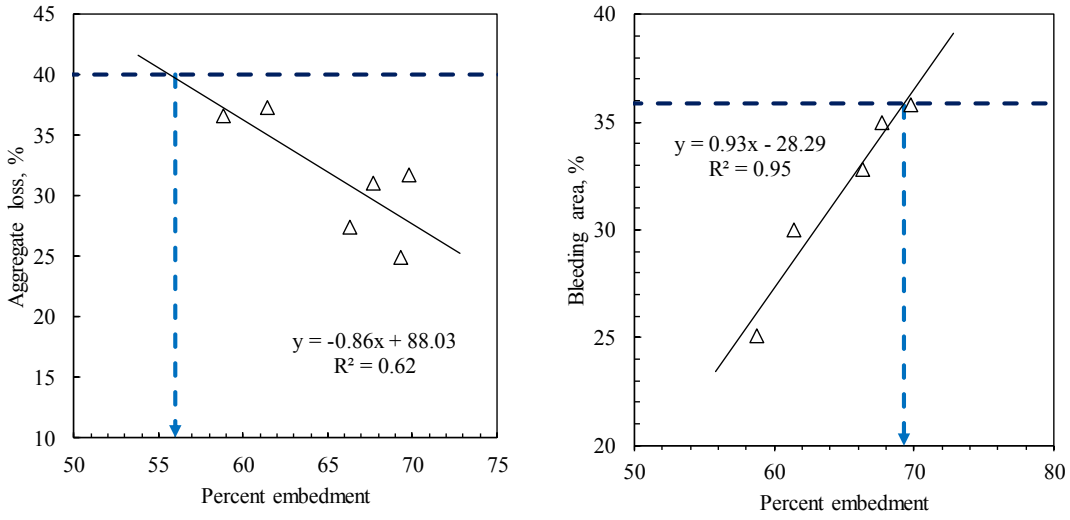

(a) Aggregate loss (b) Bleeding

Figure 8-2 Relationships between PE and chip seal performance — slag aggregates

Table 8-1 Aggregate loss rate (%) for chip seal sections over time

Age (years)	Section 1	Section 2	Section 3	Section 4	Section 5
0	0	0	0	0	0
1	7	6	5	3	3
2	14	12	10	7	6
3	23	19	15	11	9
4	32	26	21	15	12
5	43	35	27	19	15

Table 8-2 Bleeding rate (%) for chip seal sections over time

Age (years)	Section 1	Section 2	Section 3	Section 4	Section 5
0	0	3	5	8	10
1	3	6	9	12	14
2	6	10	13	16	19
3	10	14	17	21	24
4	13	18	21	26	29
5	17	22	26	31	34

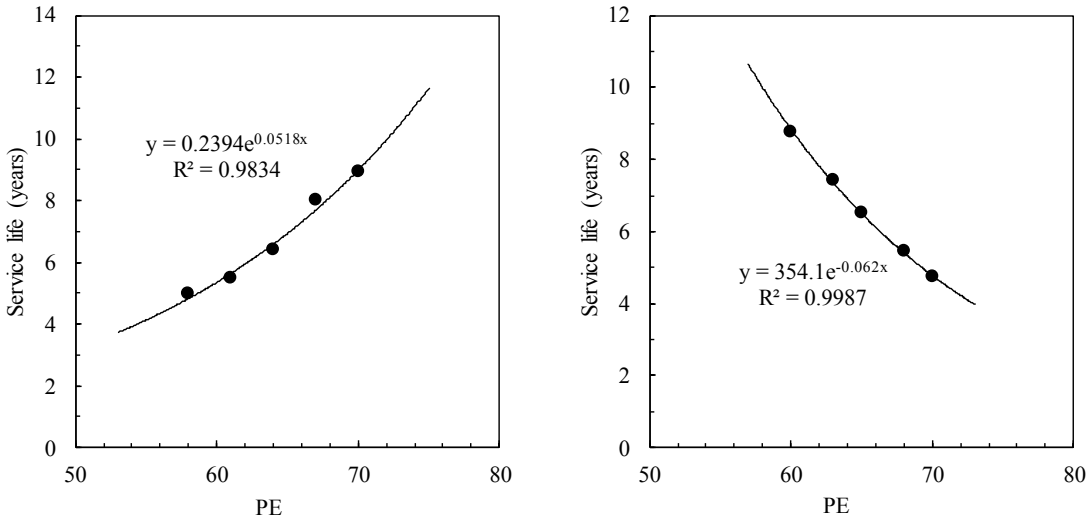

(a) Aggregate loss (b) Bleeding

Figure 8-3 Relationship between AQC and performance measures

It should be noted that such relationships can be developed by collecting field performance data and initial PE at the time of construction for a sample of projects located in different regions in Michigan.

8.4 Determine Performance Thresholds and AQC Limits

There is no single correct method for establishing specification limits. Furthermore, there is a distinct difference between the limits of AQC and quality measures. The following steps were used to establish limits for AQC and quality measures:

1. Determine AQC-performance relationships – The relationships have been substantiated in the previous section. The results in Figure 8-3 demonstrate that a relationship can be developed between percent embedment (AQC) and service lives (based on aggregate loss and bleeding). These relationships are appropriate for developing chip seal performance-related specifications.
2. Set specification limits – As described previously, performance thresholds for these specifications can be set at a maximum aggregate loss of 40% and bleeding area of about 33%. A lower limit of 58 and an upper limit of 70 were set for percent embedment and bleeding performance for chip seals. All quality measures, pay adjustments, and risks will be evaluated based on this assumption.
3. Decide on the quality measure – The recommended quality measure and one that is used often in current statistical quality control in highway construction is percent within limits (PWL) (Burati et al., 2003; Huges et al., 2011). Therefore, PWL was used as a quality measure for developing pay factors.
4. Define AQL material – As previously mentioned, PWL is used as a quality measure in pavement construction practices. The procedure to obtain to obtain the PWL value that could be used as acceptance quality limits (AQL) is demonstrated below.

5. Define RQL material –The rejectable quality limits (RQL) is also a subjective decision made by the agency or party setting the specification limits. The PWL value that could be used as RQL can be obtained from the example demonstrated below. A lot of the RQL will receive a reduced pay factor equivalent to that level of quality as specified in the payment plan. The lot may be rejected if PWL is at or below RQL.

Summary

- The AQC selected for development of chip seals PRS guidelines is percent embedment (PE). The relationships shown in Equations (8.1) and (8.2) will be used to relate PE to aggregate loss and bleeding performance measures.
- A lower specification limit of 40 percent aggregate loss (corresponding to approximately 58 PE) and upper specification limit of 33 percent bleeding area (corresponding to 70 PE) were established.
- The PWL is selected as a quality measure.
- The PWL value that can be used as AQL can be obtained from the demonstrated example below.
- The PWL value that can be used as RQL can be obtained from the demonstrated example below in accordance with the pay equation.

8.5 Specify Test Methods to Measure AQC

A previous study developed a standard test procedure to directly calculate the aggregate percent embedment into the asphalt binder in a chip seal project via digital image analysis. Three image analysis algorithms were developed and used to analyze chip seal samples (Kutay *et al.*, 2016, 2017; Ozdemir, 2016). The software named CIPS, was developed for road agencies and contractors to estimate percent embedment from field cores as an acceptance test for chip seal projects. The research team recommends such methods be used for measuring percent embedment in the field.

8.6 Establish a Sampling and Measurement Plan

The risks associated with incorrectly accepting or rejecting a lot is related to the sample size. The following procedure is suggested to develop guidelines for a sampling and measurement plan for chip seals:

1. Determine which party performs acceptance testing – The parties (contractor and agency) involved in the project must agree upon the duties of performing acceptance testing.
2. Determine the type of acceptance plan to be used – The relationships established between percent embedment (PE) and service life (SL) show varying degrees of effectiveness in terms of life extension for different levels of PE. A “variable acceptance plan” can be used to measure the change in construction quality due to statistical variation of the PE.

3. Develop verification sampling and testing procedures – Verification sampling is a standard procedure that is used to verify the accuracy of the acceptance test results. The guidelines for different sampling methods are described elsewhere (Chatti *et al.*, 2017), but the decision on whether to use split or independent sampling is unique to the goals of the agency. In practice, it is appropriate that the agency's verification test methods are used solely for verification and that acceptance methods proposed by the contractor must first be compared to the results of agency verification testing.
4. Select the appropriate verification sampling frequency –The verification sampling frequency of the agency should be approximately ten percent of the acceptance sampling rate of the contractor. In practice, verification testing frequency is decided for economic, rather than statistical, reasons. Again, this decision must be agreed upon by agency and contractor and it is assumed that the procedure is already established for the purposes of this demonstrative example.
5. Determine lot size and sample size – The quantification of percent embedment after construction needs field cores. Therefore, lots and sublots can be defined as segmented lengths of a project. Based on a survey of highway practice, most agencies report pavement segment lengths in 0.1-mile (500 foot) increments for roughness specifications (Merritt, Chang and Rutledge, 2015). For chip seals, it is possible to establish a lot size based on the coverage length of an aggregate truck and then divide the length into 5 sublots. A sample size of 5 (i.e., one core from each sublot) is recommended to estimate PWL for a lot.

8.7 Select and Evaluate Quality Measurement Methods

Tables 8-3 and 8-4 show the means and standard deviations for measured PE for several lots. The PWL of each lot was estimated using a beta distribution, and service lives (SL) were estimated based on the relationships shown in Figure 8-3 for aggregate loss and bleeding. The service lives were estimated at the mean values of PE. A higher PWL for PE illustrates a better quality of chip seal. While higher PWL values for aggregate loss show that more samples exhibit PE value of above 58 and vice versa, higher PWL values for bleeding illustrate that more samples show PE value of below 70 and vice versa. A summary of PWL values calculated for a range of PE within 16 lots are shown in Tables 8-3 and 8-4. The SL was calculated for each PE as shown in the tables. The relationships were established between PWL based on PE and SL for aggregate loss and bleeding using the simulated lots. These relationships allow the prediction of pavement performance in terms of SL as a function of quality levels (see Figure 8-4). The relationships show that better construction quality would result in higher service lives based on aggregate loss and bleeding.

Table 8-3 Summary of simulated lots for PE and aggregate loss performance

Mean PE	Std PE	n	PWL	SL (years)
55.0	10.0	5	39.4	4.1
56.3	10.0	5	43.8	4.4
57.5	10.0	5	48.2	4.7
58.8	10.0	5	52.7	5.0
60.0	10.0	5	57.1	5.4
61.3	10.0	5	61.5	5.7
62.5	10.0	5	65.8	6.1
63.8	10.0	5	70.1	6.5
65.0	10.0	5	74.3	6.9
66.3	10.0	5	78.3	7.4
67.5	10.0	5	82.1	7.9
68.8	10.0	5	85.8	8.4
70.0	10.0	5	89.2	9.0
71.3	10.0	5	92.4	9.6
72.5	10.0	5	95.2	10.2
73.8	10.0	5	97.6	10.9

Table 8-4 Summary of simulated lots for PE and bleeding performance

Mean PE	Std PE	n	PWL	SL (years)
55.0	10.0	5	96.2	11.7
56.3	10.0	5	93.6	10.8
57.5	10.0	5	90.5	10.0
58.8	10.0	5	87.2	9.3
60.0	10.0	5	83.6	8.6
61.3	10.0	5	79.8	7.9
62.5	10.0	5	75.9	7.3
63.8	10.0	5	71.8	6.8
65.0	10.0	5	67.6	6.3
66.3	10.0	5	63.2	5.8
67.5	10.0	5	58.9	5.4
68.8	10.0	5	54.4	5.0
70.0	10.0	5	50.0	4.6
71.3	10.0	5	45.6	4.3
72.5	10.0	5	41.1	4.0
73.8	10.0	5	36.8	3.7

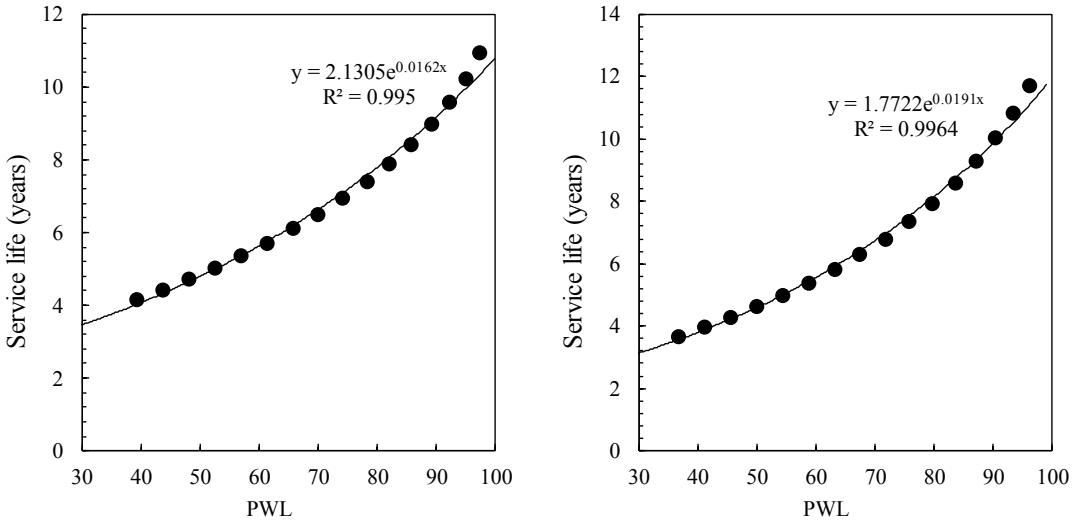

(a) Aggregate loss (b) Bleeding

Figure 8-4 Performance-based relationship between PWL and SL

8.8 Develop Pay Adjustment Factors for Incentives and Disincentives

The relevant expected pay (EP) and operating characteristic (OC) curves were developed to assign pay factors for appropriate levels of acceptable and unacceptable quality while minimizing the expected risks to both contractor and agency. The following steps illustrate the process for developing the pay adjustment factors based on expected performance of chip seals:

1. Predict pavement performance as a function of quality levels – A relationship between PWL and pavement performance in terms of service life was established. The performance in terms of quality is shown in Figure 8-4.

2. Convert the expected performance into pay adjustment – The pay factor is calculated by using Equation (3) which corresponds to the estimated change in quality ranging from 0 to 100 PWL because SL is a function of PWL (see Figure 8-4). The relationship between PWL and the pay factor is shown in Figure 8-5.

$$PF = \frac{C\left(R^D - R^E\right)}{1 - R^O} \tag{8.3}$$

where:

PF=	pay adjustment factor for new pavement or overlay (same units as C)
C=	present total cost of resurfacing use C=1 for PF
D=	design life of pavement or initial overlay
E =	expected life of pavement or overlay
O=	expected life of successive overlays
R=	$(1+INF)/(1+INT)$
INF=	long-term annual inflation rate in decimal form
INT=	long-term annual interest rate in decimal form

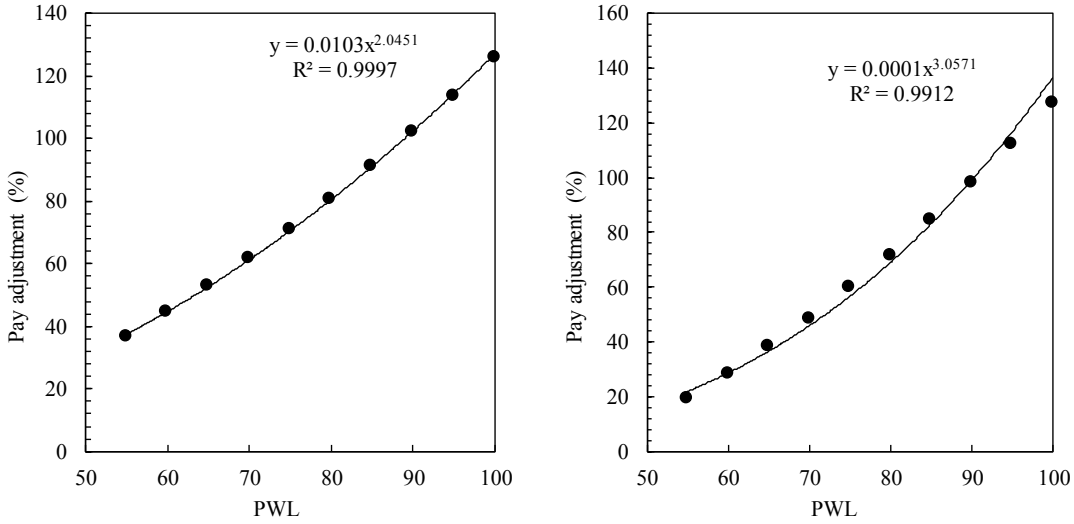

(a) Aggregate loss (b) Bleeding

Figure 8-5 EP model between *PE* and performance measures

The pay equation can be used in the risk assessment to develop OC curves, assess the associated α and β risk, and determine the appropriate AQL and RQL levels necessary to award payment factors which accurately reflect the measured levels of quality. The following are pay equations based on aggregate loss and bleeding.

$$PF(\%) = 0.0103 \times PWL^{2.045} \tag{8.4}$$

$$PF(\%) = 0.0001 \times PWL^{3.06} \tag{8.5}$$

3. Adjust the AQL, RQL, and pay relationships to minimize risk – As discussed in the determination of AQC limits, the AQL and RQL need to be established. The key principle in any fair payment plan is that a contractor should be awarded 100 percent pay for producing an AQL quality. For adjustment of AQL, the EP curves must be evaluated such that the payment plan awards 100 percent pay at AQL while incentive can be given if the quality of work is above AQL. Tables 8-5 and 8-6 show the pay factors generated from the EP curve shown by Equations 4 and 5. As seen in Tables 8-5 and 8-6, the AQL may be chosen at 90 PWL to ensure a contractor is not awarded bonus pay for AQL work. For establishing RQL, the EP curves can be used to determine the level of performance (in terms of service life) that is deemed unacceptable and should result in reduced pay. This decision is typically made to meet the needs of the agency to ensure the pavement performs to established standards. For instance, in EP curve shown in Table 8-5, an agency may decide that a service life of less than 5 years is undesirable. Therefore, the RQL will be set at 55 PWL, and any lot produced at a quality level below that will receive no pay. Further, the agency may also decide that any quality between AQL of 90 and RQL of 55 will be accepted but will receive a reduced pay or disincentive.

Table 8-5 Summary of EP curve for varying chip seal quality levels — aggregate loss

PWL	SL (years)	PF%
0	2.1	-21.41
5	2.3	-17.79
10	2.5	-13.88
15	2.7	-9.69
20	2.9	-5.18
25	3.2	-0.33
30	3.5	4.86
35	3.8	10.43
40	4.1	16.39
45	4.4	22.77
50	4.8	29.59
55 (RQL)	5.2	36.87
60	5.6	44.62
65	6.1	52.87
70	6.6	61.65
75	7.2	70.95
80	7.8	80.80
85	8.4	91.21
90 (AQL)	9.1	102.19
95	9.9	113.74
100	10.7	125.86

Table 8-6 Summary of EP curve for varying chip seal quality levels — bleeding

PWL	SL (years)	PF%
0	1.8	-43.73
5	1.9	-40.10
10	2.1	-36.12
15	2.4	-31.79
20	2.6	-27.07
25	2.9	-21.93
30	3.1	-16.34
35	3.5	-10.26
40	3.8	-3.67
45	4.2	3.48
50	4.6	11.22
55 (RQL)	5.1	19.59
60	5.6	28.60
65	6.1	38.31
70	6.7	48.74
75	7.4	59.92
80	8.2	71.86
85	9.0	84.59
90 (AQL)	9.9	98.11
95	10.9	112.42
100	11.9	127.51

A summary of the finalized AQL and RQL values for single chip seals, based on performance due to friction number (*FN*) are presented in Table 8-4. The OC curves were developed to assess the risk of receiving a payment that correctly corresponds to the level of quality sampled. These OC curves are shown in Figure 8-7.

Table 8-7 Pay factor summary for chip seals

Quality characteristics	Quality levels and pay adjustment
AQL (PWL)	90
AQL_{LE}	7 to 9 years
AQLPF (%)	100%
RQL (PWL)	55
RQL_{LE}	4 to 5 years
RQL_{PF} (%)	20% to 37%

When evaluating the risks associated with receiving appropriate pay for predicted change in PWL. The OC curves of desired quality 90 PWL (i.e. AQL) for a sample size of 3, 5, and 10 are shown in Figure 8-6. The level of quality produced by a contractor as indicated on the x-axis must be matched with the OC curve with desired quality to evaluate the probability of receiving a pay factor which corresponds to a desired quality. In this case, recall the established AQL of 90 PWL. If a contractor produces AQL quality in the field, then quality level must be matched with the OC curve at AQL. Figure 8-6 indicates that the pay adjustment plan will award pay factor greater than 1 (see Table 8-5) at a probability of 50 %for all lots sampled. This suggests that the contractor will receive pay greater than 100 percent (pay for above AQL) half of the time and receive pay less than 100 percent (pay for below AQL) half of the time. Since several lots will be sampled for quality, this averages to 100 percent pay throughout the project, which is characteristic of an unbiased and fair adjustment plan to both agency and contractor. This also incentivizes the contractor to consistently aim for above AQL quality to offset the probability of and receive bonus pay. Also, it can be seen that the greater the sample size, the higher the probability of receiving pay greater than 100 percent if the produced quality is above AQL. Similarly, less is the probability of receiving pay greater than 100 percent if the produced quality is less than AQL. A summary of the PRS specifications for chip seals is shown in Table 8-8.

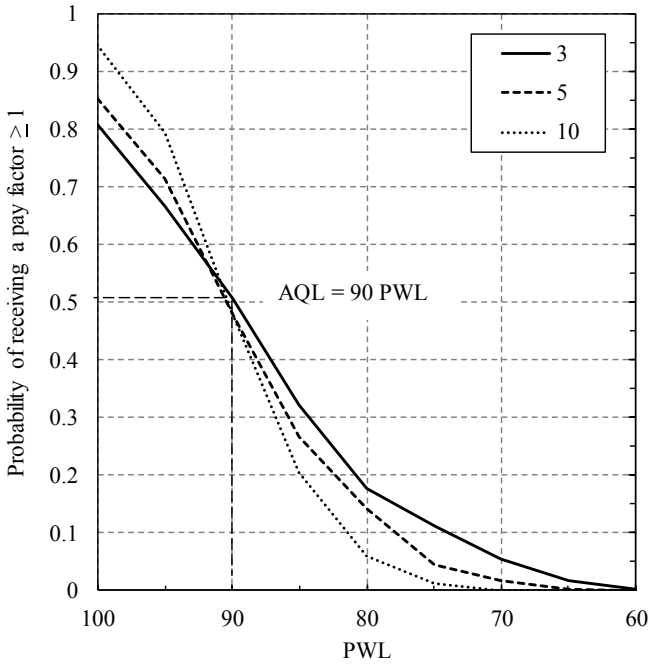

Figure 8-6 Predicted OC curves for change in quality measures

Table 8-8 PRS for chip seals

Treatment	Chip seals
AQC(s)	Percent embedment (PE)
Lot size	Dependent on agency
Sample size	Dependent on agency
AQC threshold	Minimum 58 PE (corresponds to 40% aggregate loss) Maximum 70 PE (corresponds to 33% bleeding area)
Quality measure	PWL
Quality thresholds	AQL = 90 PWL, RQL = 55 PWL
Pay Equations	$PF(\%) = 0.0103 \times PWL^{2.045}$ $PF(\%) = 0.0001 \times PWL^{3.06}$
AQL pay factor	100%
RQL pay factor	20 to 37%
P(PF>1) at AQL	50%

9. CONCLUSIONS

Microstructural characteristics of chip seals, i.e., the percent embedment and aggregate orientation, significantly affect their long-term performance. An ideal chip seal is the one which has all the aggregates embedded properly at optimum percent embedment levels. Because of this research study, performance-based threshold values for the percent embedment were developed to minimize the common chip seal distresses, i.e., bleeding and aggregate loss, which were evaluated using a retrofitted Hamburg Wheel Tracking (HWT) device. Two emulsion types (CRS-2M and CSEA), one binder (PG70-28) for hot-applied chip seal application, and three aggregate sources (one slag and two different kinds of natural aggregate) were included in the testing program. The percent embedment limits were evaluated through analysis of the laboratory performance-based test results coupled with digital image techniques to directly measure percent embedment. Based on test results, the performance-based minimum and maximum limits of the percent embedment of aggregates were established as follows;

1. Emulsion-based chip seals utilizing natural aggregates: 58.4 (min) to 71.5 (max) percent. Emulsion-based chip seals utilizing slag aggregates: 55.7 (min) to 69.3 (max) percent. For practical reasons, these values can be averaged. Consequently, *the thresholds for the emulsion-based chip seals are recommended to be 58 (min) and 70 (max) percent.*
2. The recommended thresholds for hot-applied chip seals (based on tests on Gerkin aggregates) are from 72% (min) to 84% (max).

It should be noted that the limits above assume that the type of aggregate and emulsion were chosen adequately, and proper construction practices are followed. Other major conclusions and observations from this study can be listed as follows:

3. Both aggregate loss and bleeding test results correlated very well with the image-based percent embedment results computed using the CIPS software.
4. Unlike the percent embedment computed using the image analysis technique (i.e., CIPS software), the percent embedment calculated from the macrotexture depth (which the sand patch and laser-based methods are based on) did not correlate well with the performance. This is because the percent embedment calculated from the macrotexture measurements is heavily dependent on major assumptions which do not reflect the field conditions.
5. In the chip seal bleeding test, the binder typically rises to the surface and steadily increases the percent bleeding area. However, at certain binder application rates, the binder is simply excessive and quickly rises to the surface (due to the readjustment of the aggregates), sticks to the tire and picks up the aggregates attached to the binder. At this point, 'tertiary flow' (somewhat analogous to the tertiary flow in asphalt mixture rutting tests) occurs. Tertiary flow is essentially the catastrophic failure of the chip seals and should be avoided.
6. Excessive aggregate application rates can cause aggregates to misalign and increase the possibility of failures. Even though results of aggregate orientation measurements and their effect on performance were discussed, the scope of this study did not include

extensive investigation of effect of inadequate aggregate orientation on performance, which should be studied in the future.

7. Residual aggregate rate (RAR) increased as the emulsion application rate (EAR) increased, which is somewhat expected since larger amounts of binder help retain the aggregates spread and compacted.
8. The chip seals with natural and slag aggregates exhibited an overall average aggregate loss by abrasion (ALA) values of 22.4 and 31.5 percent, respectively. It is commonly believed that chip seals with cubical aggregates (i.e., slag) perform better than the chip seals with flaky aggregates (i.e. natural), however the results presented here show otherwise. Several factors could have contributed to such outcome. First, since the aggregate types used were not the same type, the aggregate-emulsion compatibility could have played a role in such observation. Also, the gradation distributions of the aggregates were different. Moreover, the possible variations in the aggregate-binder microstructure (i.e. orientation, percent embedment, as well as aggregate interlock) between the two chip seals might have contributed to the observed trend.

In this study, rational chip seal pay factors were estimated based on the aggregate loss and bleeding performance. Using the methodology presented herein, the contractors can be paid according to work quality. The performance related specifications were developed based on the relationship between PE (AQC) and expected chip seal performance in terms of aggregate loss and bleeding. While the developed pay adjustment factors were developed based on laboratory test results, the results should be validated by collecting field data for several chip seal projects in different regions of Michigan. The following are the recommendations to validate and calibrate the pay adjustment factors in future:

- Identify at least 15 to 20 chip seals projects located in different regions of the state.
- Divide each project into lots and sublots. The number of lots can be based on amount of a day's work or to capture a uniform construction process.
- Measure PE by taking at least 4 to 5 cores within each lot just after construction.
- Monitor chip seal performance in terms of aggregate loss and bleeding for at least 5 years.
- Validate and calibrate the relationship between PWL based on PE and service life to reach a performance threshold.
- Use the approach documented in this report to adjust pay adjustment factors.

This project provided MDOT (and other road agencies in Michigan) reliable performance-based threshold values of the percent embedment that could be used as criteria in chip seal design specifications and as quality assurance and acceptance protocols for such treatments. The results of this project also provided a strong foundation for climate and traffic-based design procedures for chip seals treatments. Successful implementation of this research will result in extended service life and improved performance of the pavements in Michigan; and consequently, in significant cost savings.

10.REFERENCES

Abedini, M. *et al.* (2017) 'Low-temperature adhesion performance of polymer-modified Bitumen emulsion in chip seals using different SBR latexes', *Petroleum Science and Technology*. Taylor & Francis, 35(1), pp. 59–65. doi: 10.1080/10916466.2016.1238932.

Adams, J. M. (2014) *Development of a Performance-Based Mix Design and Performance-Related Specification for Chip Seal Surface Treatments*. North Carolina State University.

Adams, J. M. and Kim, Y. R. (2010) 'Mean profile depth analysis of field and laboratory traffic - loaded chip seal surface treatments', *Transportation Research Record*. Taylor & Francis, pp. 1–16. doi: 10.1080/10298436.2013.851790.

Adams, J. M. and Kim, Y. R. (2014) 'Mean profile depth analysis of field and laboratory traffic-loaded chip seal surface treatments', *International Journal of Pavement Engineering*. Taylor & Francis, pp. 645–656. doi: 10.1080/10298436.2013.851790.

Akilli, A. *et al.* (2012) 'Investigation of adhesion properties in chip seals with pull out test', in *5th Eurasphalt & Eurobitume Congress (Istambul, Turkey)*.

Aktaş, B. *et al.* (2011) 'Comparative Analysis of Macrotexture Measurement Tests for Pavement Preservation Treatments', *Transportation Research Record: Journal of the Transportation Research Board*, 2209, pp. 34–40. doi: 10.3141/2209-05.

Aktaş, B. *et al.* (2013) 'Effect of aggregate surface properties on chip seal retention performance', *Construction and Building Materials*, 44, pp. 639–644. doi: 10.1016/j.conbuildmat.2013.03.060.

Anderson, R. M. *et al.* (2014) *Optimal Timing of Preventive Maintenance for Addressing Environmental Aging in Hot-Mix Asphalt Pavements*. Department of Transportation, Research Services & Library.

ASTM-D6372 (2005) 'Standard Practice for Design , Testing , and Construction of Micro-Surfacing 1', i, pp. 1–7. doi: 10.1520/D6372-05.2.

ASTM-D6943 (2015) 'Standard Practice for Immersion Testing of Industrial Protective Coatings and Linings'. doi: 10.1520/D6943-15.2.

ASTM-D7000 (2011) 'Standard Test Method for Sweep Test of Bituminous Emulsion Surface Treatment Samples', *Astm D7000*, 11(C), pp. 1–4. doi: 10.1520/D7000-11.

ASTM-E1845 (2015) *Standard Practice for Calculating Pavement Macrotexture Mean Profile Depth*.

ASTM-E2157 (2015) 'Standard Test Method for Measuring Pavement Macrotexture Properties Using the Circular Track Meter', *ASTM International*. doi: 10.1520/E2157-09.2.

ASTM-E2380 (2015) ‘Standard Test Method for Measuring Pavement Macrotexture Depth Using an Outflow meter’, *ASTM International*. doi: 10.1520/E2380.

ASTM D4541 (2009) ‘Standard Test Method for Pull-Off Strength of Coatings Using Portable Adhesion’, *ASTM International*, (April), p. 16 p. doi: 10.1520/D4541-09E01.2.

ASTM E965 (2015) ‘Standard Test Method for Measuring Pavement Macrotexture Depth Using a Volumetric technique’, *ASTM International*, i, pp. 1–4. doi: 10.1520/E0965-15.2.

Bhattacharjee, S. *et al.* (2004) ‘Use of MMLS3 scaled accelerated loading for fatigue characterization of Hot Mix Asphalt (HMA) in the laboratory’, *2nd International Conference on Accelerated Pavement Testing*, (September 2004). Available at: http://www.mrr.dot.state.mn.us/research/MnROAD_Project/index_files/pdfs/Bhattacharjee_S.pdf.

Burati, J. L. *et al.* (2003) ‘Optimal procedures for quality assurance specifications’. Turner-Fairbank Highway Research Center. Available at: https://rosap.ntl.bts.gov/view/dot/755 (Accessed: 14 May 2018).

Chatti, K. *et al.* (2017) *Performance-related specifications for pavement preservation treatments*, *NCHRP Research Report*.

Chaturabong, P., Hanz, A. J. and Bahia, H. U. (2015) ‘Development of Loaded Wheel Test for Evaluating Bleeding in Chip Seals’, *Transportation Research Record: Journal of the Transportation Research Board*, pp. 48–55. doi: 10.3141/2481-07.

Das, B. and Sobham, K. (2013) *Principles of Geotechnical Engineering*. doi: 10.1017/CBO9781107415324.004.

Epps-Martin, A., Glover, C. J. and Barcena, R. (2001) *A performance-graded binder specification for surface treatments*.

Epps, J., Chaffin, C. W. and Hill, A. J. (1980) *FIELD EVALUATION OF A SEAL COAT DESIGN METHOD*.

Gransberg, D. D. (2005) ‘Chip Seal Program Excellence in the United States’, *Transportation Research Record: Journal of the Transportation Research Board*, 1933(1933), pp. 72–82. doi: 10.3141/1933-09.

Gransberg, D. D. (2007) ‘Using a New Zealand Performance Specification to Evaluate U.S. Chip Seal Performance’, *Journal of Transportation Engineering*, 133(12), pp. 688–695. doi: 10.1061/(ASCE)0733-947X(2007)133:12(688).

Gransberg, D. D. and James, D. M. (2005) *Chip seal best practices*.

Gransberg, D. D. and Zaman, M. (2005) ‘Analysis of emulsion and hot asphalt cement chip seal performance’, *Journal of Transportation Engineering-Asce*, 131(3), pp. 229–238. doi: 10.1061/(ASCE)0733-947X(2005)131:3(229).

Gransberg, D. and James, D. M. B. (2005) *Chip seal best practices*.

Guirguis, M. and Buss, A. (2017) 'Performance Evaluation of Emulsion and Hot Asphalt Cement Chip Seal Pavements', *Journal of Materials in Civil Engineering*, 29(11)(11), pp. 1–10. doi: 10.1061/(ASCE)MT.1943-5533.0002057.

Gürer, C. *et al.* (2012) 'Effects of construction-related factors on chip seal performance', *Construction and Building Materials*, 35, pp. 605–613. doi: 10.1016/j.conbuildmat.2012.04.096.

Howard, I. L. *et al.* (2009) 'Chip and Scrub Seal Binder Evaluation by Frosted Marble Aggregate Retention Tes', *Transportation Research Board 88th Annual Meeting*.

Howard, I. L. *et al.* (2017) 'Material selection and traffic opening guidance for chip or scrub seals', *Road Materials and Pavement Design*. Taylor & Francis, 0(0), pp. 1–23. doi: 10.1080/14680629.2017.1340327.

Huges, C. S. *et al.* (2011) *Guidelines for Quality Related Pay Adjustment Factors for Pavements*.

Huurman, M. (2010) 'Developments in 3D surfacing seals FE modelling', *International Journal of Pavement Engineering*, 11(1), pp. 1–12. doi: 10.1080/10298430600949852.

Im, J. H. and Kim, Y. R. (2016) 'Performance Evaluation of Chip Seals for Higher Volume Roads Using Polymer-Modified Emulsions : Laboratory and Field Study in North Carolina', 44, pp. 484–497. doi: 10.1520/JTE20140544.

Islam, S. and Hossain, M. (2011) 'Chip Seal with Lightweight Aggregates for Low-Volume Roads', *Transportation Research Record: Journal of the Transportation Research Board*, 2205, pp. 58–66. doi: 10.3141/2205-08.

Janisch, D. W. and Gaillard, F. S. (1998) 'Minnesota Seal Coat Handbook', (April).

Johannes, P. T., Johannes, P. T. and Bahia, H. U. (2013) 'Asphalt Emulsion Sprayability and Drain-Out Characteristics in Chip Seals', *Transportation Research Record Journal of the Transportation Research Board Transportation Research Board of the National Academies*, (2361), pp. 80–87. doi: 10.3141/2361-10.

Johannes, P. T., Mahmoud, E. and Bahia, H. (2011) 'Sensitivity of ASTM D7000 Sweep Test to Emulsion Application Rate and Aggregate Gradation', *Transportation Research Record: Journal of the Transportation Research Board*, 2235, pp. 95–102. doi: 10.3141/2235-11.

Jordan, W. S. and Howard, I. L. (2010) 'Applicability of Modified Vialit Adhesion Test for Seal Treatment Specifications', *Transportation Research Board 89th Annual Meeting*.

Kandhal, P. S. and Motter, J. B. (1991) 'Criteria for Accepting Precoated Aggregates for Seal Coats and Surface Treatments', *Transportation Research Record Journal of the Transportation Research Board Transportation Research Board of the National Academies*, (January), pp. 80–89. Available at: https://www.google.com.my/url?sa=t&rct=j&q=&esrc=s&source=web&cd=164&cad=rja&uact=

8&ved=0CCsQFjADOKAB&url=http://www.ncat.us/files/reports/1991/rep91-02.pdf&ei=AZ7JVKmlN6LQmwXu5YLwAQ&usg=AFQjCNHhU8mQ1wFcNKpVkul7uH4eYZkLvA&sig2=6XsZUySRZqAJAJolwoOoPQ&bvm=b.

Kim, Y. R. *et al.* (2017) *Performance-Related Specifications for Emulsified Asphaltic Binders Used in Preservation Surface Treatments*. National Academies Press. doi: 10.17226/24694.

Kumbargeri, Y., Boz, I. and Kutay, M. E. (2018) 'Quantifying the effect of binder/aggregate application rates on chip seal characteristics via digital image processing and sweep tests', in *Transportation Research Board 2018 Annual Meeting*. Washington D.C.

Kutay, M. E. *et al.* (2016) *An Acceptance Test for Chip Seal Projects Based on Image Analysis*. Michigan State University. Center for Highway Pavement Preservation.

Kutay, M. E. *et al.* (2017) *Development of an Acceptance Test for Chip Seal Projects, Michigan Department of Transportaion, report no. SPR 1649*. Available at: http://www.michigan.gov/documents/mdot/SPR1649_554816_7.pdf.

Lee, J. *et al.* (2013) 'Calibration of Seal Coat Application Rate Design', *Journal of Testing and Evaluation*, 41(2), p. 20120021. doi: 10.1520/JTE20120021.

Lee, J. and Kim, R. Y. (2012) 'Evaluation of polymer-modified chip seals at low temperatures', *International Journal of Pavement Engineering*, 15(3), pp. 1–10. doi: 10.1080/10298436.2012.655738.

Lee, J. and Kim, Y. (2008) 'Understanding the Effects of Aggregate and Emulsion Application Rates on Performance of Asphalt Surface Treatments', *Transportation Research Record: Journal of the Transportation Research Board*, 2044, pp. 71–78. doi: 10.3141/2044-08.

Lee, J. and Kim, Y. (2009) 'Performance-Based Uniformity Coefficient of Chip Seal Aggregate', *Transportation Research Record: Journal of the Transportation Research Board*, 2108(2108), pp. 53–60. doi: 10.3141/2108-06.

Lee, J. and Kim, Y. (2010) 'Evaluation of Performance and Cost-Effectiveness of Polymer-Modified Chip Seals', *Transportation Research Record: Journal of the Transportation Research Board*, 2150, pp. 79–86. doi: 10.3141/2150-10.

Lee, J., Kim, Y. and McGraw, E. (2006) 'Performance Evaluation of Bituminous Surface Treatment Using Third-Scale Model Mobile Loading Simulator', *Transportation Research Record: Journal of the Transportation Research Board*, 1958, pp. 59–70. doi: 10.3141/1958-07.

Lee, S. (2003) *Long-term performance assessment of asphalt concrete pavements using the third scale model mobile loading simulator and fiber reinforced asphalt concrete*. North Carolina State University. Available at: http://repository.lib.ncsu.edu/ir/handle/1840.16/3887.

Louw, K., Rossman, D. and Cupido, D. (2004) 'The Vialit Adhesion Test: Is It An Appropriate Test To Predict Low Temperature Binder/Aggregate Failure?', *8th Conference on Asphalt Pavements for Southern Africa (CAPSA'04)*, 12(September 2004).

Marasteanu, M. O. and Anderson, D. A. (1999) 'Improved Model for Bitumen Rheological Characterization', in *Eurobitume Workshop on Performance Related Properties for Bituminous Binders*.

Mcleod, N. (1969) 'A General Method of Design for Seal Coats and Surface Treatments', *Proceedings of the Association of Asphalt Paving Technologists*, 38.

Mendez Larrain, M. M. (2015) *Analytical Modeling of Rutting Potential of Asphalt Mixes Using Hamburg Wheel Tracking Device*. University of New Mexico. Available at: http://digitalrepository.unm.edu/ce_etds/116.

Merritt, D. K., Chang, G. K. and Rutledge, J. L. (2015) *Best Practices for Achieving and Measuring Pavement Smoothness, A Synthesis of State-of-Practice*.

Miller, T., Arega, Z. and Bahia, H. (2010) 'Correlating Rheological and Bond Properties of Emulsions to Aggregate Retention of Chip Seals', *Transportation Research Record: Journal of the Transportation Research Board*, 2179, pp. 66–74. doi: 10.3141/2179-08.

Ozdemir, U. (2016) *An acceptance test for chip seal projects based on image analysis*. Michigan State University.

Ozdemir, U. *et al.* (2018) 'Quantification of aggregate embedment in chip seals using image processing', *Journal of Transportation Engineering-Part B: Pavements*.

Ozdemir, U. *et al.* (no date) 'Quantification of aggregate embedment in chip seals using image processing', *Journal of Transportation Engineering, Part B: pavements*.

Peshkin, D. G. and Hoerner, T. E. (2005) 'PAVEMENT PRESERVATION: PRACTICES, RESEARCH PLANS, AND INITIATIVES'. Available at: http://citeseerx.ist.psu.edu/viewdoc/download?doi=10.1.1.129.5584&rep=rep1&type=pdf (Accessed: 14 May 2018).

Peshkin, D. G., Hoerner, T. E. and Zimmerman, K. A. (2004) *Optimal timing of pavement preventive maintenance treatment applications*. Transportation Research Board.

Pierce, L. M. and Kebede, N. (2015) 'Chip Seal Performance Measures — Best Practices Chip Seal', (March).

Praticò, F. G., Vaiana, R. and Iuele, T. (2016) 'Surface Performance Characterization of Single-Layer Surface Dressing: A Macrotexture Prediction Model', in *8th RILEM International Symposium on Testing and Characterization of Sustainable and Innovative Bituminous Materials*, pp. 459–470. doi: 10.1007/978-94-017-7342-3.

Rada, G. R. *et al.* (2013) *Guide for Conducting Forensic Investigations of Highway Pavements*. Transportation Research Board, .

Rizzutto, S. J. *et al.* (2015) 'Use of a Variable Rate Spray Bar to Minimize Wheel Path Bleeding for Asphalt-Rubber Chip Seal Applications', *Journal of Materials in Civil Engineering*, 27(3),

pp. 1–8. doi: 10.1061/(ASCE)MT.1943-5533.0001035.

Roque, R., Anderson, D. avi. and Thompson, M. (1991) 'Effect of material, design, and construction variables on seal-coat performance. ', *Transportation Research Record: Journal of the Transportation Research Board*, 1300(August), pp. 108–115.

Santagata, F. A. *et al.* (2009) 'Modified PATTI Test for the Characterization of Adhesion and Cohesion Properties of Asphalt Binders'. Available at: https://trid.trb.org/view/899139 (Accessed: 14 May 2018).

Senadheera, S., Gransberg, D. D. and Kologlu, T. (2000) *Statewide Seal Coat Constructability Review*. doi: 10.1016/j.ijrobp.2011.04.014.

Sendheera, S. *et al.* (2006) *A testing and evaluation protocol to assess seal coat binder-aggregate compatibility*.

Shuler, S. (2011) *Manual for emulsion-based chip seals for pavement preservation*.

Shuler, S. *et al.* (2011) *Manual for Emulsion-Based Chip Seals for Pavement Preservation*. doi: 10.17226/14421.

Tenison, J. (2009) 'Pre-Overlay Treatment of Existing Pavements'. Available at: https://scholar.google.com/scholar?hl=en&as_sdt=0%2C23&q=Tenison+J.%2C+H.%2C+D.%2C+%22Pre-Overlay+Treatment+of+Existing+Pavements%2C%22+National+Cooperative+Highway+Research+Program%2C+NCHRP+Synthesis+388%2C+2009.&btnG= (Accessed: 14 May 2018).

Texas Department of Transporation (2010) 'Seal Coat and Surface Treatment Manual', (July).

TNZ report (2005) *Chipsealing in New Zealand*.

Uz, V. E. and Gökalp, İ. (2017) 'Comparative laboratory evaluation of macro texture depth of surface coatings with standard volumetric test methods', *Construction and Building Materials*, 139, pp. 267–276. doi: 10.1016/j.conbuildmat.2017.02.059.

Wasiuddin, N. M. *et al.* (2013) 'Use of Sweep Test for Emulsion and Hot Asphalt Chip Seals: Laboratory and Field Evaluation', *Journal of Testing and Evaluation*, 41(2), p. 20120051. doi: 10.1520/JTE20120051.

Watson, B. (no date) 'Elcometer 110 PATTI Pneumatic Adhesion Tester'. Available at: https://www.elcometer.com/images/stories/PDFs/InstructionBooks/110.pdf (Accessed: 14 May 2018).